DEVELOPING FLOW IN AN ELLIPTICAL DUCT

A Thesis Submitted
In Partial Fulfilment of the Requirements
for the Degree of

MASTER OF TECHNOLOGY

by
K. VELUSAMY

to the

DEPARTMENT OF MECHANICAL ENGINEERING
INDIAN INSTITUTE OF TECHNOLOGY, KANPUR
MAY, 1985

ME-1985-M-VEL-DEV

To

my teacher
Prof. Garg

CERTIFICATE

CERTIFIED that the thesis titled, "DEVELOPING FLOW IN AN ELLIPTICAL DUCT" has been submitted by K. Velusamy under my supervision and that this work has not been submitted elsewhere for award of a degree.

I.I.T. Kanpur
May 1985.

(Dr. Vijay K. Garg)
Professor
Department of Mechanical Engineering
INDIAN INSTITUTE OF TECHNOLOGY, KANPUR

ACKNOWLEDGEMENT

I deeply express my sincere thanks and sense of gratitude to my guide Dr. V.K. Garg who initiated me into this work and guided me with valuable suggestions throughout the course of this work.

Besides thanking Mr. G.L. Misra for his neat typing of the manuscript, I also thank all my friends and colleagues for their help and encouragement.

K. VELUSAMY

CONTENTS

LIST OF FIGURES

LIST OF TABLES

NOMENCLATURE

a = semi major-axis of the elliptical duct

A = $\cosh^2(\pi Z/2) - \cos^2(\pi Y/2)$

b = semi minor-axis of the elliptical duct

B = $\dfrac{\cot(\pi Y/2) + \coth^2 \eta_w \tan(\pi Y/2)}{\coth(\pi Z/2) - \coth^2 \eta_w \tanh(\pi Z/2)}$

c = focal length of the elliptical duct

C = $\dfrac{(\pi/2)\sinh(\pi Z)}{2A^{1/2}}$

D = $\dfrac{(\pi/2)\sin(\pi Y)}{2A^{1/2}}$

E = $(E_1, E_2, E_3, \ldots, E_n)$ is the row vector arising from the coefficients of axial velocity component at location $(i+1)$ in eqn. (3.17)

G = is the unsymmetric banded matrix arising from coefficients of axial velocity component at location $(i+1)$ in eqn. (3.2)

G^* = is the upper triangular matrix with diagonal elements unity

H = $\{H_1, H_2, H_3, \ldots, H_n\}$ is the column vector arising from the pressure at location $(i+1)$ in the momentum eqn. (3.2)

H^* = operated vector $\{H\}$

i = represents location in X-direction

j = represents location in Y-direction

J = Jacobian of the transformation divided by the square of the focal length

k = represents location in Z-direction

$K(X)$ = pressure defect

K_1 = constant in eqn. (2.7)

K_2 = constant in eqn. (2.9)

K_∞ = Pressure defect K(X) at $X \to \infty$

L = entrance length

p = pressure

p_o = pressure p at x = 0

P = dimensionless pressure $(p-p_o)/\rho u_o^2$

Q = is the known right hand side of eqn.(3.17)

R = $\{R_1, R_2, R_3, \ldots, R_n\}$ is the known right hand side column vector arising from the terms at location (i) in eqn. (3.2)

R^* = operated vector {R}

S = is the coefficient matrix arising from eqns. (3.17) and (3.2)

u = velocity component along x-direction

u_o = velocity u at x = 0

U = dimensionless velocity component along X-direction, u/u_o

v = velocity component along y-direction

v_η = velocity component along η-direction

v_Ψ = velocity component along Ψ-direction

V = dimensionless velocity component along Y-direction, $\dfrac{(\pi c/2)\, v_\Psi}{\nu}$

w = velocity component along z-direction

W = dimensionless velocity component along Z-direction, $\dfrac{(\pi c/2) v_\eta}{\nu}$

x = Cartesian coordinate along the duct centre-line

X = dimensionless axial coordinate, $\dfrac{\nu x}{(\pi c/2)^2 u_o}$

X_∞ = dimensionless entrance length, $\dfrac{\nu L}{(\pi c/2)^2 u_o}$

X^* = $X(\pi c/2b)^2$

y = Cartesian coordinate along the duct minor-axis

Y = dimensionless coordinate along Ψ-direction, $\Psi/(\pi/2)$

z = Cartesian coordinate along the duct major-axis

Z = dimensionless coordinate along η-direction, $\eta/(\pi/2)$

δ = small length FF^1 fig. (3.3)

ΔX = step size in the X-direction

ΔY = step size in the Y-direction

ΔZ = step size in the Z-direction

η = coordinate in the elliptic cylinder coordinate system fig. (A.1)

η_w = represents the duct wall

θ_1 = ratio of step sizes $\Delta Z2/\Delta Z1$

θ_2 = ratio of step sizes $\Delta Y1/\Delta Y2$

θ_3 = ratio of step sizes $\Delta Y3/\Delta Y2$

λ = duct aspect ratio, a/b

μ = dynamic viscosity of the fluid

ν = kinematic viscosity of the fluid

ρ = density of the fluid

σ = $\eta_w/(\pi/2)$

Φ_1 = ratio of step sizes $\Delta Z2/\Delta Z1$

Φ_2 = ratio step sizes $\Delta Y2/\Delta Y1$

Φ_3 = $\Phi_1 \cdot \Phi_2$

Φ_4 = ratio of step sizes $\Delta Y3/\Delta Y1$

Φ_5 = $\Phi_1 \cdot \Phi_4$

Ψ = coordinate in the elliptic-cylinder coordinate system fig. (A.1).

Chapter 1

INTRODUCTION

Whenever a viscous fluid enters a stationary duct, a layer of the fluid sticks to the wall of the duct creating a velocity gradient in the transverse direction of flow. In order to satisfy the mass balance, transverse velocity components towards the duct-centre and consequent acceleration of the core surrounding the duct centreline are set up. The cross-flow and acceleration proceed till the fluid reaches a station in the axial coordinate beyond which the velocity profile remains constant and the cross-flow vanishes. The region in the duct between this station and the entrance is known as the hydrodynamic entry region. In this flow development region the momentum of the fluid increases as the velocity distribution becomes less uniform, and viscous dissipation of the energy occurs in establishing the velocity profile. Hence the pressure gradient in this region is higher than that in the fully developed region. Entrance-region heat and mass transfer coefficients are also larger than those for a developed flow, owing to the presence of cross flow and smaller boundary-layer thickness. The calculation of these coefficients requires detailed knowledge of the velocity field in the entrance-region of the duct.

Though circular ducts are common, non-circular ducts may occur, for example, in nuclear reactors and in compact

heat-exchange equipment. Since nuclear reactors use low Prandtl number (and hence less viscous) liquid metals, the flow development length is significant. In a compact heat-exchange equipment the entrance length would constitute a significant portion of the total duct-length.

The hydrodynamic development of flow, in the entrance-region of tubes and ducts, has been a subject of study from as early as 1922 when Schiller [1] presented an analysis. Even for laminar conditions, the flow development in the entrance-region does not permit an exact solution for any shape of the duct cross-section. The difficulty in the analysis is traced to the nonlinear nature of the inertia terms which appear in the equations of motion. In the past, various approximate methods of solution have been developed to provide the requisite information relating to the velocity and pressure fields. These methods may be brought together under four general classes which will be explained subsequently.

In the first class are methods which linearize the inertia terms. With the usual boundary-layer assumptions of negligible axial momentum diffusion, and negligible dependence of pressure on the transverse coordinates, Langhaar [2] linearized the inertia terms of the Navier-Stokes equations, and solved the same for a steady flow in the entrance-region of a straight circular tube to get a family of velocity profiles defined by Bessel functions. His results are in close agreement with the experimental results of Nikuradse [3]. Such linearized

solutions with some refinement or the other are presented for a circular tube by Slezkin [4], and for a parallel-plate channel by Sparrow, et al. [5]. Later Lundgren, et al. [6], with the usual boundary-layer assumptions, devised a general analytical method for determining the entrance pressure-drop for ducts of arbitrary cross sections. Their analysis has two drawbacks. First, it does not predict the actual entrance-length. Second, since the pressure-drop calculation is based on the momentum and mechanical energy equations, knowledge of the exact velocity field is essential.

McComas [7] extended the work of Lundgren, et al. [6] for the determination of hydrodynamic entrance-lengths from the fully developed velocity profile. Comparison of his results with the detailed analysis of development region for circular tube and parallel-plate channel [8,9], rectangular ducts [10], and annular ducts [11] indicates that his predictions of the entrance-lengths are far smaller than those predicted by [8-11]. Also the centreline velocity and the axial pressure gradient are in substantial error.

Flemming and Sparrow [12] generalised the method given in [8] for ducts of arbitrary cross section. They express the entrance-region velocity in terms of a deviation from the fully developed velocity. This deviation is determined by a least squares method satisfying the wall boundary conditions. They also use the questionable assumption that the pressure drop in

the entrance-region from the momentum equation is equal to that from the mechanical energy equation. Though their method of solution is applicable to all cross-sectional ducts, results have been presented only for triangular and rectangular ducts.

In the second class are methods which divide the entrance-region into two parts, one near the entrance of the duct where a perturbation solution of the boundary-layer model is assumed, and the other far away from the entrance where a perturbation solution of the fully developed velocity profile is assumed. These two solutions are then patched at some appropriate axial location. Schlichting [13] determined the approximate velocity profile in the entrance-region of a parallel plate channel using this approach. Atkinsen and Goldstein [14] extended the work of Schlichting for a circular duct.

In the third class of analysis, initially developed by Schiller [1], the duct cross-section of the entrance region is considered to be composed of two regions, a boundary-layer developing near the wall and an inviscid fluid core. An integral representation of the momentum conservation principle is employed assuming a suitable velocity distribution inside the boundary-layer and estimating pressure from the Bernoulli equation applicable to the unsheared core. For circular ducts and parallel plate channels Schiller used parabolic boundary-layer velocity profiles, whereas Shapiro, et al. [15] and Siegel [16] assumed modified cubic and modified quartic boundary-layer velocity

profiles and Bogue [17] assumed cubic boundary-layer velocity profiles and power law flow. Bogue also included the radial momentum term in the Von-Karman's integral method [18, p. 137]. The reported velocity profiles from all these integral method solutions vary little with the assumed boundary-layer velocity profile. Tomita [19,20] achieved similar results for power law flow and by the variational method. For a circular tube Campbell and Slattery [21] modified Schiller's method to take into account viscous dissipation of energy in the boundary-layer. Their solution yields much better results than those given by Schiller's method especially at larger distances from the entrance where an increasingly larger part of the fluid is in boundary-layer shear and viscous dissipation of energy is increasingly important. More information about this is available in [22].

Chen [23] extended the integral momentum method for developing flow in a pipe and in a parallel-plate channel at low Reynolds numbers. Bhatti [24] obtained a closed form analytical solution for the development of centreline velocity and pressure-drop in the entrance-region of elliptical ducts. Alongwith the usual boundary-layer assumptions he also assumed that the core is also elliptical and concentric with the duct cross-section. However, for a three-dimensional flow such as the flow in the entrance-region of an elliptical duct, the integral method requires that the velocity profile in the

boundary layer as well as the variation of boundary-layer thickness along the duct be assumed. For a two-dimensional flow such as the flow in the entrance-region of circular tube or a parallel-plate channel, only the velocity profile in the boundary-layer needs to be assumed. Bhatti also assumes that at the elliptical duct inlet, the streamwise growth of the boundary-layer is identical to that on a flat plate at zero incidence. However, while the former is influenced by the favourable pressure gradient, the latter has no pressure gradient. Bhatti's results are therefore suspect.

This integral method has been used by Han and Coopar [25] for triangular ducts and by Sparrow [26] for rectangular ducts.

In the last class are solutions obtained numerically, by writing various derivatives that appear in the Navier-Stokes equations in the finite-difference form and solving the resulting set of linear or non-linear simultaneous equations. Extending the work of Rouleau [27], Bodoia and Osterle [28] solved the entrance-region flow development in a parallel-plate channel. With the usual boundary-layer assumptions the Navier-Stokes equations are parabolic enabling numerical marching in the flow direction. They linearised the non-linear inertia terms with the known upstream velocity field. Wang and Longwell [29], without any boundary-layer assumptions solved the entire Navier-Stokes equations using finite-difference technique for a parallel-plate channel with Reynolds number 300. They introduced

stream function and vorticity in the continuity and momentum equations to reduce the number of equations and to eliminate the pressure terms. They experienced some convergence problems at low Reynolds number values.

Schmidt and Zeldin [30] proceeded exactly in the same way as Wang and Longwell [29] and calculated the pressure-defect for circular ducts and parallel-plate channels for Reynolds number values of 100, 500 and 10,000. The kinks in the developing velocity profile reported by Wang and Longwell have also been observed by Brandt and Gillis [31]. Later Abarbanel, et al. [32] proved that the kinks belong to the exact mathematical solution and are not merely mathematical consequence of the non-physical singularities, though the boundary-layer theory precludes such a kink. Besides Bhatti's analysis for a developing flow in an elliptical duct, other analyses that consider three-dimensional developing flows confine themselves to the triangular [33-37], rectangular [34-39] or square [33,34,40-43] ducts.

The foregoing brief survey of the literature indicates that the problem of flow development in the entrance-region of elliptical ducts remains to be solved satisfactorily. It is this problem that we solve by a finite-difference method. The fluid is taken to be incompressible and Newtonian, and the usual boundary-layer approximations are used.

Chapter 2

ANALYSIS

The complete equations of motion for a laminar, incompressible, uniform property flow in the Cartesian coordinate system (x, y, z), with the velocity components (u, v, w), density ρ, pressure p, and dynamic viscosity μ are [18].

continuity :

$$\frac{\partial u}{\partial x} + \frac{\partial v}{\partial y} + \frac{\partial w}{\partial z} = 0 \qquad (2.1)$$

x-momentum :

$$\rho\left(u\frac{\partial u}{\partial x} + v\frac{\partial u}{\partial y} + w\frac{\partial u}{\partial z}\right) = -\frac{\partial p}{\partial x} + \mu\left(\frac{\partial^2 u}{\partial x^2} + \frac{\partial^2 u}{\partial y^2} + \frac{\partial^2 u}{\partial z^2}\right) \qquad (2.2)$$

y-momentum :

$$\rho\left(u\frac{\partial v}{\partial x} + v\frac{\partial v}{\partial y} + w\frac{\partial v}{\partial z}\right) = -\frac{\partial p}{\partial y} + \mu\left(\frac{\partial^2 v}{\partial x^2} + \frac{\partial^2 v}{\partial y^2} + \frac{\partial^2 v}{\partial z^2}\right) \qquad (2.3)$$

z-momentum :

$$\rho\left(u\frac{\partial w}{\partial x} + v\frac{\partial w}{\partial y} + w\frac{\partial w}{\partial z}\right) = -\frac{\partial p}{\partial z} + \mu\left(\frac{\partial^2 w}{\partial x^2} + \frac{\partial^2 w}{\partial y^2} + \frac{\partial^2 w}{\partial z^2}\right). \qquad (2.4)$$

For the elliptical duct (Fig. 2.1) with major axis = 2a and minor axis = 2b, and with origin at the centre of the duct cross-section, the boundary conditions are

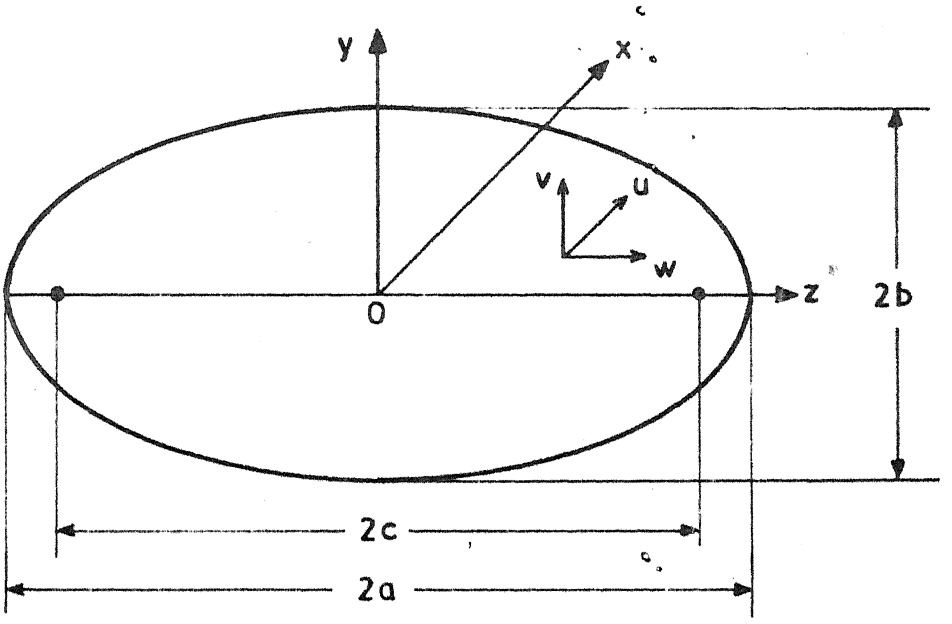

Fig. 2.1 Duct cross-section

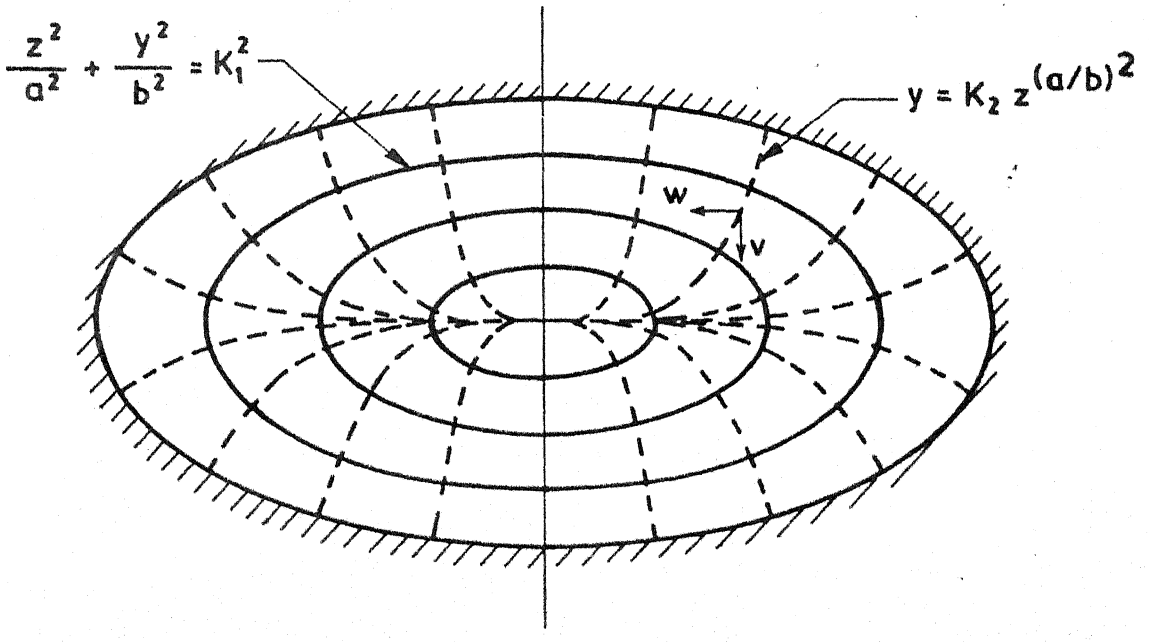

Fig. 2.2 Equal speed curves (——) and vorticity diffusion curves (- - - -)

$$\left.\begin{aligned} u(x,0 \le y \le b,\ a\left[1-y^2/b^2\right]^{1/2}) &= 0 \\ \frac{\partial u}{\partial z}(x,y,0) &= 0 \\ \frac{\partial u}{\partial y}(x,0,z) &= 0 \end{aligned}\right\} \qquad (2.5a)$$

$$\left.\begin{aligned} v(x,0 \le y \le b,\ a\left[1-y^2/b^2\right]^{1/2}) &= 0 \\ v(x,0,z) &= 0 \\ \frac{\partial v}{\partial z}(x,y,0) &= 0 \end{aligned}\right\} \qquad (2.5b)$$

$$\left.\begin{aligned} w(x,0 \le y \le b,\ a\left[1-y^2/b^2\right]^{1/2}) &= 0 \\ w(x,y,0) &= 0 \\ \frac{\partial w}{\partial y}(x,0,z) &= 0 \end{aligned}\right\} \qquad (2.5c)$$

$$\left.\begin{aligned} u(0,y,z) &= u_o \\ p(0,y,z) &= p_o \end{aligned}\right\} \qquad (2.5d)$$

$$\left.\begin{aligned} \frac{\partial p}{\partial y}(x,0,z) &= 0 \\ \frac{\partial p}{\partial z}(x,y,0) &= 0 \\ v(0,y,z) &= 0 \\ w(0,y,z) &= 0. \end{aligned}\right\} \qquad (2.5e)$$

For the present analysis u_o has been assumed uniform, although the effect of the duct on the flow propagates upstream. A lucid discussion of various boundary conditions used for $u(0,y,z)$ for a circular duct is given by Shah and London [44]. We note, however, that the assumption of a uniform u_o at the duct-entrance is very common.

An order of magnitude analysis, essentially that of Carlson [45], may now be applied to eqns. (2.1) to (2.4). Taking a representative length in the axial direction x, along the duct-axis, to be of the order of development length L, and in the transverse directions y and z to be of the order of maximum half-widths of the duct b and a respectively, we assume that $L \gg a$ or b. Then, if terms of $O(a/L)$ or $O(b/L)$ or lower compared to those of $O(1)$ are neglected, eqns. (2.2) to (2.4) reduce to

$$\rho\left(u\frac{\partial u}{\partial x} + v\frac{\partial u}{\partial y} + w\frac{\partial u}{\partial z}\right) = -\frac{dp}{dx} + \mu\left(\frac{\partial^2 u}{\partial y^2} + \frac{\partial^2 u}{\partial z^2}\right), \qquad (2.6)$$

and the dependence of p on the transverse coordinates ceases.

Eqns. (2.1) and (2.6) constitute two equations in the three velocity components u, v and w and are hence insolvable. An additional equation must be specified in order to complete the set[+]. Carlson [45] has proposed and verified that for a square duct one possible choice is to assume that at each point in the duct cross-section, the transverse velocity vector is directed towards the duct centreline. This provides the required additional relation between v and w. Garg [46] has verified that this relation can be extended to rectangular ducts of moderate aspect ratios. Feldman, et al. [47] have also developed a relation between transverse velocity components for the developing flow in an eccentric annular duct. Following these successes, we also develop this additional relation on the basis of the following hypothesis.

In a confined flow, the vorticity diffuses normally from the duct wall owing to a balance of pressure and viscous forces at the wall, and the fact that pressure is impressed normally upon the wall. Also in an elliptical duct, owing to the absence of any sharp corners, the vorticity diffusion curves emanating normally from the duct-wall remain normal to all equal speed curves. This is analogous to the orthogonality of heat flux lines and isotherms in a thermal problem. Such a normal diffusion of vorticity is possible if and only if the equal speed curves have the same slope at the corresponding points. Since the duct wall itself is an equal speed curve representing zero speed, all the other equal speed curves should have the same shape as the duct wall and are therefore concentric ellipses.

Let the equation of these equal speed curves (Fig. 2.2) be

$$\frac{z^2}{a^2} + \frac{y^2}{b^2} = K_1^2 , \qquad (2.7)$$

with $0 < K_1 \leq 1$. The slope of the normal to the curves represented by eqn. (2.7) is

$$\frac{dy}{dz} = \left(\frac{a}{b}\right)^2 \frac{y}{z} . \qquad (2.8)$$

Eqn. (2.8) represents the slope of the tangent to the vorticity diffusion curves at any general point (z, y). Upon integration, it gives the equation of the vorticity diffusion curves

$$y = K_2 z^{(a/b)^2}, \qquad (2.9)$$

here K_2 is the constant of integration. Eqn. (2.9) indicates hat the shape of the vorticity diffusion curves is a function f the aspect ratio $\lambda = a/b$. For a circular duct with the aspect atio unity, Eqn. (2.9) represents a family of straight lines $= K_2 z$ which are readily recognised as the radial lines.

The above discussion indicates that the transverse elocity vector is directed towards the centre of the duct along he vorticity diffusion curves represented by eqn. (2.9). Based n this a third relation between v and w of the form

$$\frac{v}{w} = \left(\frac{a}{b}\right)^2 \frac{y}{z} \qquad (2.10)$$

is assumed.

Eqns. (2.1), (2.6) and (2.10) constitute a complete set+ with the boundary conditions in eqns. (2.5a,b,c,d). A rigorous solution of this set, by the finite-difference method, in the Cartesian coordinate system is cumbersome because of the curved boundary of the duct. The treatment for curved boundaries by the finite-difference method are available in [48,49]. Herein we transform the set of eqns. (2.1), (2.6) and (2.10) alongwith the boundary conditions into an elliptic-cylindrical coordinate system (x, Ψ, η) with velocity components (u, v_Ψ, v_η) respectively. The constant η surfaces are confocal elliptic cylinders, orthogonal to the confocal hyperbolic cylinders represented by

---

+Also see footnote on p.11.

constant Ψ surfaces (see Appendix. A). The foci of both the families are same and are situated at $(c,0)$ in the (z,y) plane. It is to be noted that $\eta = \eta_w$ represents the duct wall.

After some lengthy algebra (see Appendix. B), the complete set of equations reduces to

$$c\,J\,\frac{\partial u}{\partial x} + \frac{\partial}{\partial \Psi}\,(v_\Psi\,J^{1/2}) + \frac{\partial}{\partial \eta}\,(v_\eta\,J^{1/2}) = 0, \qquad (2.11)$$

$$u\,\frac{\partial u}{\partial x} + \frac{1}{cJ^{1/2}}\,(v_\Psi\,\frac{\partial u}{\partial \Psi} + v_\eta\,\frac{\partial u}{\partial \eta}) = -\,\frac{1}{\rho}\,\frac{dp}{dx}$$

$$+\,\frac{\nu}{c^2\,J}\,(\frac{\partial^2 u}{\partial \Psi^2} + \frac{\partial^2 u}{\partial \eta^2}), \qquad (2.12)$$

$$\frac{v_\Psi}{v_\eta} = -\,\frac{(\coth\eta - \coth^2\eta_w\,\tanh\eta)}{(\cot\Psi + \coth^2\eta_w\,\tan\Psi)}, \qquad (2.13)$$

$$\left.\begin{aligned} u(x,\Psi,\eta_w) &= 0,\\ \frac{\partial u}{\partial \Psi}\,(x,\pi/2,\eta) &= 0,\\ \frac{\partial u}{\partial \Psi}\,(x,0,0 < \eta \le \eta_w) &= 0,\\ \frac{\partial u}{\partial \eta}\,(x,0 < \Psi \le \frac{\pi}{2},0) &= 0, \end{aligned}\right\} \qquad (2.14a)$$

$$\left.\begin{aligned} v_\Psi\,(x,\Psi,\eta_w) &= 0,\\ v_\Psi(x,0,0 < \eta \le \eta_w) &= 0,\\ v_\Psi(x,\pi/2,\eta) &= 0,\\ \frac{\partial v_\Psi}{\partial \eta}\,(x,0 < \Psi \le \frac{\pi}{2},0) &= 0, \end{aligned}\right\} \qquad (2.14b)$$

$$\left.\begin{aligned} v_\eta\ (x, \Psi, \eta_w) &= 0, \\ v_\eta\ (x, 0 < \Psi \leq \pi/2, 0) &= 0, \\ \frac{\partial v_\eta}{\partial \Psi}\ (x, 0, 0 < \eta \leq \eta_w) &= 0, \\ \frac{\partial v_\eta}{\partial \Psi}\ (x, \pi/2, \eta) &= 0, \end{aligned}\right\} \qquad (2.14c)$$

$$\left.\begin{aligned} u(0, \Psi, \eta) &= u_o, \\ p(0) &= p_o, \end{aligned}\right\} \qquad (2.14d)$$

where ν is the kinematic viscosity of the fluid and

$J\ (= (\frac{\partial z}{\partial \eta}\frac{\partial Y}{\partial \Psi} - \frac{\partial Y}{\partial \eta}\frac{\partial z}{\partial \Psi})/c^2)$ is the Jacobian of the transformation divided by the square of the focal length c.

It should be noted that the Jacobian of the transformation vanishes at the focus and therefore eqns. (2.11) to (2.13) do not hold at the focal point. Elimination of this singularity in the finite-difference procedure will be explained in the next chapter.

After non-dimensionalisation with

$$X = \frac{\nu x}{(\pi c/2)^2 u_o},$$

$$Y = \frac{\Psi}{\pi/2},$$

$$Z = \frac{\eta}{\pi/2},$$

$$U = \frac{u}{u_o},$$

$$V = \frac{(\pi c/2)\, v_\psi}{\nu} ,$$

$$W = \frac{(\pi c/2)\, v_\eta}{\nu} ,$$

and

$$P = \frac{(p - p_o)}{\rho u_o^2} ,$$

the set of eqns. (2.11) to (2.14) reduces to

$$A \frac{\partial U}{\partial X} + A^{1/2} \left(\frac{\partial V}{\partial Y} + \frac{\partial W}{\partial Z}\right) + DV + CW = 0 , \qquad (2.15)$$

$$AU \frac{\partial U}{\partial X} + A^{1/2}\left(V \frac{\partial U}{\partial Y} + W \frac{\partial U}{\partial Z}\right) = -A \frac{dP}{dX} + \frac{\partial^2 U}{\partial Y^2} + \frac{\partial^2 U}{\partial Z^2} , \qquad (2.16)$$

$$V = -W/B , \qquad (2.17)$$

$$\left.\begin{aligned} U(X,Y,\sigma) &= 0 , \\ \frac{\partial U}{\partial Y}(X,1,Z) &= 0 , \\ \frac{\partial U}{\partial Y}(X,0,0 < Z \leq \sigma) &= 0 , \\ \frac{\partial U}{\partial Z}(X,0 < Y \leq 1,0) &= 0 , \end{aligned}\right\} \qquad (2.18a)$$

$$\left.\begin{aligned} V(X,Y,\sigma) &= 0 , \\ V(X,0,0 < Z \leq \sigma) &= 0 , \\ V(X,1,Z) &= 0 , \\ \frac{\partial V}{\partial Z}(X,0 < Y \leq 1,0) &= 0 , \end{aligned}\right\} \qquad (2.18b)$$

$$\left.\begin{aligned} W(x,Y,\sigma) &= 0\,, \\ W(X,0 < Y \leq 1,\ 0) &= 0\,, \\ \frac{\partial W}{\partial Y}(X,0,0 < Z \leq \sigma) &= 0\,, \\ \frac{\partial W}{\partial Y}(X,1,Z) &= 0\,, \end{aligned}\right\} \qquad (2\text{-}18c)$$

$$\left.\begin{aligned} U(0,Y,Z) &= 1\,, \\ P(0) &= 0\,, \end{aligned}\right\} \qquad (2\text{-}18d)$$

and

where

$$A = \cosh^2(\pi Z/2) - \cos^2(\pi Y/2),$$

$$B = \frac{\cot(\pi Y/2) + \coth^2 \eta_w \cdot \tan(\pi Y/2)}{\coth(\pi Z/2) - \coth^2 \eta_w \cdot \tanh(\pi Z/2)}\,,$$

$$C = \frac{\partial A^{1/2}}{\partial Z} = \frac{(\pi/2)\ \sinh(\pi Z)}{2A^{1/2}}\,,$$

$$D = \frac{\partial A^{1/2}}{\partial Y} = \frac{(\pi/2)\ \sin(\pi Y)}{2A^{1/2}}\,,$$

and

$$\sigma = \frac{\eta_w}{(\pi/2)}\,.$$

Chapter 3
THE FINITE-DIFFERENCE METHOD

Eqn. (2.16) is parabolic in the axial coordinate X, so that the classical forward marching scheme in the axial direction can be employed. Since eqns. (2.15), (2.16) and (2.17) do not involve any derivatives of the transverse velocity components with respect to the axial coordinate, their specification at the entrance as initial conditions is unnecessary in the true mathematical sense. But for the finite-difference method that we employ, their specification at the entrance is required to start the marching procedure. Though theoretically the transverse velocities can be proved to be infinite at the entrance singular point, we specify them as zero. This choice of the transverse velocities affects only the region near the entrance, and its effect dies out as we march [50] in the flow direction.

A non uniform finite-difference grid (Figs. 3.1,2) is imposed on the flow field. Step sizes ΔX, ΔY, and ΔZ are taken respectively in the X,Y, and Z directions. Backward differencing in the marching X-direction and central differencing in the Y and Z-directions are employed in eqn. (2.16) whereas only backward differencing is employed in eqn. (2.15). The finite-difference forms of eqns. (2.15), (2.16) and (2.17), with no-slip condition on the duct-wall and linearization of the non-linear inertia terms by the upstream flow field are

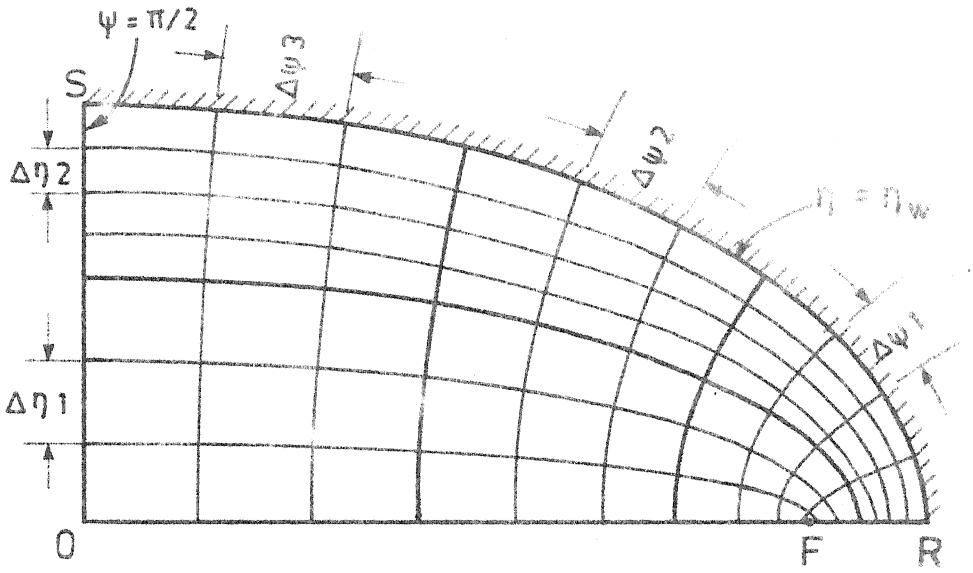

Fig. 3.1 Finite-difference grid in physical plane.

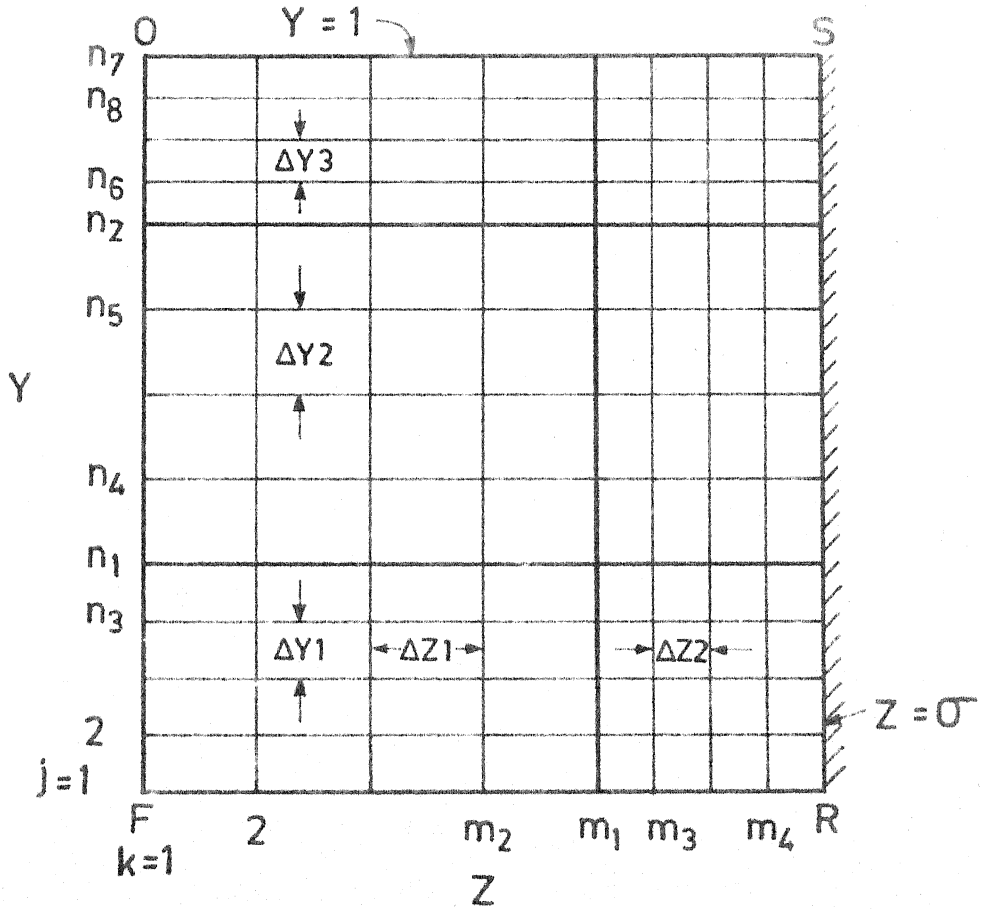

Fig. 3.2 Finite-difference grid in transformed (computational) plane.

$$A^{1/2}_{j,k}\frac{(V_{i+1,j+1,k}-V_{i+1,j,k})}{(\Delta Y)}+A^{1/2}_{j,k}\frac{(W_{i+1,j,k+1}-W_{i+1,j,k})}{(\Delta Z)}$$

$$+D_{j,k}V_{i+1,j,k}+C_{j,k}W_{i+1,j,k}+A_{j,k}\frac{(U_{i+1,j,k}-U_{i,j,k})}{(\Delta X)}=0, \tag{3.1}$$

$$A^{1/2}_{j,k}V_{i,j,k}\frac{(U_{i+1,j+1,k}-U_{i+1,j-1,k})}{2(\Delta Y)}$$

$$+A^{1/2}_{j,k}W_{i,j,k}\frac{(U_{i+1,j,k+1}-U_{i+1,j,k-1})}{2(\Delta Z)}$$

$$+A_{j,k}U_{i,j,k}\frac{(U_{i+1,j,k}-U_{i,j,k})}{(\Delta X)}=-A_{j,k}\frac{(P_{i+1}-P_i)}{(\Delta X)}$$

$$+\frac{(U_{i+1,j+1,k}-2U_{i+1,j,k}+U_{i+1,j-1,k})}{(\Delta Y)^2}$$

$$+\frac{(U_{i+1,j,k+1}-2U_{i+1,j,k}+U_{i+1,j,k-1})}{(\Delta Z)^2}, \tag{3.2}$$

and

$$V_{i+1,j,k}=-\frac{W_{i+1,j,k}}{B_{j,k}}, \tag{3.3}$$

where the subscripts i, j, and k represent location in X, Y, and Z directions respectively and

$$\Delta Z = \begin{cases} \Delta Z1 & \text{for } k = 1(1)m1 \\ \Delta Z2 & \text{for } k = m1(1)m4+1 \end{cases}$$

and

$$\Delta Y = \begin{cases} \Delta Y1 & \text{for } j = 1(1)n1 \\ \Delta Y2 & \text{for } j = n1(1)n2 \\ \Delta Y3 & \text{for } j = n2(1)n7. \end{cases}$$

Eqns. (3.1) and (3.2) need to be modified at the boundary lines, i.e., for j = 1 and n7, and for k = 1. Moreover, eqn. (3.2) needs modification at lines where the grid size changes, i.e., for j = n1 and n2, and for k = m1. With the inclusion of the boundary conditions (2.18), eqns. (3.1) and (3.2) take the following forms (see Fig. 3.2) :

(a) along the boundary FR (j = 1, k ≠ 1) :

$$A^{1/2}_{1,k} \frac{V_{i+1,2,k}}{(\Delta Y1)} + A^{1/2}_{1,k} \frac{(W_{i+1,1,k+1} - W_{i+1,1,k})}{(\Delta Z)} + C_{1,k} W_{i+1,1,k} + A_{1,k} \frac{(U_{i+1,1,k} - U_{i,1,k})}{(\Delta X)} = 0, \qquad (3.4)$$

and

$$A^{1/2}_{1,k} W_{i,1,k} \frac{(U_{i+1,1,k+1} - U_{i+1,1,k-1})}{2(\Delta Z)} + A_{1,k} U_{i,1,k} \frac{(U_{i+1,1,k} - U_{i,1,k})}{(\Delta X)}$$

$$= -A_{1,k}\frac{(P_{i+1}-P_i)}{(\Delta X)} + \frac{(2U_{i+1,2,k}-2U_{i+1,1,k})}{(\Delta Y_1)^2}$$

$$+ \frac{(U_{i+1,1,k+1}-2U_{i+1,1,k}+U_{i+1,1,k-1})}{(\Delta Z)^2}. \qquad (3.5)$$

(b) along the boundary FO ($k = 1,\ j \neq 1$) :

$$A^{1/2}_{j,1}\frac{(V_{i+1,j+1,1}-V_{i+1,j,1})}{(\Delta Y)} + A^{1/2}_{j,1}\frac{W_{i+1,j,2}}{(\Delta Z_1)} + D_{j,1}V_{i+1,j,1}$$

$$+ A_{j,1}\frac{(U_{i+1,j,1}-U_{i,j,1})}{(\Delta X)} = 0, \qquad (3.6)$$

and

$$A^{1/2}_{j,1}V_{i,j,1}\frac{(U_{i+1,j+1,1}-U_{i+1,j-1,1})}{2(\Delta Y)}$$

$$+ A_{j,1}U_{i,j,k}\frac{(U_{i+1,j,1}-U_{i,j,1})}{(\Delta X)}$$

$$= -A_{j,1}\frac{(P_{i+1}-P_i)}{(\Delta X)} + \frac{(U_{i+1,j+1,1}-2U_{i+1,j,1}+U_{i+1,j-1,1})}{(\Delta Y)^2}$$

$$+ \frac{(2U_{i+1,j,2}-2U_{i+1,j,1})}{(\Delta Z_1)^2}. \qquad (3.7)$$

(c) along the boundary OS ($j = n7$):

$$-A^{1/2}_{n7,k}\frac{V_{i+1,n8,k}}{(\Delta Y3)}+A^{1/2}_{n7,k}\frac{(W_{i+1,n7,k+1}-W_{i+1,n7,k})}{(\Delta Z)}$$

$$+C_{n7,k}W_{i+1,n7,k}+A_{n7,k}\frac{(U_{i+1,n7,k}-U_{i,n7,k})}{(\Delta X)}=0, \qquad (3.8)$$

and

$$A^{1/2}_{n7,k}W_{i,n7,k}\frac{(U_{i+1,n7,k+1}-U_{i+1,n7,k-1})}{2(\Delta Z)}$$

$$+A_{n7,k}U_{i,n7,k}\frac{(U_{i+1,n7,k}-U_{i,n7,k})}{(\Delta X)}$$

$$=-A_{n7,k}\frac{(P_{i+1}-P_i)}{(\Delta X)}+\frac{(2U_{i+1,n8,k}-2U_{i+1,n7,k})}{(\Delta Y3)^2}$$

$$+\frac{(U_{i+1,n7,k+1}-2U_{i+1,n7,k}+U_{i+1,n7,k-1})}{(\Delta Z)^2}. \qquad (3.9)$$

Let us now derive the form of eqns. (3.1) and (3.2) applicable at the focal point j = 1, k = 1.

We know that the focal point of the ellipse is a singular point of transformation since the Jacobian of the transformation vanishes at that point. To avoid use of this point in the computations, a point F^1 is considered very near to the right of focal point F such that $FF^1 = \delta$ (Fig. 3.3). The reason for not considering F^1 on the line FG will be explained later. Hence

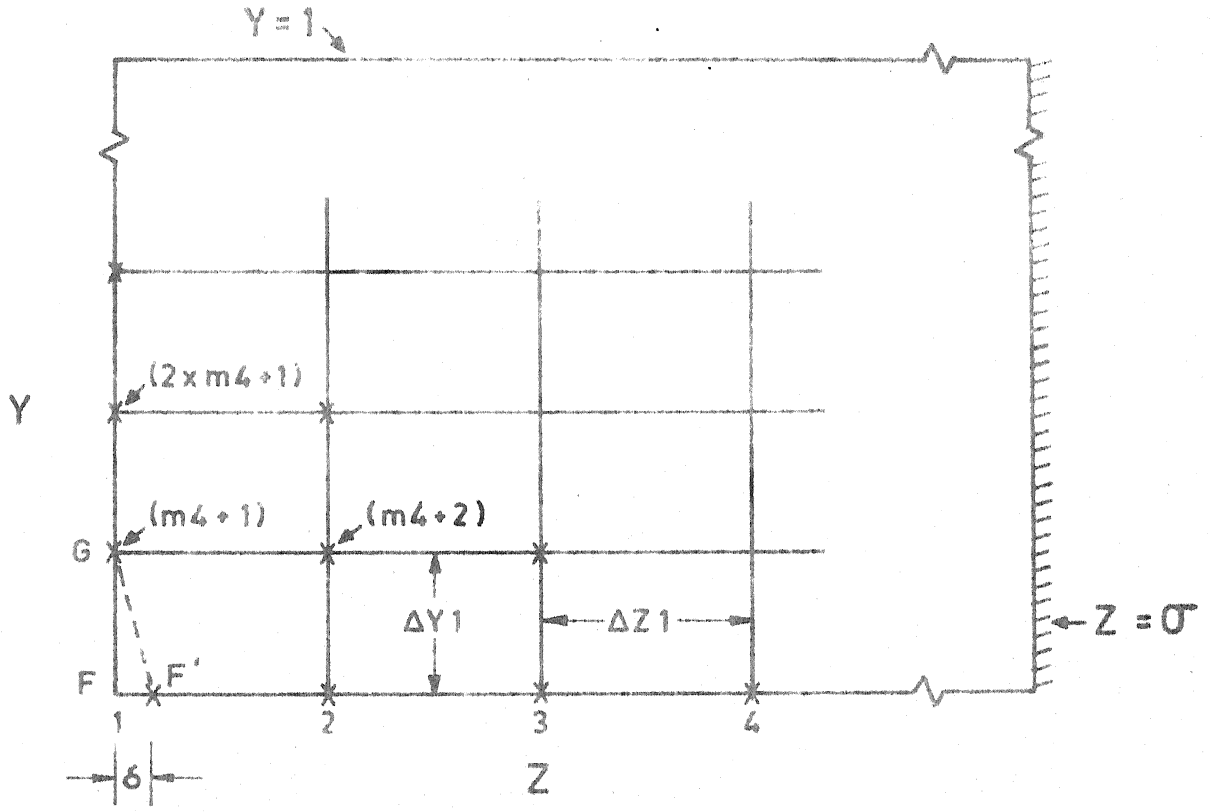

Fig. 3.3 Computational grid near the focus.

for the finite-difference procedure, F^1 would be the first point $(i,1,1)$. The discretised form of the axial momentum eqn. (2.16) at $(i,1,1)$ takes the form,

$$A_{1,1}U_{i,1,1}\frac{(U_{i+1,1,1}-U_{i,1,1})}{(\Delta X)} + A_{1,1}^{1/2}W_{i,1,1}\frac{(-3U_{i+1,1,1}+4U_{i+1,1,2}-U_{i+1,1,3})}{2(\Delta Z_1)}$$

$$= -A_{1,1}\frac{(P_{i+1}-P_i)}{(\Delta X)} + \frac{(6U_{i+1,1,1}-15U_{i+1,1,2}+12U_{i+1,1,3}-3U_{i+1,1,4})}{3(\Delta Z_1)^2}$$

$$+ \frac{(2U_{i+1,2,1}-2U_{i+1,1,1})}{(\Delta Y_1)^2}, \qquad (3.10)$$

when $\frac{\partial U}{\partial Z}$ and $\frac{\partial^2 U}{\partial Z^2}$ are expressed by the second order accurate forward differences [51], as the boundary condition $\frac{\partial U}{\partial Z}(X,Y,0) = 0$ does not hold at F^1 and hence use of central differences is not possible.

Had we considered F^1 on the line FG (Fig. 3.3), the discretised form of (2.16) at the new F^1 would have been

$$A_{1,1}U_{i,1,1}\frac{(U_{i+1,1,1}-U_{i,1,1})}{(\Delta X)} + A_{1,1}^{1/2}V_{i,1,1}\frac{(-3U_{i+1,1,1}+4U_{i+1,2,1}-U_{i+1,3,1})}{2(\Delta Y_1)}$$

$$= -A_{1,1} \frac{(P_{i+1} - P_i)}{(\Delta X)} + \frac{(2U_{i+1,1,2} - 2U_{i+1,1,1})}{(\Delta Z_1)^2}$$

$$+ \frac{(6U_{i+1,1,1} - 15U_{i+1,2,1} + 12U_{i+1,3,1} - 3U_{i+1,4,1})}{3(\Delta Y_1)^2},$$

since the boundary condition $\frac{\partial U}{\partial Y}(X,0,Z) = 0$ is not applicable at the new F^1. It is clear from the last term of the above equation that the band width of the coefficient matrix (to be explained later) of the resulting set of linear simultaneous equations would have been doubled in comparison to that using eqn. (3.10). The consequence of this increase is additional computer time and storage requirements.

The discretised continuity equation at F^1 is

$$A_{1,1}^{1/2} \frac{V_{i+1,2,1}}{(\Delta Y_1)} + A_{1,1}^{1/2} \frac{W_{i+1,1,2}}{(\Delta Z_1)} + A_{1,1} \frac{(U_{i+1,1,1} - U_{i,1,1})}{(\Delta X)} = 0. \qquad (3.11)$$

It is to be noted that no correction for ΔZ_1 has been applied either to eqn. (3.10) or to eqn. (3.11) and $W_{i,1,1}$ is taken to be zero as δ is negligibly small.

Along lines where grid size changes take place, eqn. (3.2) takes the following form [see Ref. 50, Appendix D].

(a) Along the line k = m1 (all j except j = n1 and n2) :

$$A_{j,m1}^{1/2} V_{i,j,m1} \frac{(U_{i+1,j+1,m1} - U_{i+1,j-1,m1})}{2(\Delta Y)}$$

$$-A^{1/2}_{j,m1}\ W_{i,j,m1}\ \frac{(-U_{i+1,j,m3}+(1-\theta_1^2)U_{i+1,j,m1}+\theta_1^2 U_{i+1,j,m2})}{(1+\theta_1)(\Delta Z2)}$$

$$+\ A_{j,m1}\ U_{i,j,m1}\ \frac{(U_{i+1,j,m1}\ -\ U_{i,j,m1})}{(\Delta X)}\ =\ -A_{j,m1}\ \frac{(P_{i+1}-P_i)}{(\Delta X)}$$

$$+\ \frac{(U_{i+1,j+1,m1}\ -\ 2U_{i+1,j,m1}\ +\ U_{i+1,j-1,m1})}{(\Delta Y)^2}$$

$$+\ \frac{2\theta_1(U_{i+1,j,m3}\ -\ (1+\theta_1)\ U_{i+1,j,m1}\ +\ \theta_1 U_{i+1,j,m2})}{(1+\theta_1)(\Delta Z2)^2}\ , \qquad (3\cdot12)$$

where $\theta_1 = \dfrac{\Delta Z2}{\Delta Z1} \leq 1$.

(b) Along the line j = n1 (all k except k = m1) :

$$A^{1/2}_{n1,k}\ V_{i,n1,k}\ \frac{(\theta_2^2 U_{i+1,n4,k}\ +\ (1-\theta_2^2)U_{i+1,n1,k}\ -\ U_{i+1,n3,k})}{(1+\theta_2)(\Delta Y1)}$$

$$+\ A^{1/2}_{n1,k}\ W_{i,n1,k}\ \frac{(U_{i+1,n1,k+1}\ -\ U_{i+1,n1,k-1})}{2(\Delta Z)}$$

$$+\ A_{n1,k}\ U_{i,n1,k}\ \frac{(U_{i+1,n1,k}\ -\ U_{i,n1,k})}{(\Delta X)}$$

$$=\ -A_{n1,k}\ \frac{(P_{i+1}-P_i)}{(\Delta X)}\ +\ \frac{2\theta_2(\theta_2 U_{i+1,n4,k}-(1+\theta_2)U_{i+1,n1,k}+U_{i+1,n3,k})}{(1+\theta_2)(\Delta Y1)^2}$$

$$+\ \frac{(U_{i+1,n1,k+1}\ -\ 2U_{i+1,n1,k}\ +\ U_{i+1,n1,k-1})}{(\Delta Z)^2} \qquad (3\cdot13)$$

where $\theta_2 = \dfrac{\Delta Y1}{\Delta Y2} \leq 1$.

(c) Along the line j = n2 (all k except k = m1) :

$$A^{1/2}_{n2,k}\, V_{i,n2,k}\, \frac{(U_{i+1,n6,k} - (1-\theta_3^2)U_{i+1,n2,k} - \theta_3^2 U_{i+1,n5,k})}{(1+\theta_3)(\Delta Y3)}$$

$$+ A^{1/2}_{n2,k}\, W_{i,n2,k}\, \frac{(U_{i+1,n2,k+1} - U_{i+1,n2,k-1})}{2(\Delta Z)}$$

$$+ A_{n2,k}\, U_{i,n2,k}\, \frac{(U_{i+1,n2,k} - U_{i,n2,k})}{(\Delta X)}$$

$$= -A_{n2,k}\, \frac{(P_{i+1} - P_i)}{(\Delta X)}$$

$$+ \frac{2\theta_3(U_{i+1,n6,k} - (1+\theta_3)U_{i+1,n2,k} + \theta_3 U_{i+1,n5,k})}{(1+\theta_3)(\Delta Y3)^2}$$

$$+ \frac{(U_{i+1,n2,k+1} - 2U_{i+1,n2,k} + U_{i+1,n2,k-1})}{(\Delta Z)^2} \qquad (3.14)$$

where $\theta_3 = \dfrac{\Delta Y3}{\Delta Y2} \leq 1$.

(d) At the point j = n1 and k = m1 :

$$A^{1/2}_{n1,m1} V_{i,n1,m1}\, \frac{[\theta_2^2 U_{i+1,n4,m1} + (1-\theta_2^2)U_{i+1,n1,m1} - U_{i+1,n3,m1}]}{(1+\theta_2)(\Delta Y1)}$$

$$+ A^{1/2}_{n1,m1} W_{i,n1,m1} \frac{[U_{i+1,n1,m3} - (1-\theta_1^2)U_{i+1,n1,m1} - \theta_1^2 U_{i+1,n1,m2}]}{(1+\theta_1)(\Delta Z2)}$$

$$+ A_{n1,m1} U_{i+1,n1,m1} \frac{[U_{i+1,n1,m1} - U_{i,n1,m1}]}{(\Delta X)}$$

$$= -A_{n1,m1} \frac{[P_{i+1} - P_i]}{(\Delta X)}$$

$$+ \frac{2\theta_2 [\theta_2 U_{i+1,n4,m1} - (1+\theta_2)U_{i+1,n1,m1} + U_{i+1,n3,m1}]}{(1+\theta_2)(\Delta Y1)^2}$$

$$+ \frac{2\theta_1 [U_{i+1,n1,m3} - (1+\theta_1)U_{i+1,n1,m1} + \theta_1 U_{i+1,n1,m2}]}{(1+\theta_1)(\Delta Z2)^2}$$

(3.15)

(e) At the point j = n2 and k = m1 :

$$A^{1/2}_{n2,m1} V_{i,n2,m1} \frac{[U_{i+1,n6,m1} - (1-\theta_3^2)U_{i+1,n2,m1} - \theta_3^2 U_{i+1,n5,m1}]}{(1+\theta_3)(\Delta Y3)}$$

$$+ A^{1/2}_{n2,m1} W_{i,n2,m1} \frac{[U_{i+1,n2,m3} - (1-\theta_1^2)U_{i+1,n2,m1} - \theta_1^2 U_{i+1,n2,m2}]}{(1+\theta_1)(\Delta Z2)}$$

$$+ A_{n2,m1} U_{i,n2,m1} \frac{[U_{i+1,n2,m1} - U_{i,n2,m1}]}{(\Delta X)} = -A_{n2,m1} \frac{[P_{i+1} - P_i]}{(\Delta X)}$$

$$\frac{2\theta_3 \left[U_{i+1,n6,m1} - (1+\theta_3)\, U_{i+1,n2,m1} + \theta_3\, U_{i+1,n5,m1}\right]}{(1+\theta_3)\,(\Delta Y3)^2}$$

$$+\ \frac{2\theta_1 \left[U_{i+1,n2,m3} - (1+\theta_1) U_{i+1,n2,m1} + \theta_1\, U_{i+1,n2,m2}\right]}{(1+\theta_1)\,(\Delta Z2)^2} \qquad (3.16)$$

Eqns. (3.1) to (3.16) constitute a set of (3xm4xn8+m4-n8+1) linear simultaneous equations in that many unknowns, viz.

$U_{i+1,j,k}$ (for j = 1(1) n8+1, k = 1(1)m4),

$V_{i+1,j,k}$ (for j = 2(1) n8, k = 1(1)m4),

$W_{i+1,j,k}$ (for j = 1(1) n8+1, k = 2(1)m4),

$W_{i+1,1,1}$,

and

P_{i+1} .

This rather large set of equations can be reduced to a set of only (m4(n8+1)+1) equations in that many unknowns, viz.

$U_{i+1,j,k}$ (for j = 1(1) n8+1 , k = 1(1) m4),

and

P_{i+1} .

by the use of axial momentum equation along with the integral form of continuity equation. Once U's and P are known at the (i+1) location, V's and W's can be found from the continuity eqn. (3.1) and the relation (3.3).

The continuity eqn. (2.15) integrated over the duct cross-section by the application of the trapezoidal rule is

$$\left[\frac{A_{1,1}U_{i+1,1,1}}{4} + \sum_{k=2}^{m2}\frac{A_{1,k}U_{i+1,1,k}}{2} + \frac{A_{1,m1}U_{i+1,1,m1}(1+\Phi_1)}{4}\right.$$

$$+ \sum_{k=m3}^{m4}\frac{A_{1,k}U_{i+1,1,k}\Phi_1}{2} + \sum_{j=2}^{n3}\frac{A_{j,1}U_{i+1,j,1}}{2}$$

$$+ \frac{A_{n1,1}U_{i+1,n1,1}(1+\Phi_2)}{4} + \sum_{j=n4}^{n5}\frac{A_{j,1}U_{i+1,j,1}\Phi_2}{2}$$

$$+ \frac{A_{n2,1}U_{i+1,n2,1}(\Phi_2+\Phi_4)}{4} + \sum_{j=n6}^{n8}\frac{A_{j,1}U_{i+1,j,1}\Phi_4}{2}$$

$$+ \frac{A_{n7,1}U_{i+1,n7,1}\Phi_4}{4} + \sum_{j=2}^{n3}\sum_{k=2}^{m2}A_{j,k}U_{i+1,j,k}$$

$$+ \sum_{j=2}^{n3}\frac{A_{j,m1}U_{i+1,j,m1}(1+\Phi_1)}{2} + \sum_{j=2}^{n3}\sum_{k=m3}^{m4}A_{j,k}U_{i+1,j,k}\Phi_1$$

$$+ \sum_{k=2}^{m2}\frac{A_{n1,k}U_{i+1,n1,k}(1+\Phi_2)}{2} + \frac{A_{n1,m1}U_{i+1,n1,m1}(1+\Phi_1+\Phi_2+\Phi_3)}{4}$$

$$+\sum_{k=m3}^{m4}\frac{A_{n1,k}U_{i+1,n1,k}(\Phi_1+\Phi_3)}{2}+\sum_{j=n4}^{n5}\sum_{k=2}^{m2}A_{j,k}U_{i+1,j,k}\,\Phi_2$$

$$+\sum_{j=n4}^{n5}\frac{A_{j,m1}U_{i+1,j,m1}(\Phi_2+\Phi_3)}{2}+\sum_{j=n4}^{n5}\sum_{k=m3}^{m4}A_{j,k}U_{i+1,j,k}\,\Phi_3$$

$$+\sum_{k=2}^{m2}\frac{A_{n2,k}U_{i+1,n2,k}(\Phi_2+\Phi_4)}{2}+\frac{A_{n2,m1}U_{i+1,n2,m1}(\Phi_2+\Phi_3+\Phi_4+\Phi_5)}{4}$$

$$+\sum_{k=m3}^{m4}\frac{A_{n2,k}U_{i+1,n2,k}(\Phi_3+\Phi_5)}{2}+\sum_{j=n6}^{n8}\sum_{k=2}^{m2}A_{j,k}U_{i+1,j,k}\,\Phi_4$$

$$+\sum_{j=n6}^{n8}\frac{A_{j,m1}U_{i+1,j,m1}(\Phi_4+\Phi_5)}{2}+\sum_{j=n6}^{n8}\sum_{k=m3}^{m4}A_{j,k}U_{i+1,j,k}\,\Phi_5$$

$$+\sum_{k=2}^{m2}\frac{A_{n7,k}U_{i+1,n7,k}\,\Phi_4}{2}+\frac{A_{n7,m1}U_{i+1,n7,m1}(\Phi_4+\Phi_5)}{4}$$

$$+\sum_{k=m3}^{m4}\frac{A_{n7,k}U_{i+1,n7,k}\,\Phi_5}{2}\Big]\;(\Delta Z1)(\Delta Y1)=\int_0^1\int_0^\sigma U\cdot A\cdot dZ\;dY$$

$$=\frac{\sinh(2\eta_w)}{2\pi}\,, \qquad (3\cdot17)$$

where

$$\Phi_1=\frac{\Delta Z2}{\Delta Z1}\,, \qquad \Phi_2=\frac{\Delta Y2}{\Delta Y1}$$

$$\Phi_3 = \Phi_1 \cdot \Phi_2 \qquad , \qquad \Phi_4 = \frac{\Delta Y_3}{\Delta Y_1}$$

and

$$\Phi_5 = \Phi_1 \cdot \Phi_4 \cdot$$

Chapter 4

COMPUTATIONAL DETAILS

For the solution of finite-difference equations given in Chapter 3, the following steps are followed

1. $U_{i+1,j,k}$ and P_{i+1} are calculated from eqn. (3.2) and eqn. (3.17) solving a set of [m4(n8+1)+1] simultaneous equations (solution procedure to be explained later).

2. $V_{i+1,j,k}$ are calculated from the continuity eqn.(3.1) in a step-wise manner, starting at j = n8, k = m4 and moving in the negative Z-direction upto k = 1, utilising the above $U_{i+1,j,k}$ and the relation (3.3). Simultaneously $W_{i+1,j,k}$ are calculated using the relation (3.3).

3. Step 2 is repeated in the negative Y-direction to j = 1.

4. $W_{i+1,n7,k}$ are calculated starting from k = m4 to k = 1, utilising the boundary condition $\frac{\partial W}{\partial Y}(X,1,Z) = 0$ and antisymmetric nature of the function $B_{j,k}$ (in the relation 3.3). This completes the solution at the location (i+1).

5. Steps 1 to 4 are repeated till the flow is found to be fully developed. Mathematically this would occur at $X \to \infty$. Practically, computation is terminated when the centre-line velocity attains a

value equal to 99% of the fully developed centre-line velocity which is 2.0 in dimensionless terms.

4.1 Solution Procedure

The system of (n+1) simultaneous equations resulting from eqns. (3.17) and (3.2) can be written as

$$[S] \begin{Bmatrix} U \\ P \end{Bmatrix} = \begin{Bmatrix} Q \\ R \end{Bmatrix} \qquad (4.1)$$

where $n = m4(m8+1)$,

$S = \begin{bmatrix} E & O \\ G & H \end{bmatrix}$ is the coefficient matrix of order (n+1),

$E = (E_1, E_2, E_3, \ldots, E_n)$ is the row vector arising from the coefficients of axial velocity component U at location (i+1) in eqn. (3.17),

$H = \{H_1, H_2, H_3, \ldots, H_n\}$ is the column vector arising from the pressure at location (i+1) in the momentum eqn. (3.2),

$[G]$ is an unsymmetric banded matrix of order n and band-width (2xm4+1) arising from coefficients of axial velocity component U at location (i+1) in eqn. (3.2),

P is the unknown pressure at location (i+1),

Q is the known right hand side of eqn. (3.17),

and

$R = \{R_1, R_2, R_3, \ldots, R_n\}$ is the known right hand side column vector arising from the terms at location (i) in eqn. (3.2).

Solution of the system (4.1) by the inversion method is highly expensive even on the present-day computers since the number of steps required is of order $(n+1)^3$ and the storage requirement isof order $(n+1)^2$. A futile attempt was made to use the sparse-solver routines MA28AD, MA28BD and MA28CD of the Harwell library in order to utilise the sparsity of the matrix [S]. The counterparts of these routines in the NAG library also did not work due to some untraceable problem in the particular NAG library routine on our system. The algorithm suggested by Gupta and Tanji [52] also did not work due to the first row of [S] consisting of the vector (E) being too full. Gupta and Tanji's algorithm required that no row should be more than half filled in single precision mode and more than one third filled in double precision mode.

An algorithm was therefore developed to solve the system (4.1) based on the partitioning of [S] into the row vector (E), column vector {H}, and the unsymmetric banded matrix [G]. The banded matrix [G] is converted to an upper triangular matrix by Gauss elimination [53] with column pivoting. The same operations are simultaneously carried out for {H} and {R} also. Then the operated matrix takes the form

$$\begin{bmatrix} E & O \\ G^* & H^* \end{bmatrix} \begin{Bmatrix} U \\ P \end{Bmatrix} = \begin{Bmatrix} Q \\ R^* \end{Bmatrix}, \qquad (4.2)$$

where $[G^*]$ is the upper triangular matrix with diagonal elements unity and $\{H^*\}$ and $\{R^*\}$ are the operated vectors $\{H\}$ and $\{R\}$ respectively. If we define

$$D_n = H_n^*,$$

and

$$D_i = H_i^* - \sum_{j=1}^{n-i} G_{i,i+j}^* D_{i+j}, \quad (\text{for } i = n-1, n-2, \ldots, 2, 1)$$

and

$$C_n = R_n^*,$$

and

$$C_i = R_i^* - \sum_{j=1}^{n-i} G_{i,i+j}^* C_{i+j}, \quad (\text{for } i = n-1, n-2, \ldots, 2, 1)$$

then

$$U_n = C_n - P \cdot D_n,$$

and (4.3)

$$U_i = C_i - P \cdot D_i \qquad (\text{for } i = n-1, n-2, \ldots, 2, 1).$$

The first equation of the system (4.1) is

$$\sum_{i=1}^{n} E_i U_i = Q. \qquad (4.4)$$

Substitution of eqn. (4.3) into eqn. (4.4) leads to

$$P = \frac{\left(\sum_{i=1}^{n} E_i C_i\right) - Q}{\sum_{i=1}^{n} E_i D_i}, \qquad (4.5)$$

and back substitution in the system (4.2) gives the axial velocity vector $\{U\}$.

4.2 Correction to the uniform inlet velocity u_o

With the assumption of uniform inlet velocity $U_{o,j,k} = 1$, the integral form of the continuity eqn. (3.17) is not fully satisfied since the left hand side of (3.17) contains errors $O(\Delta Z)$ and $O(\Delta Y)$ injected through the application of the trapezoidal rule. Hence a correction to the uniform inlet velocity $U_{o,j,k}$ is applied such that eqn. (3.17) gets satisfied at $X = 0$ itself. This corrected inlet velocity $U_{o,j,k}$ is given in Table 4.1 for various aspect ratios λ. In fact, it was observed that the pressure P increased for about 7 initial marching steps ($i = 1, 2, \ldots, 7$) when this correction was not applied.

4.3 Problem with the transverse velocity components near the focus

Very high wiggles were observed in the transverse velocity components V and W in the immediate vicinity of the focal point of the ellipse. These wiggles were found to grow rather than damp out in the marching X-direction. This was found to be more pronounced at higher aspect ratios and at finer grid sizes ΔZ and ΔY due to very finely spaced points near the focus. It is clearly due to the singularity of the transformation at the focus. To avoid these wiggles, the values of W near line OF (Fig. 4.1) were extrapolated from

Lambda	U_o	delta-Z	delta-Y
1.001	1.2166	0.1210	0.1
1.1	1.1699	0.0963	0.1
1.2	1.1326	0.0763	0.1
1.4	1.1014	0.0570	0.1
2.0	1.0726	0.0350	0.1
4.0	1.0571	0.0163	0.1

Table 4.1 Corrected initial velocity U_o and step sizes delta-Z and delta-Y

Lambda=1.1		Lambda=1.2		Lambda=1.4		Lambda=2.0		Lambda=4.0	
delta-X	No.of steps	delta-X	No.of steps	delta-X	No.of steps	delta-X	No.of steps	delta-X	No.of steps
1.0E-6	100	5.0E-7	100	2.0E-7	100	1.0E-6	100	1.0E-6	100
2.0E-6	50	1.0E-6	100	5.0E-7	100	1.0E-5	90	2.0E-6	50
5.0E-6	60	2.0E-6	100	1.0E-6	100	2.0E-5	100	5.0E-6	60
1.0E-5	50	5.0E-6	130	2.0E-6	65	5.0E-5	100	1.0E-5	50
2.0E-5	40	1.0E-5	100	5.0E-6	140	1.0E-4	220	2.0E-5	100
5.0E-5	124	2.0E-5	100	1.0E-5	100	2.0E-4	400	5.0E-5	100
1.0E-4	120	5.0E-5	120	2.0E-5	100	-		1.0E-4	100
2.0E-4	100	1.0E-4	100	5.0E-5	120	-		-	
5.0E-4	60	2.0E-4	200	1.0E-4	999	-		-	
1.0E-3	254	5.0E-4	80	1.0E-4	30	-		-	
-		1.0E-3	88	-		-		-	

Table 4.2 Step size delta-X and Number of steps

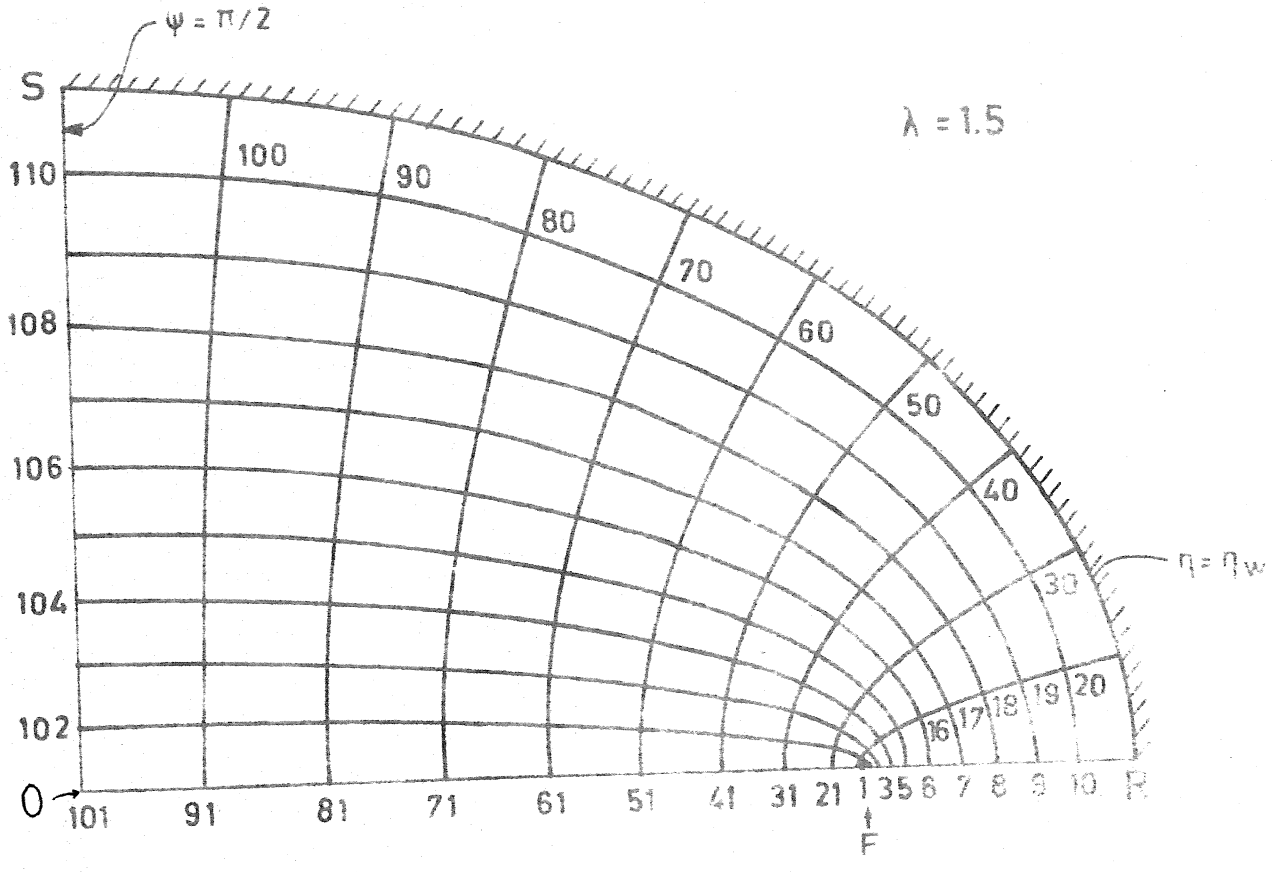

Fig. 4.1 Finite-difference grid (to scale)

those away from the focus such that $W(X,Y,0) = 0$. After some numerical experimentation, it was found that a fifth order polynomial (exact fit) provided results accurate to fourth decimal place for all aspect ratios.

It should be noted that this extrapolation has been carried out only over 25% of the real flow domain.

4.4 Selection of a value for δ

A numerical experiment was conducted for the aspect ratio $\lambda = 4$ with various values of $\delta = FF^1$ (Fig. 3.3) viz. 10^{-3}, 10^{-5}, 10^{-7}, 10^{-9} and 10^{-12}. Variations in the values of pressure and velocity components were observed respectively in the fifth and sixth places of decimal between $\delta = 10^{-3}$ and 10^{-5}. For lower δ values the variations were observed only in the tenth place of decimal. For the results presented here, δ was therefore taken to be 10^{-3} for all aspect ratios.

4.5 Step sizes

For computational efficiency but without sacrificing the accuracy the step size ΔX was changed systematically along the X-direction for various aspect ratios (Table 4.2). It is to be noted that the dimensionless axial distance is defined as

$$X = \frac{\nu x}{(\pi c/2)^2 u_o} \quad \text{where } c^2 = a^2 - b^2.$$

For higher aspect ratios such as $\lambda = 2$ and 4 the denominator

$(\pi c/2)^2 u_o$ becomes large. Hence ΔX must be inversely proportional to the square of the focal length c.

Computer codes (Appendix C) were developed for

a) uniform ΔY and ΔZ values, and

b) non-uniform ΔY and ΔZ values (specifically, three step sizes in the Y-direction and two in the Z-direction).

However since we did not have enough time to experiment with non-uniform grid code, the results presented here were computed using the uniform grid code with ΔY and ΔZ values as given in Table 4.1. Computations were carried out in double precision mode (15 significant digits) on the DEC-1090 system at IIT Kanpur.

Chapter 5

RESULTS AND DISCUSSION

Results for the computed axial velocity U(X,Y,Z), centre-line velocity U(X,1,0), pressure P(X) and the pressure defect K(X) are presented for various values of the aspect ratio. In order to limit the number of plots to a reasonable number, the axial velocity U(X,Y,Z) is shown only along the major and minor axes. Comparison is made with the already available results for elliptical ducts [6, 24] and in the limiting case for a circular duct [50].

5.1 Axial Velocity U(X,Y,Z)

As the transformation from the Cartesian to the elliptic-cylinder system does not hold for $\lambda = 1$, an elliptical duct of aspect ratio 1.001 was considered so as to check the computer programme against well known results for the developing flow in a circular pipe [50]. For this aspect ratio the focus is very near the origin (c/b being only 0.045). Fig. 5.1(a) shows the developing axial velocity at the major or minor axis for $\lambda = 1.001$ (solid lines) and the same for a circular pipe by Hornbeck's method [50] (dashed lines). The velocity profiles at the major and minor axes exactly coincide which itself is a check of the present analysis, as the velocity profile for a circular pipe is the same at any radial line. The small

differences could be attributed to the aspect ratio being not exactly one.

Having gained this confidence, higher values of the aspect ratio were tried. Figs. 5.1(b) to 5.1(j) show the developing flow axial velocity profiles at the major and minor axes for aspect ratio λ = 1.1, 1.2, 1.4, 2.0 and 4.0. Both the elliptic-cylinder coordinates and the Cartesian coordinates are indicated. Numerical values are listed in Tables 5.1(a) to 5.1(j). The small kinks observed in the velocity profiles along the major axis in the region surrounding the focus, specially at higher aspect ratios, are due to the fact that the elliptic-cylinder coordinate system clusters more grid points near the focus, specially at higher aspect ratios. From the Cartesian coordinates shown, it is clear that a uniform ΔY in the elliptic-cylinder coordinate system corresponds to a highly non-uniform Δz in the Cartesian coordinate system. These kinks disappear when U along the major axis is plotted against the Cartesian z, as is evident from Figs. 5.1(k) to 5.1(r).

These figures show that the difference in the velocity profiles between the present analysis and Bhatti's analysis [50] increases, in the viscous boundary-layer region, with the aspect ratio at the small X values. By assumption Bhatti's velocity profile in the boundary-layer region is almost linear at the small X values for all λ. Bhatti also assumed a value for the boundary-layer thickness in the developing region, and

it turns out to be smaller than that found in the present analysis. The above differences increase with λ but decrease as the flow develops. The later is expected since Bhatti's velocity profile in the developing region is based on the fully developed velocity profile.

5.2 Centre-line Velocity

The centre-line velocity development for elliptical ducts of higher aspect ratios is shown in Fig. 5.2(a) (solid lines) alongwith Bhatti's results (dashed lines). As mentioned above the boundary-layer thickness in Bhatti's analysis is small. Thus only a smaller portion of the fluid is in boundary-layer shear according to Bhatti's analysis. Consequently the centre-line velocity is under-predicted. The difference between these two analyses is therefore maximum at the smaller X values for all aspect ratios. As X increases, this difference decreases for all aspect ratios. Infact, for $\lambda = 4$, Bhatti's analysis underpredicts the centre-line velocity at small X but overpredicts it at larger X.

Fig. 5.2(b) shows the centre-line velocity development for nearly circular duct with $\lambda = 1.001$ for the present analysis, Bhatti's analysis [24] and for the circular pipe [50]. The present results compare better with those using Hornbeck's analysis [50] than Bhatti's results. While the maximum difference between the present and circular pipe results [50]

is only 4.2% that between Bhatti's and circular pipe results [50] is as much as 10.5%. It should be noted that Bhatti's results for circular pipe do not compare well with the experimental data, especially at the small X values [24, Fig. 3]. His velocity underpredicts the experimental data just as it underpredicts the theoretical results.

5.3 Entrance Length

The hydrodynamic entrance lengths for various aspect ratios are given in Table 5.2 in terms of X and X* (X* being $X.(\pi c/2b)^2$). Computations were terminated when the centre-line velocity reaches 99% of the fully developed centre-line velocity, which is 2.0 in dimensionless terms. In the computations 'b' is always kept unity while 'a' is varied to achieve different values for the aspect ratio. As per discussion in Sec. 5.2, Bhatti's analysis overpredicts the entrance-length for small λ values and underpredicts the same for high λ values.

5.4 Axial Pressure Drop and Pressure Defect

The axial pressure drop P(X) and the pressure defect K(X) are shown in figs. 5.3(a) to 5.3(e) for various values of λ. Values of P are also listed in Tables 5.1(a) to 5.1(j). The pressure defect is the difference between the actual pressure drop and the ideal pressure drop resulting from the assumption of fully developed flow at X = 0. This ideal

pressure drop can be easily shown to be

$$dP/dX = \pi^2(\lambda^2 - \lambda^{-2})$$

since the fully developed velocity profile is

$$U = 2(1 - (z/a)^2 - (y/b)^2).$$

The difference between the present analysis and Bhatti's analysis is high in the initial development region for all aspect ratios. As expected from the above discussion, this difference decreases as the flow develops. However as X increases, it vanishes for moderate aspect ratios (λ = 1.1, 1.2 and 1.4) but reduces to a non-zero value for higher aspect ratios (λ = 2.0 and 4.0).

When the flow becomes fully developed as $X \to \infty$, K attains a fully developed value, K_∞, which for various aspect ratios is given in Table 5.2. Bhatti's analysis predicts K_∞ to be 7/12 while the analysis of Lundgren, et al. [6] predicts it to be 2/3. However, it is known that the latter value is over predicted. The present analysis shows that it depends weakly on the aspect ratio.

From the above comparison, it appears that Bhatti's analysis does not provide good results in the initial developing region due perhaps to somewhat arbitrary assumptions in his analysis regarding the growth of boundary layer region and the velocity profile in this region. However, a firm judgement must await comparison with experimental data for developing flow in an elliptical duct.

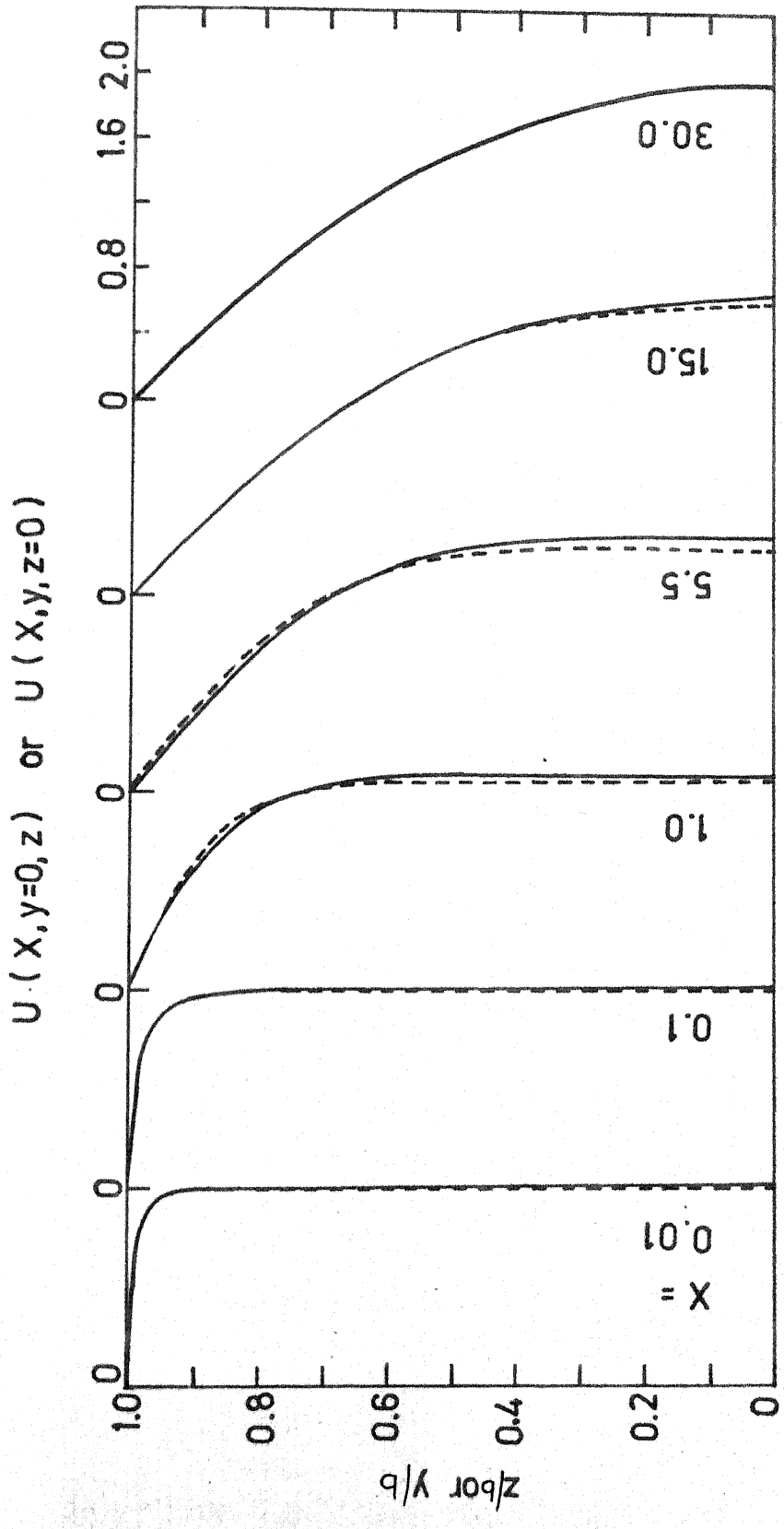

Fig. 5.1 (a) Development of axial velocity. $\lambda = 1.001$
——— Present Analysis ; - - - - - Circular pipe

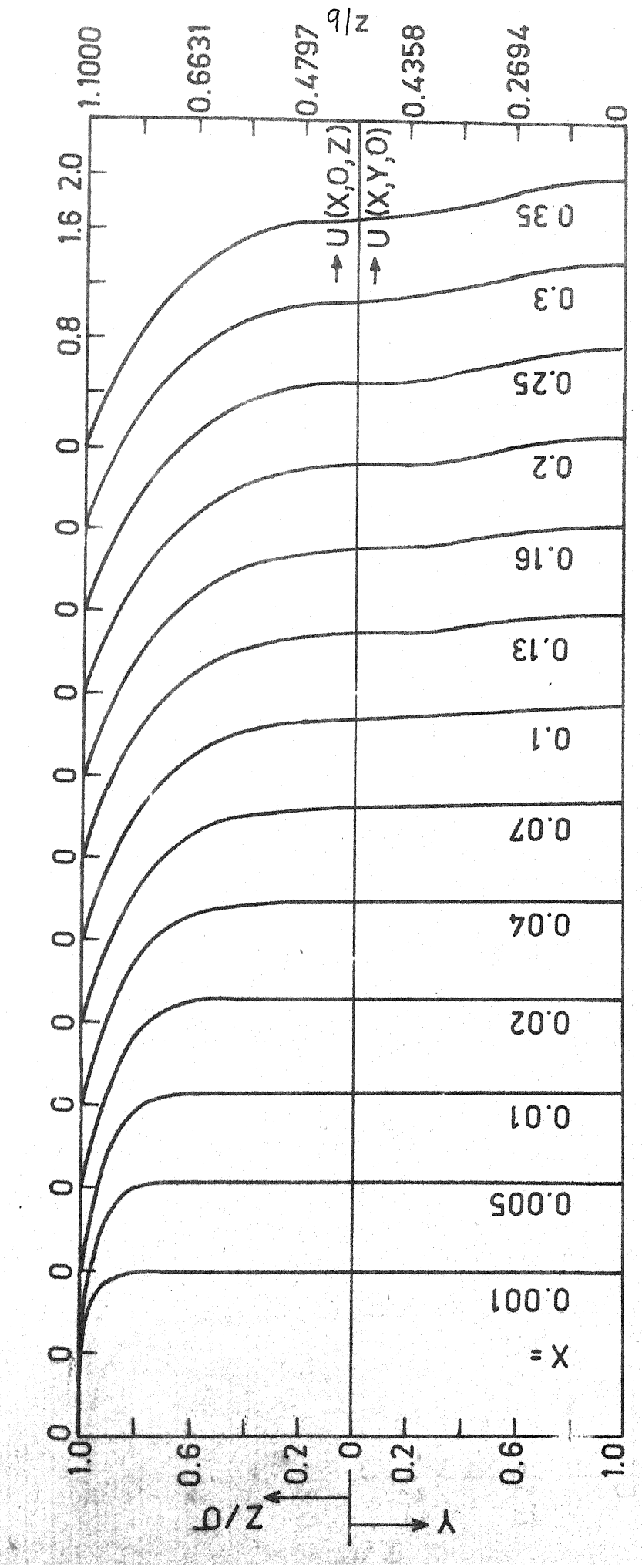

Fig. 5.1 (b) Development of axial velocity at the major axis. $\lambda = 1.1$

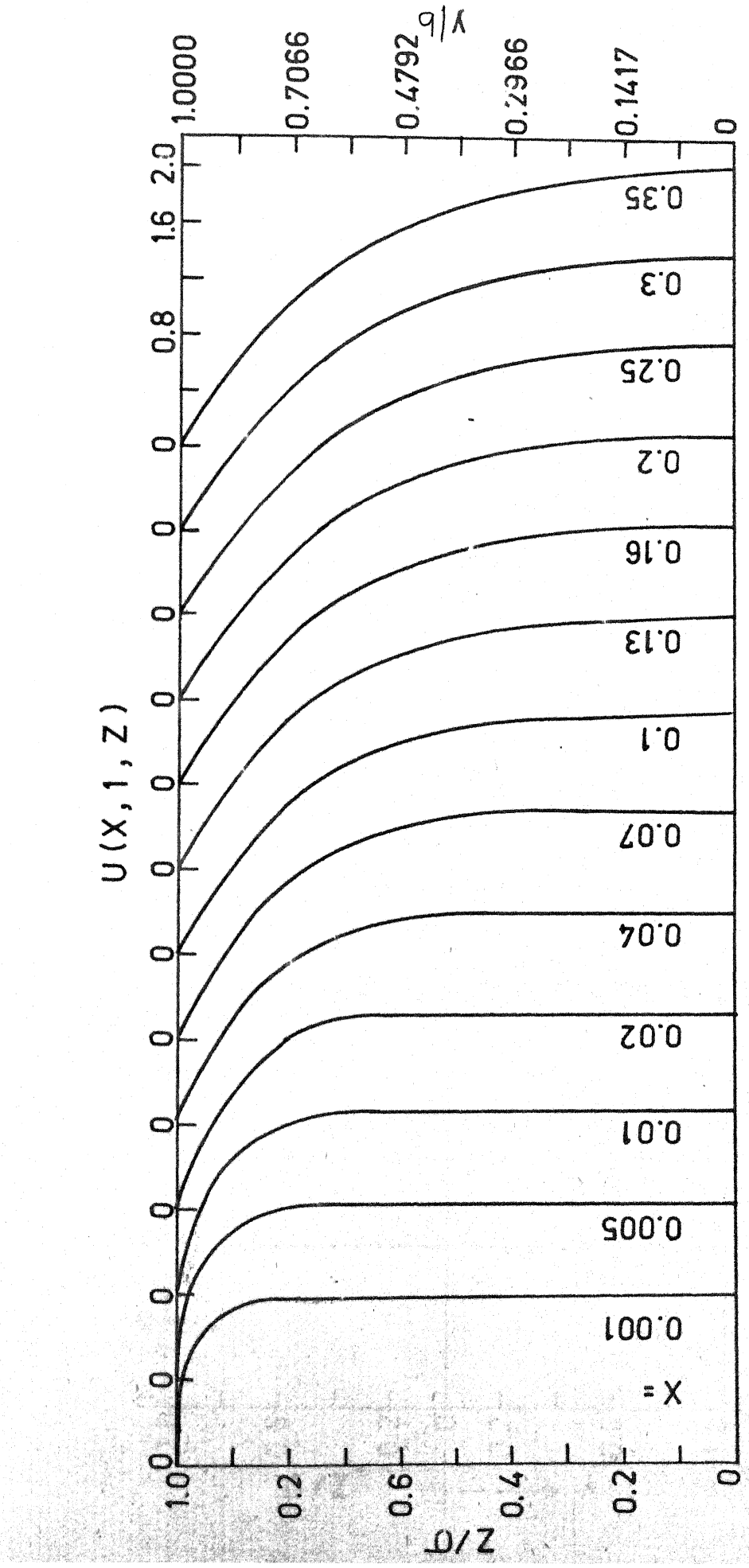

Fig. 5.1 (c) Development of axial velocity at the minor-axis. $\lambda = 1.1$

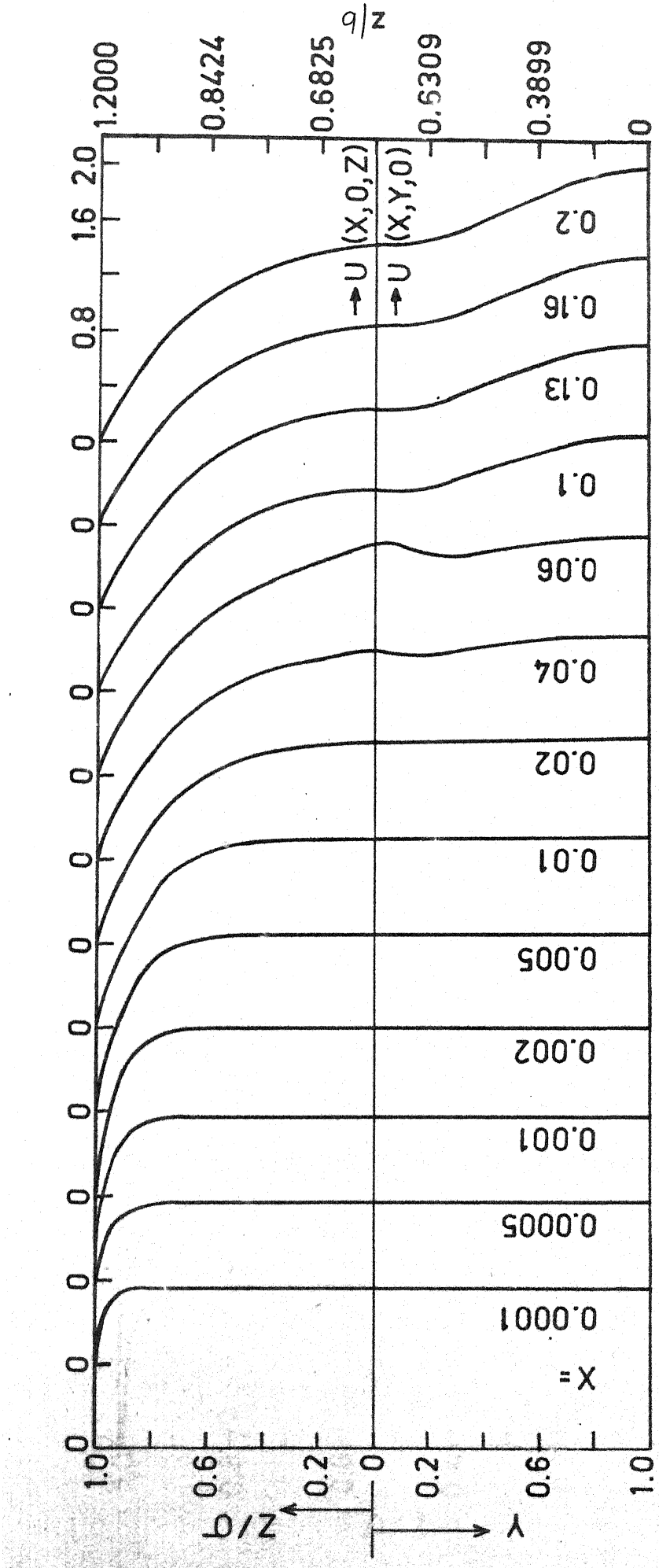

Fig. 5.1 (d) Development of axial velocity at the major axis. $\lambda = 1.2$

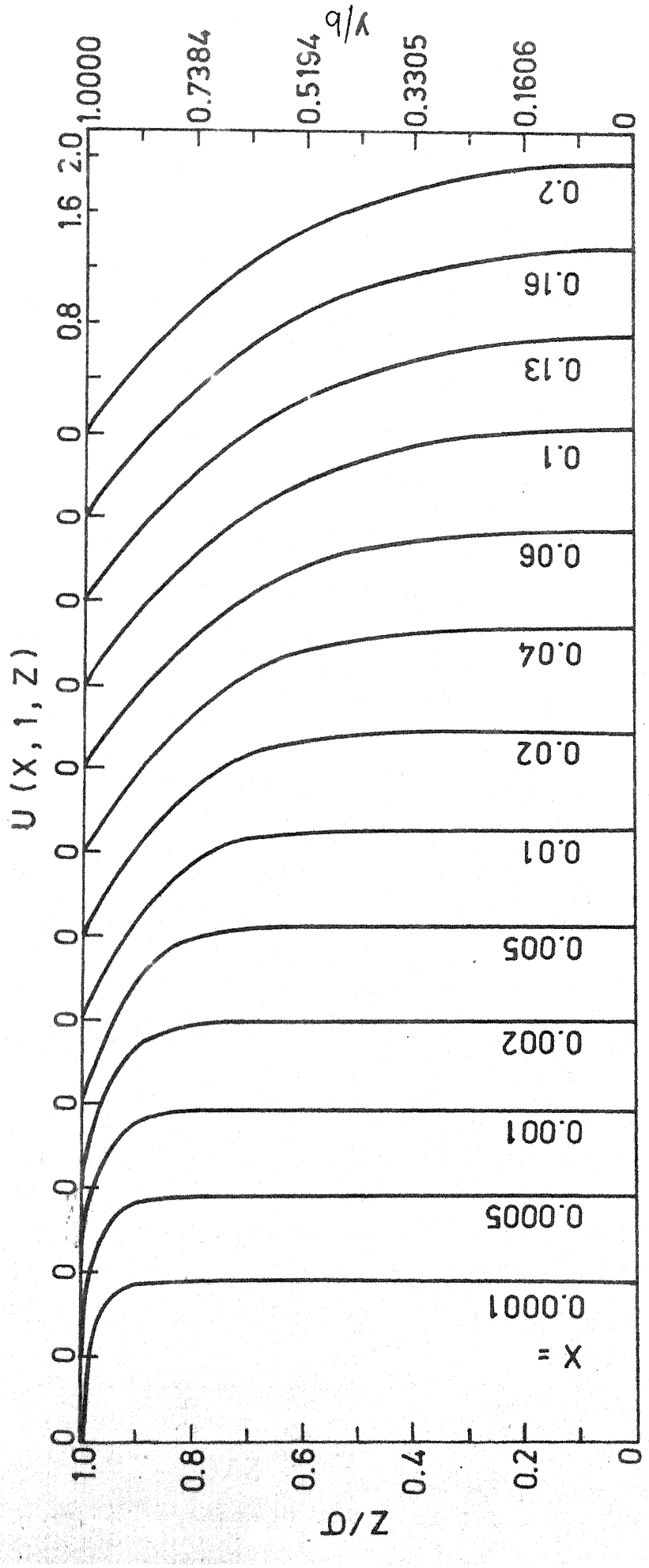

Fig. 5.1 (e) Development of axial velocity at the minor-axis. $\lambda = 1.2$

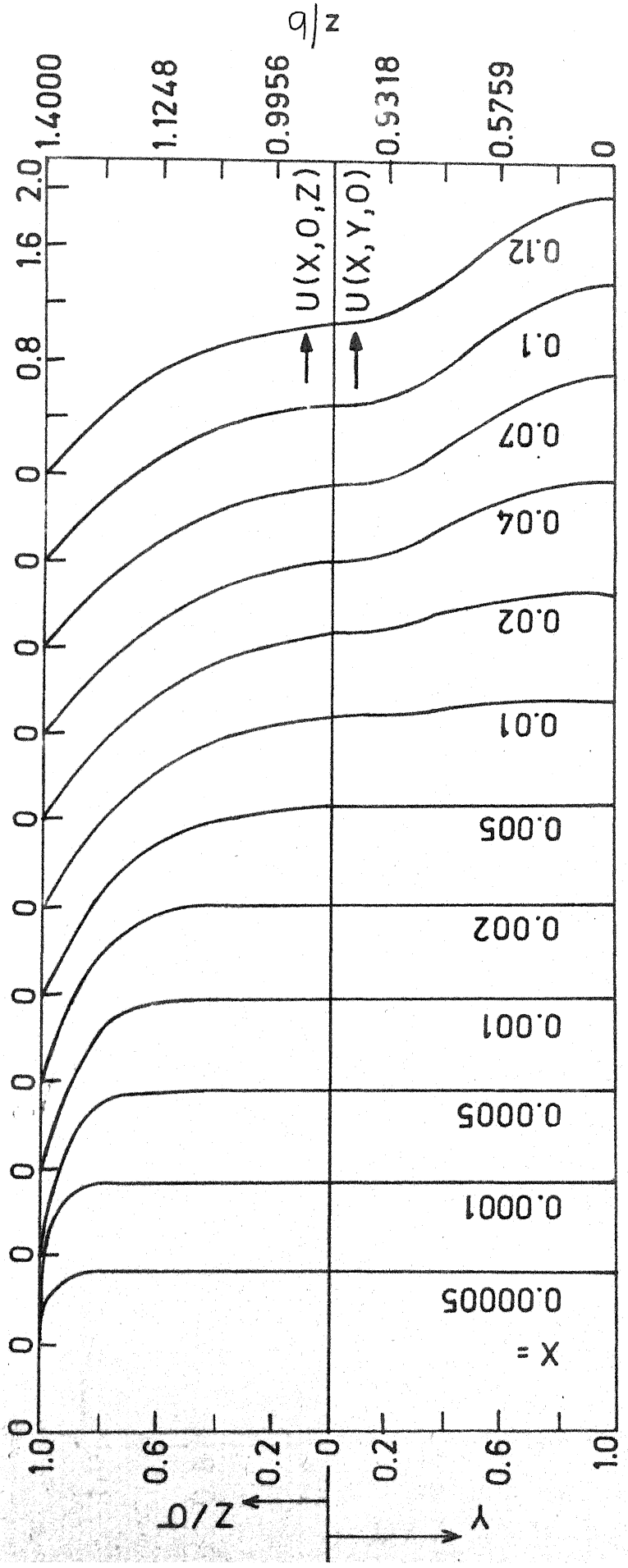

Fig. 5.1 (f) Development of axial velocity at the major - axis $\lambda = 1.4$

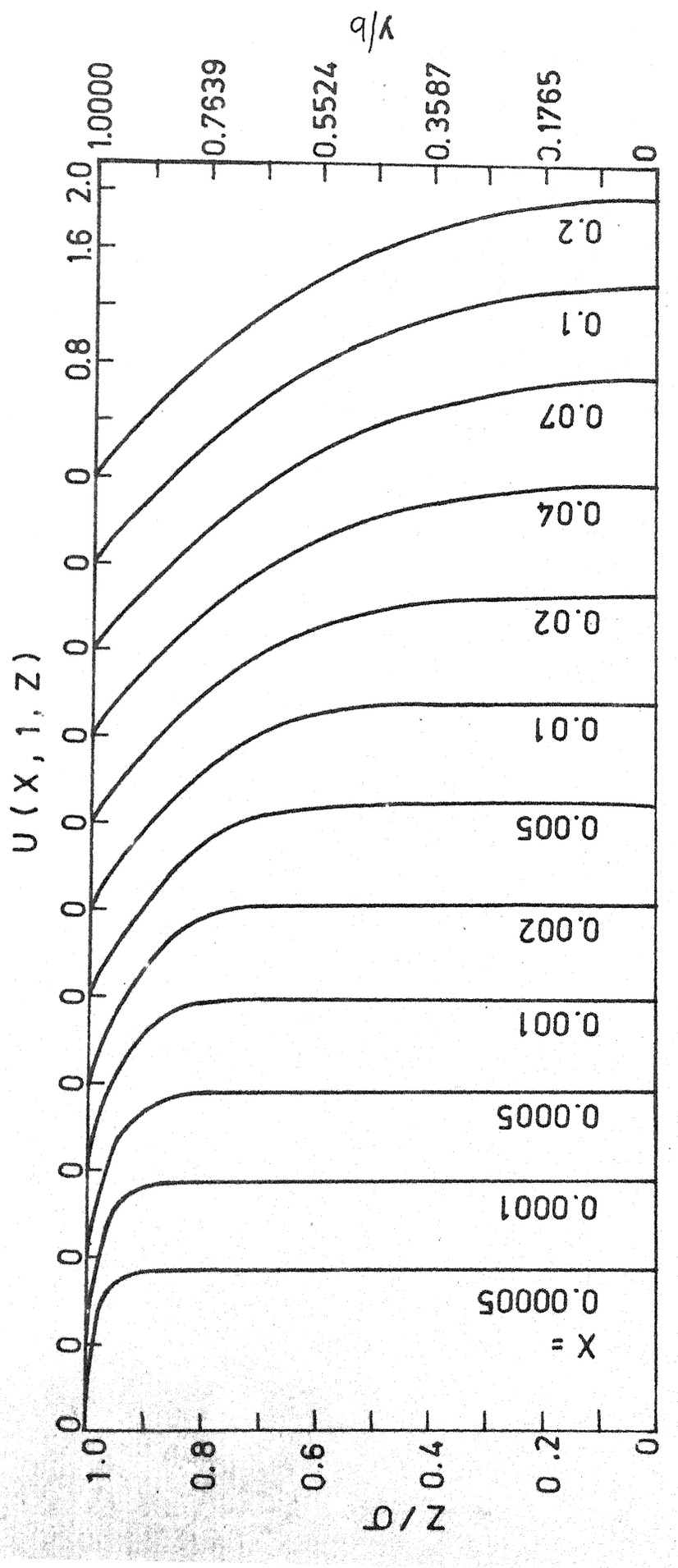

Fig. 5.1 (g) Development of axial velocity at the minor-axis. $\lambda = 1.4$

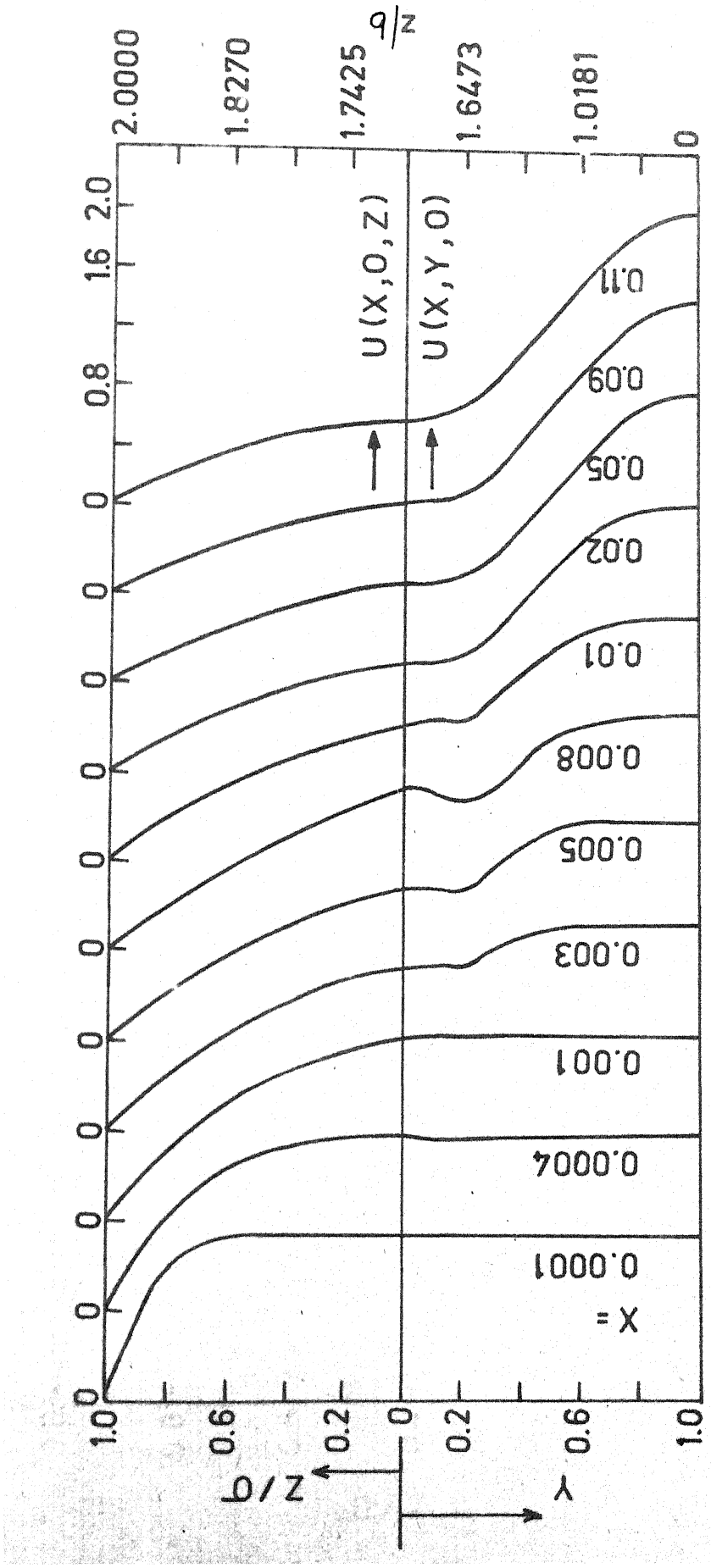

Fig. 5.1 (h) Development of axial velocity at the major-axis. $\lambda = 2$

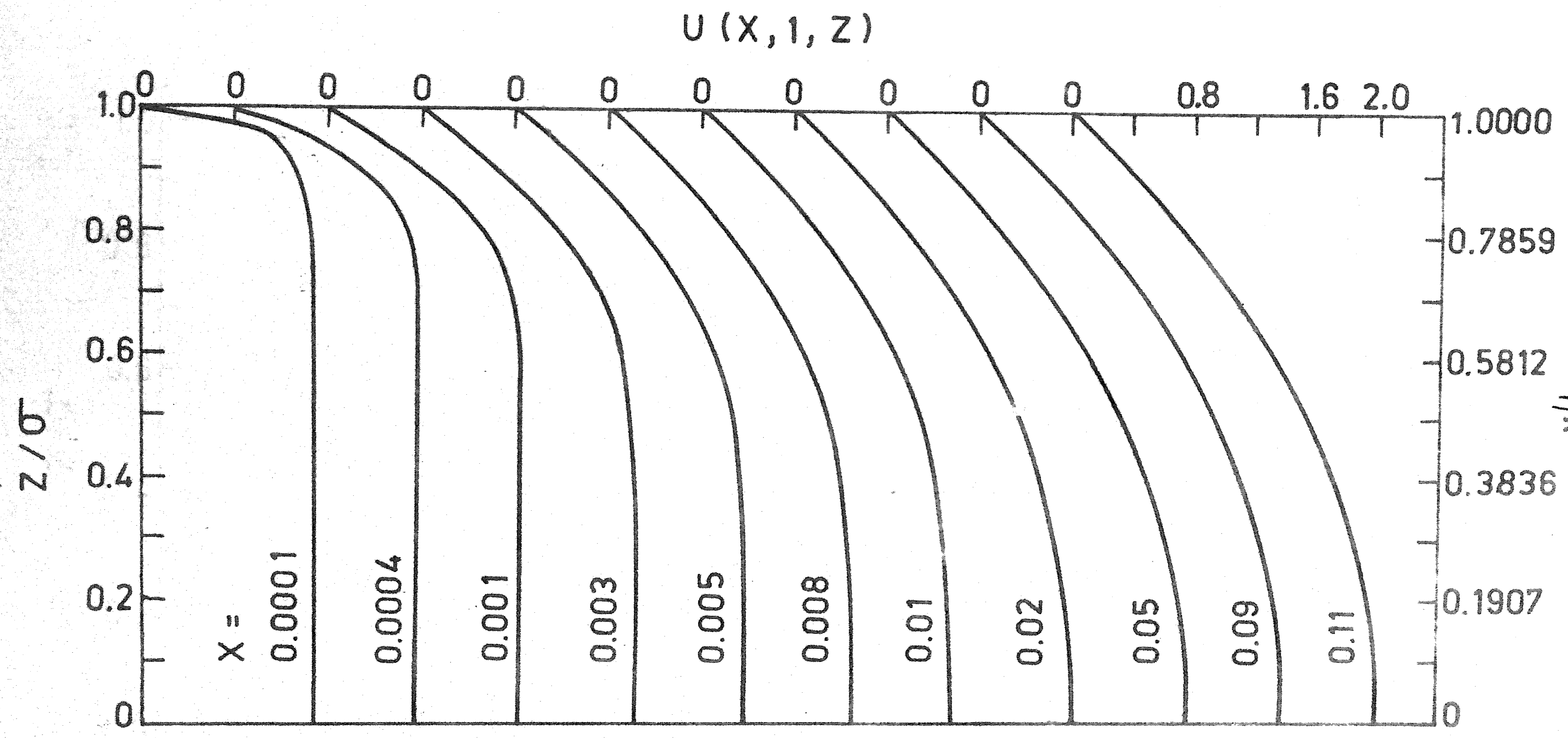

Fig. 5.1 (i) Development of axial velocity at the minor-axis. λ = 2.

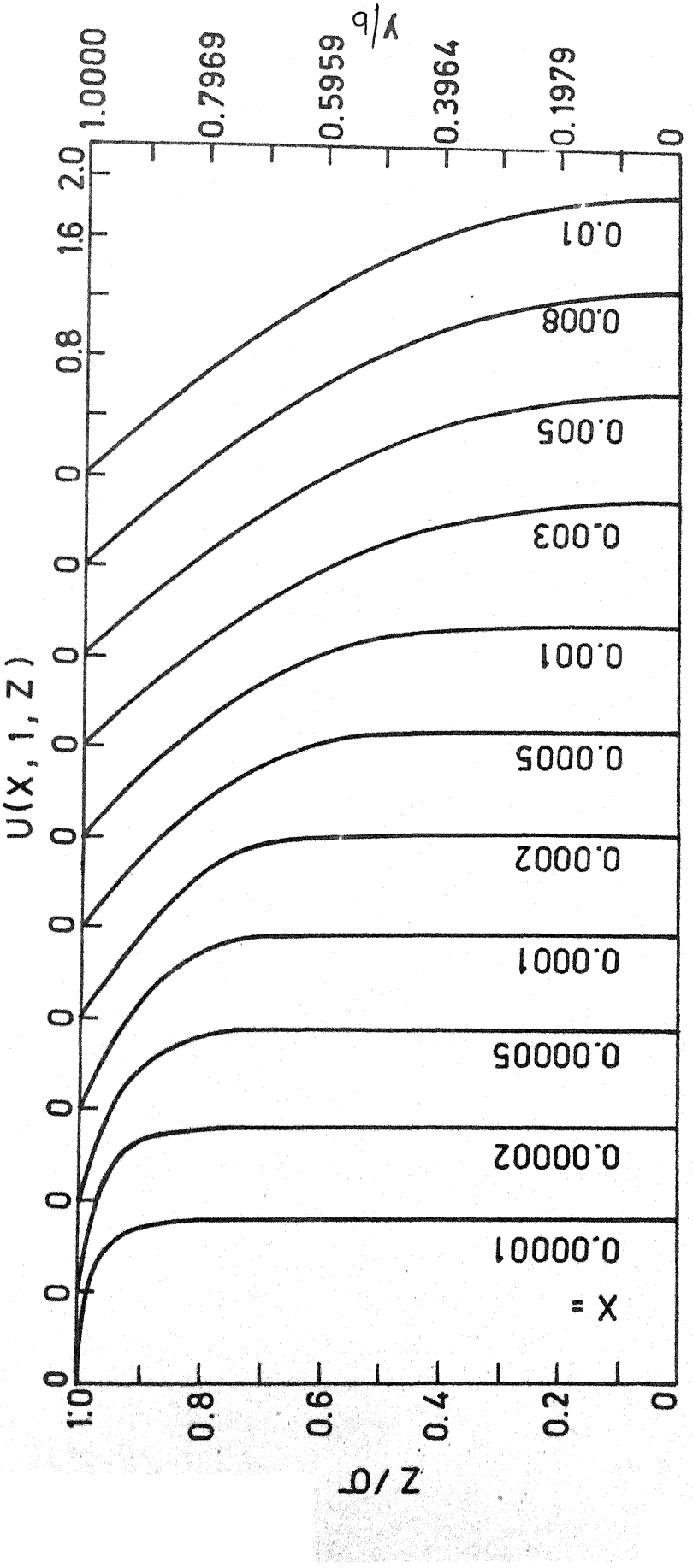

Fig.5.1 (j) Development of axial velocity at the minor axis. $\lambda = 4$

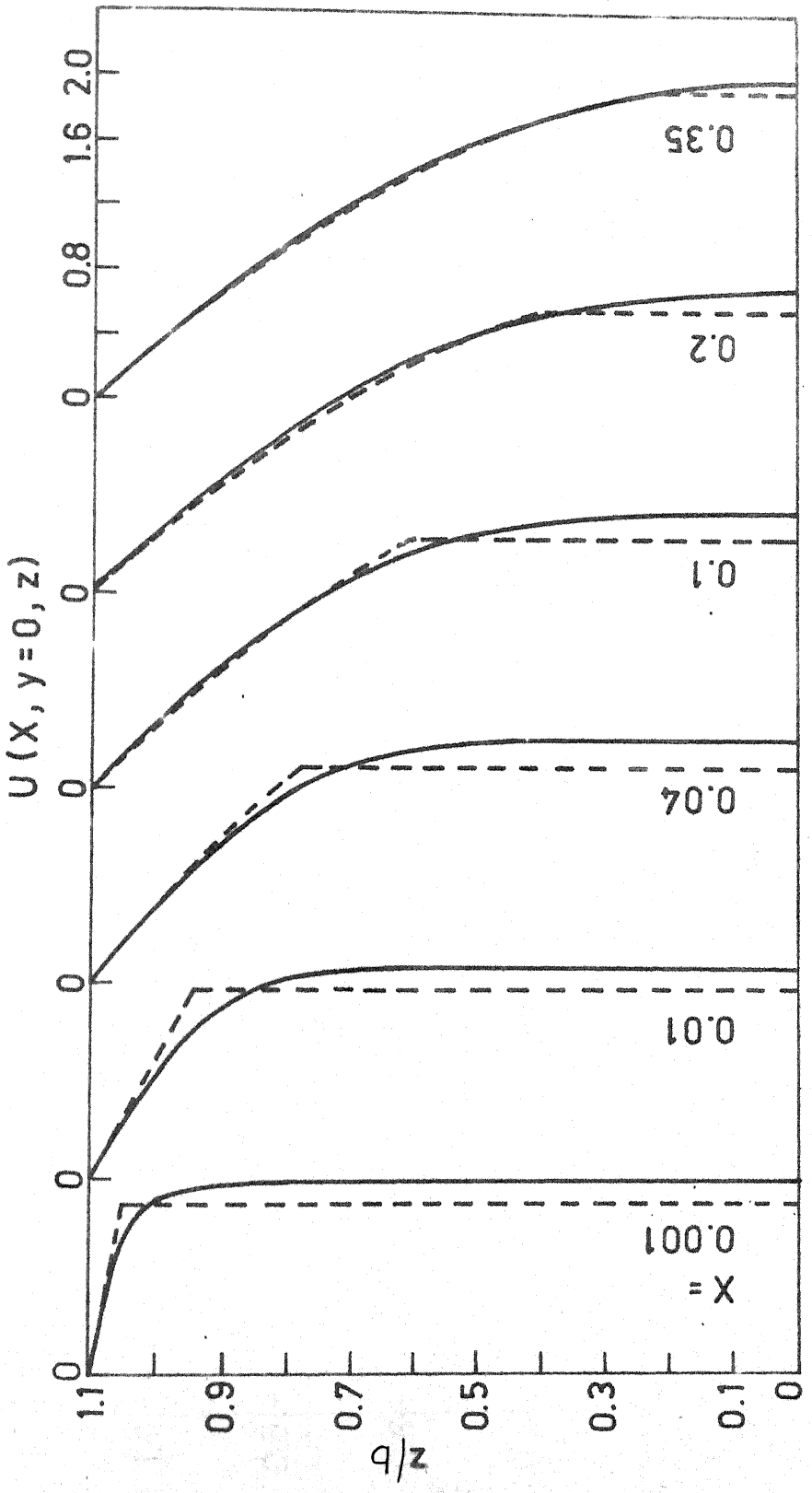

Fig.5.1 (k) Development of axial velocity at the major axis. $\lambda = 1.1$
——— Present Analysis; ----- Bhatti's Analysis

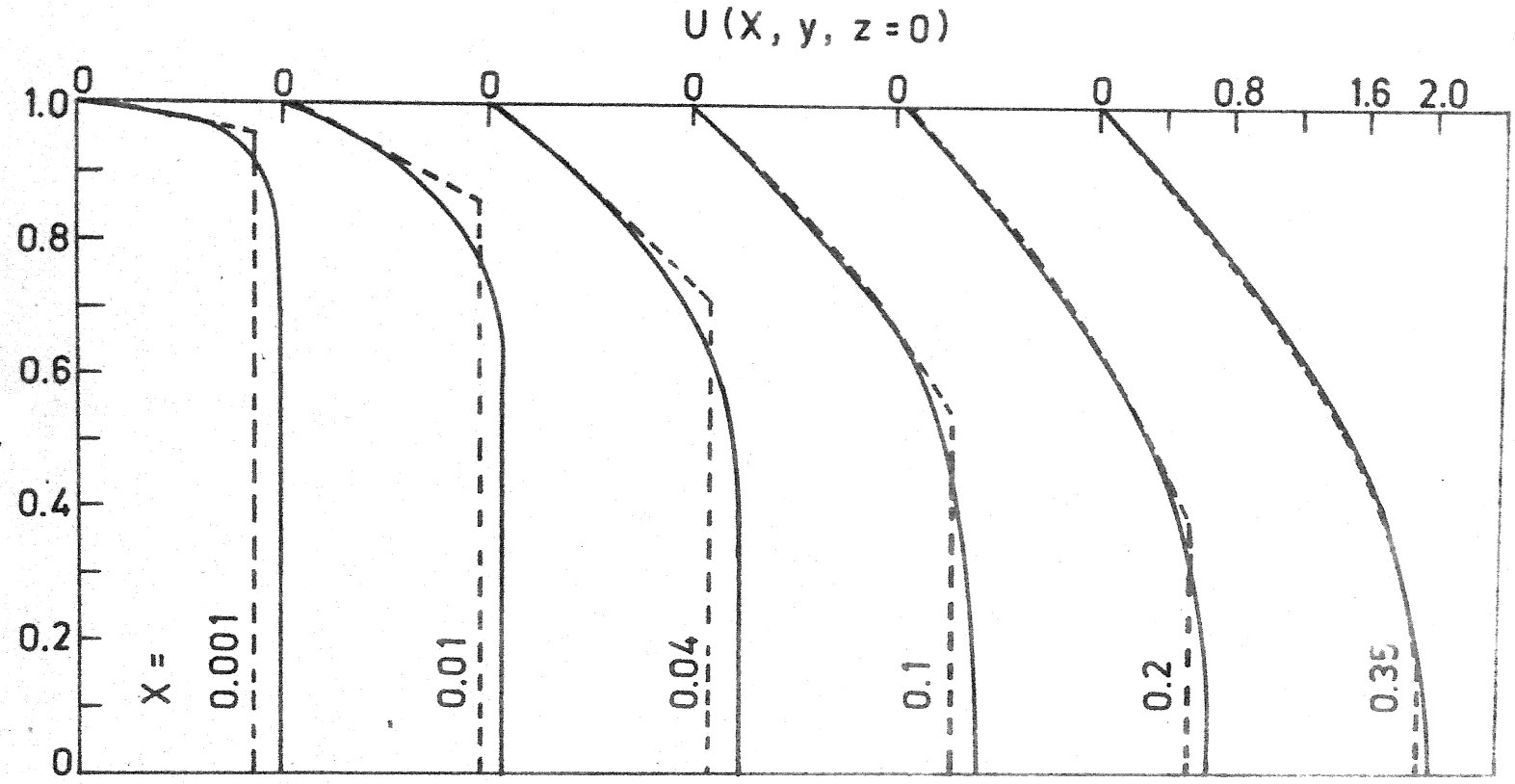

Fig. 5.1 (I) Development of axial velocity at the minor-axis. $\lambda = 1.1$
——— Present Analysis; ----- Bhatti's Analysis.

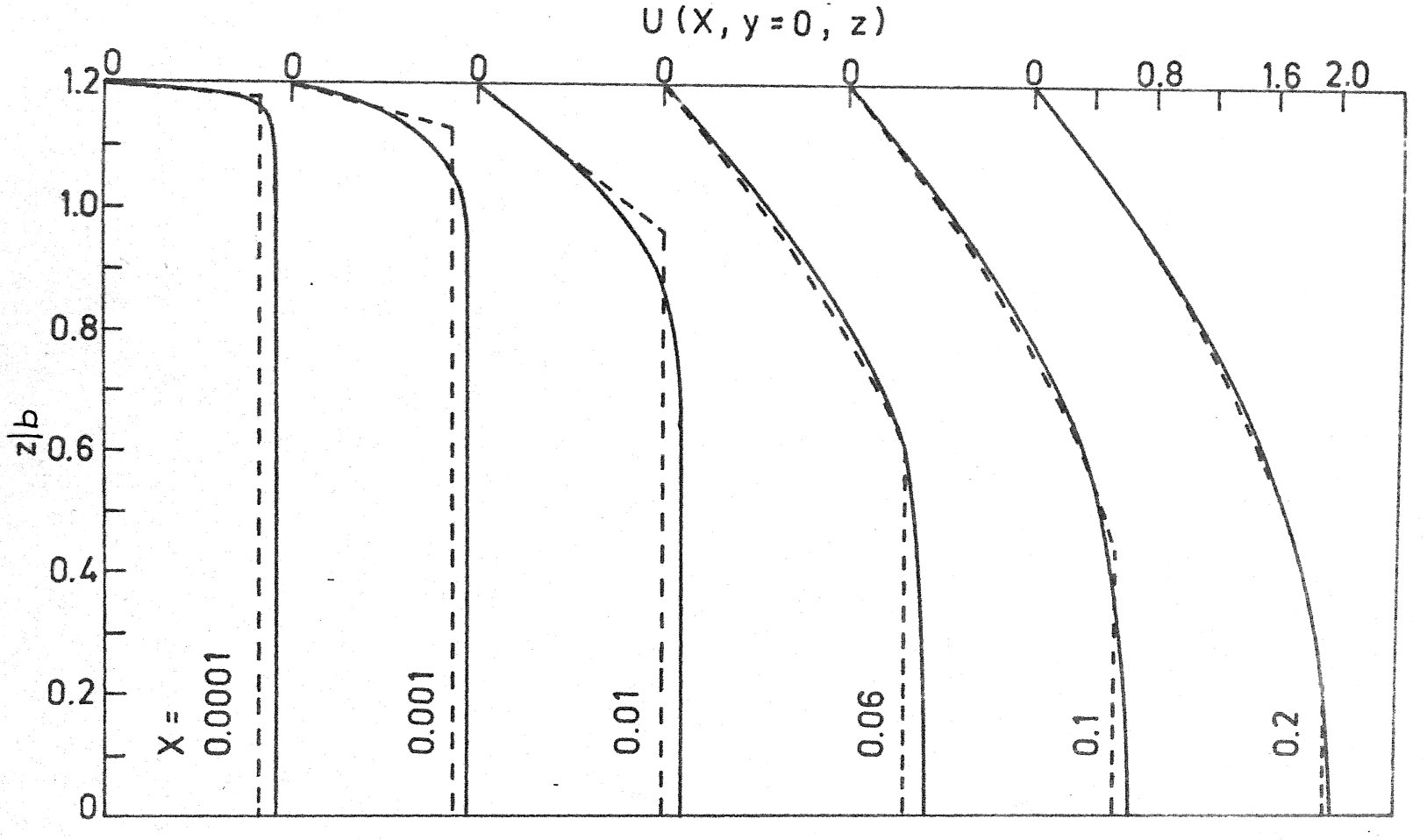

Fig.5.1(m) Development of axial velocity at the major-axis. $\lambda = 1.2$

——— Present Analysis; – – – – Bhatti's Analysis

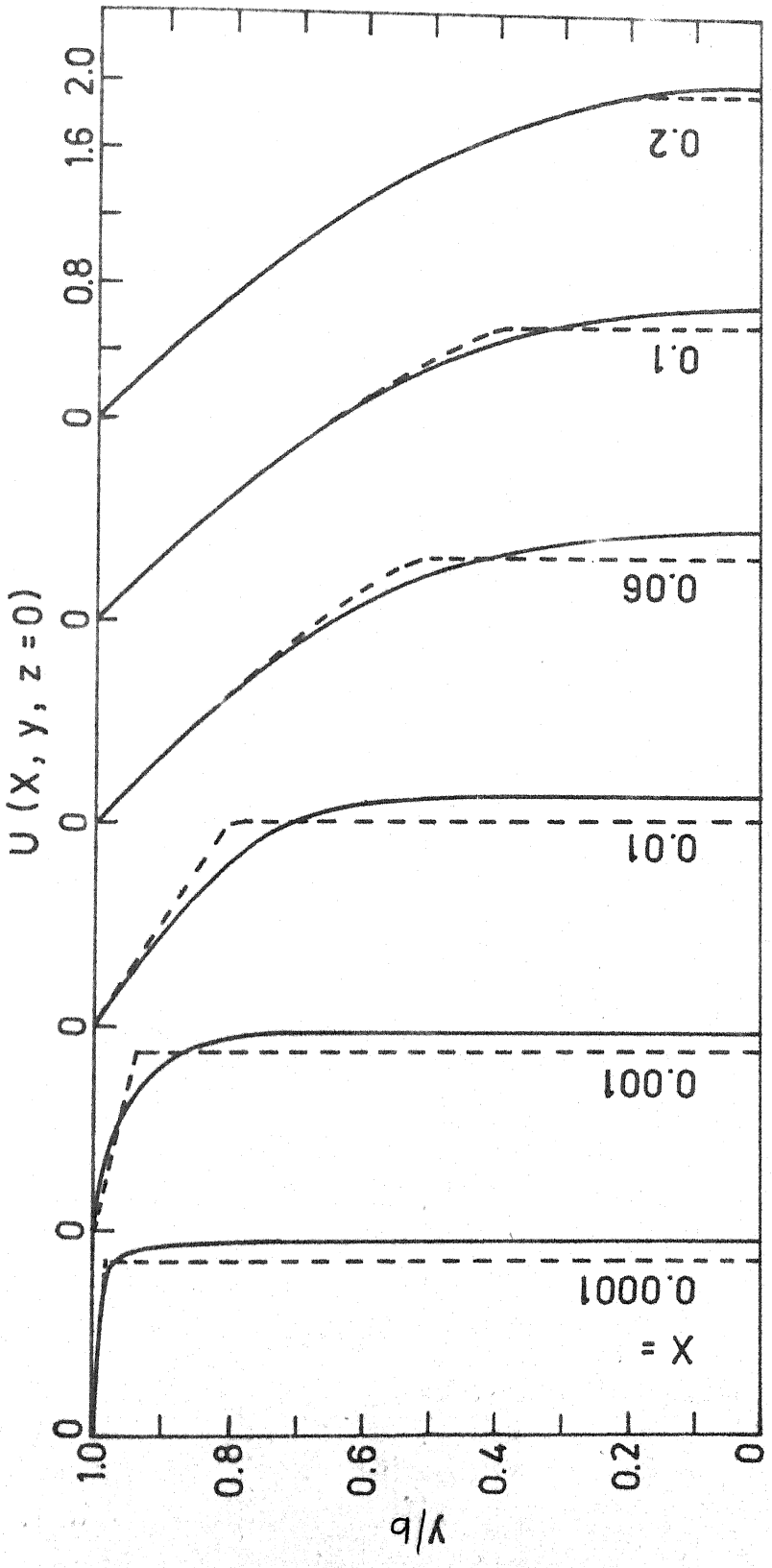

Fig. 5.1 (n) Development of axial velocity at the minor-axis. $\lambda = 1.2$
——— Present Analysis ; - - - - Bhatti's Analysis

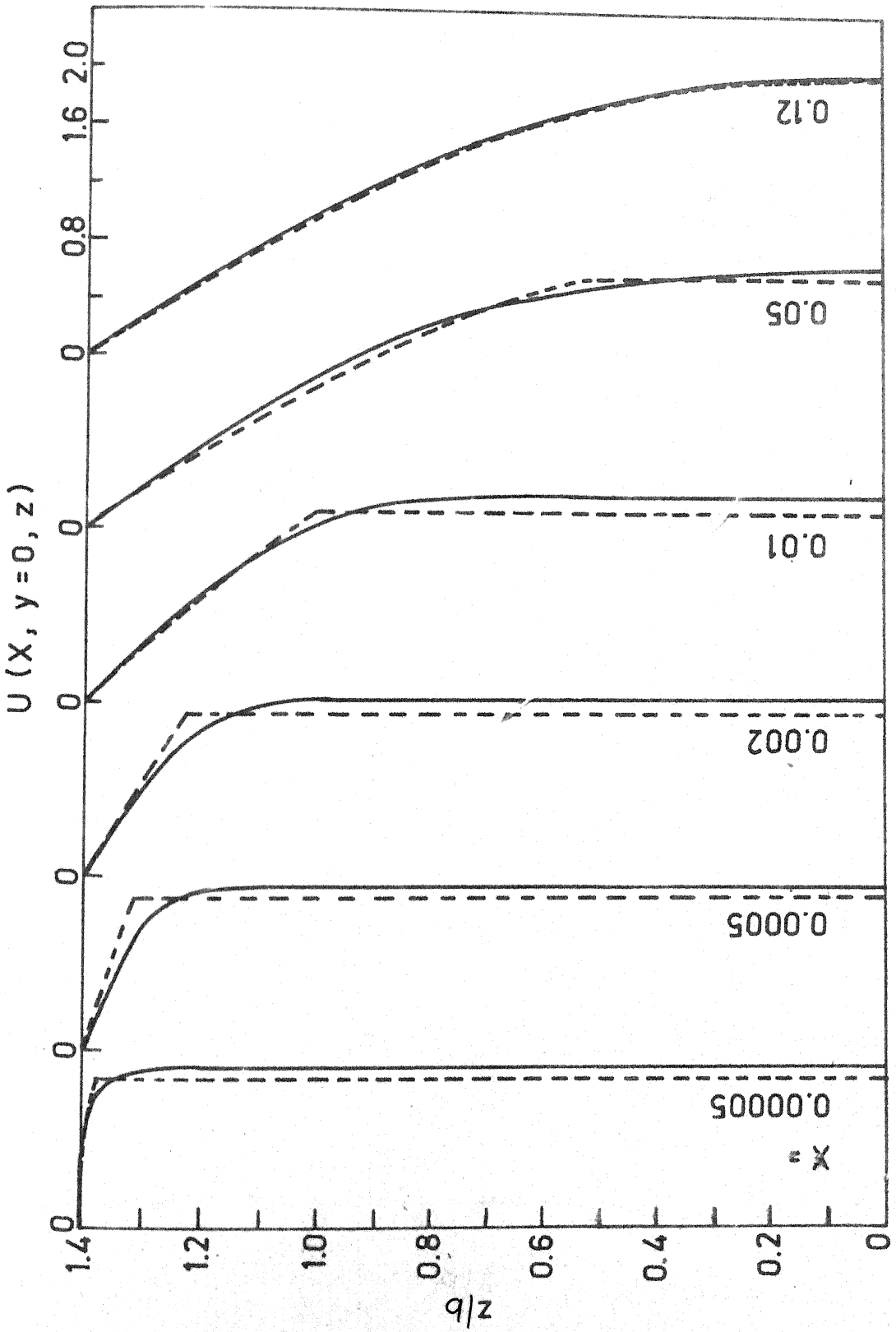

Fig. 5.1 (o) Development of axial velocity at the major-axis. $\lambda = 1.4$
—— Present Analysis; - - - - Bhatti's Analysis.

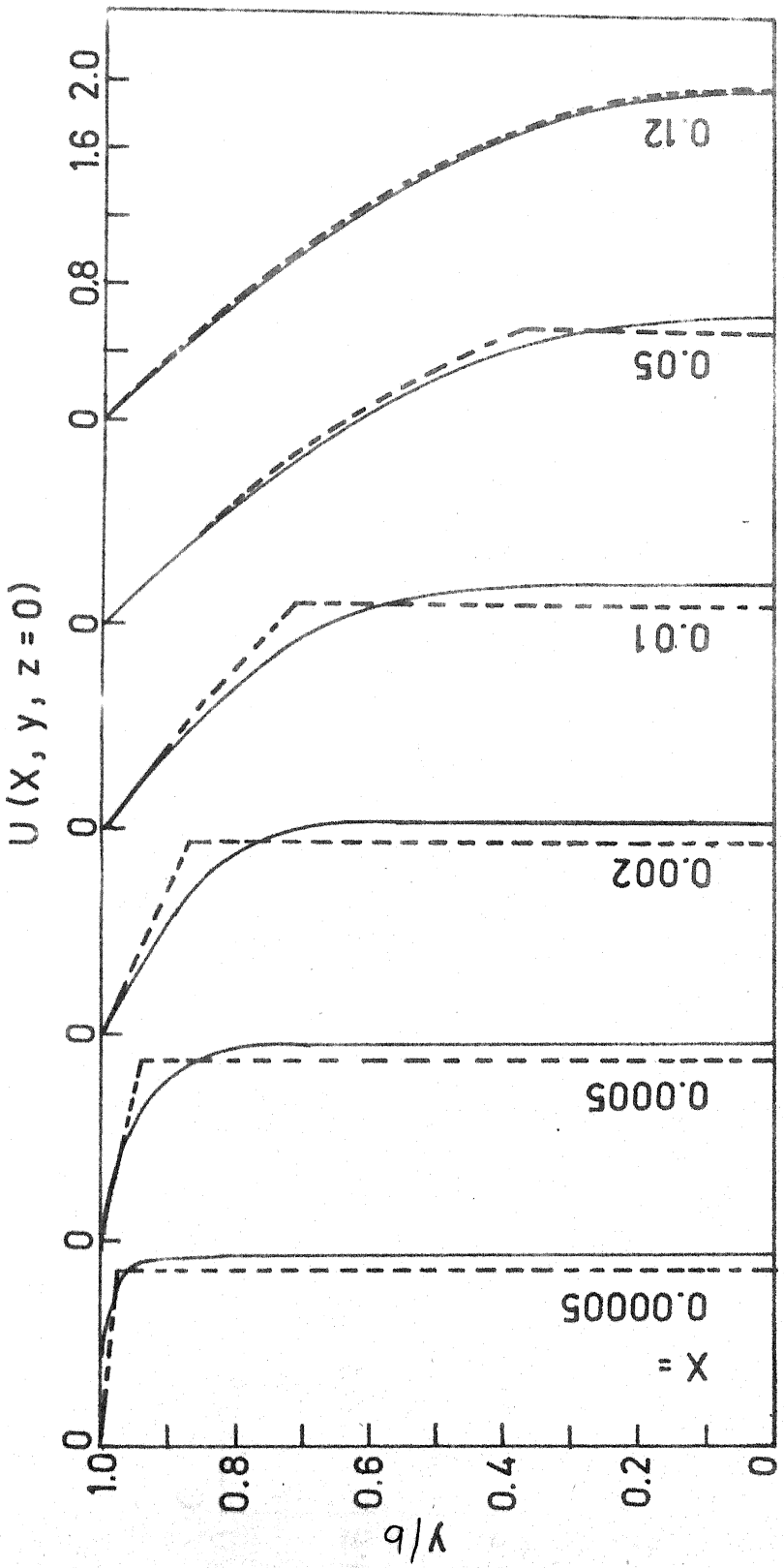

Fig. 5.1 (p) Development of axial velocity at the minor axis $\lambda = 1.4$
——— Present Analysis ; - - - - Bhatti's Analysis.

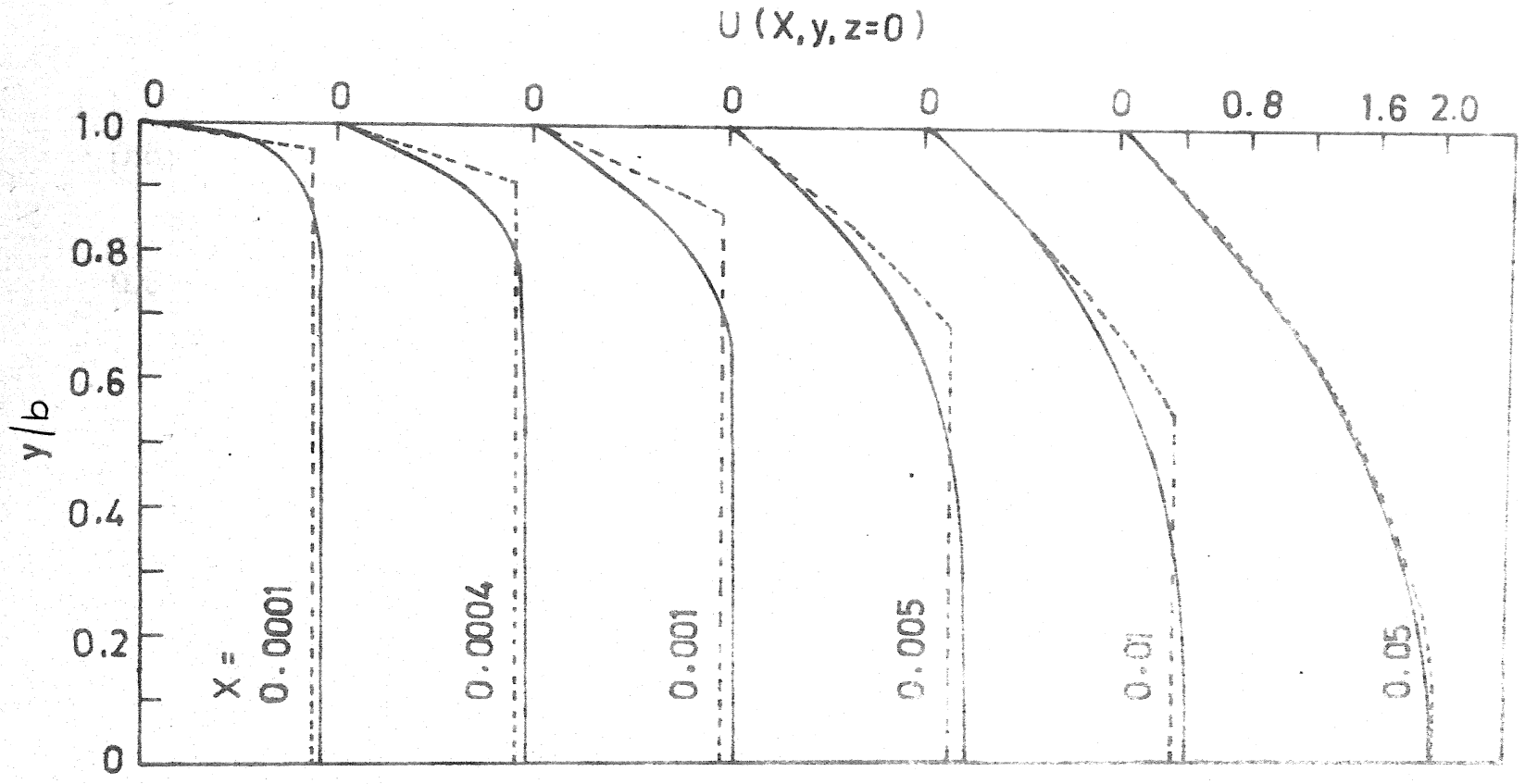

Fig. 5.1 (q) Development of axial velocity at the minor-axis. $\lambda = 2$

——— Present Analysis; - - - - Bhatti's Analysis

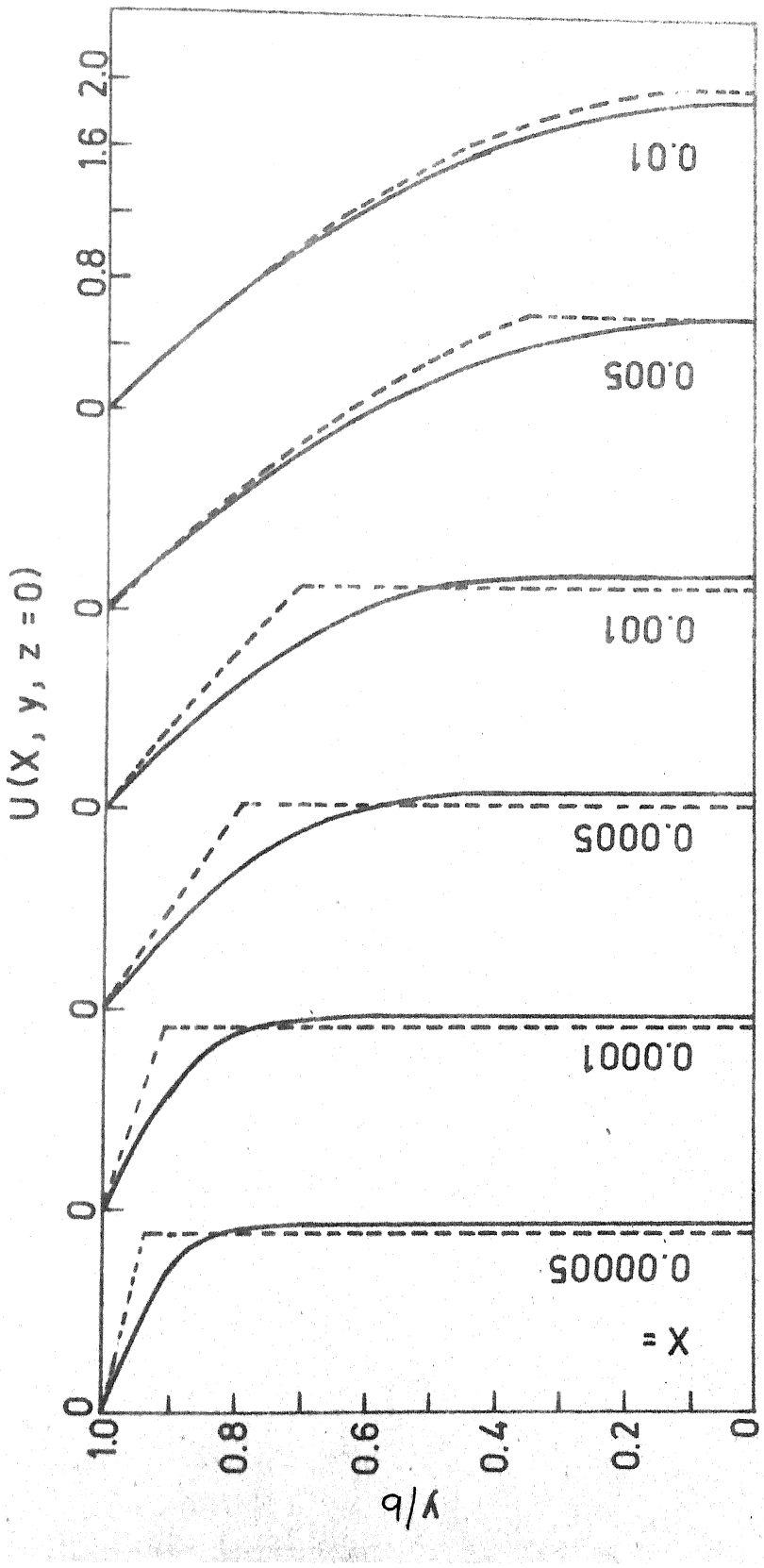

Fig. 5.1 (r) Development of axial velocity at the minor axis. $\lambda = 4$
——— Present Analysis; - - - - - Bhatti's Analysis

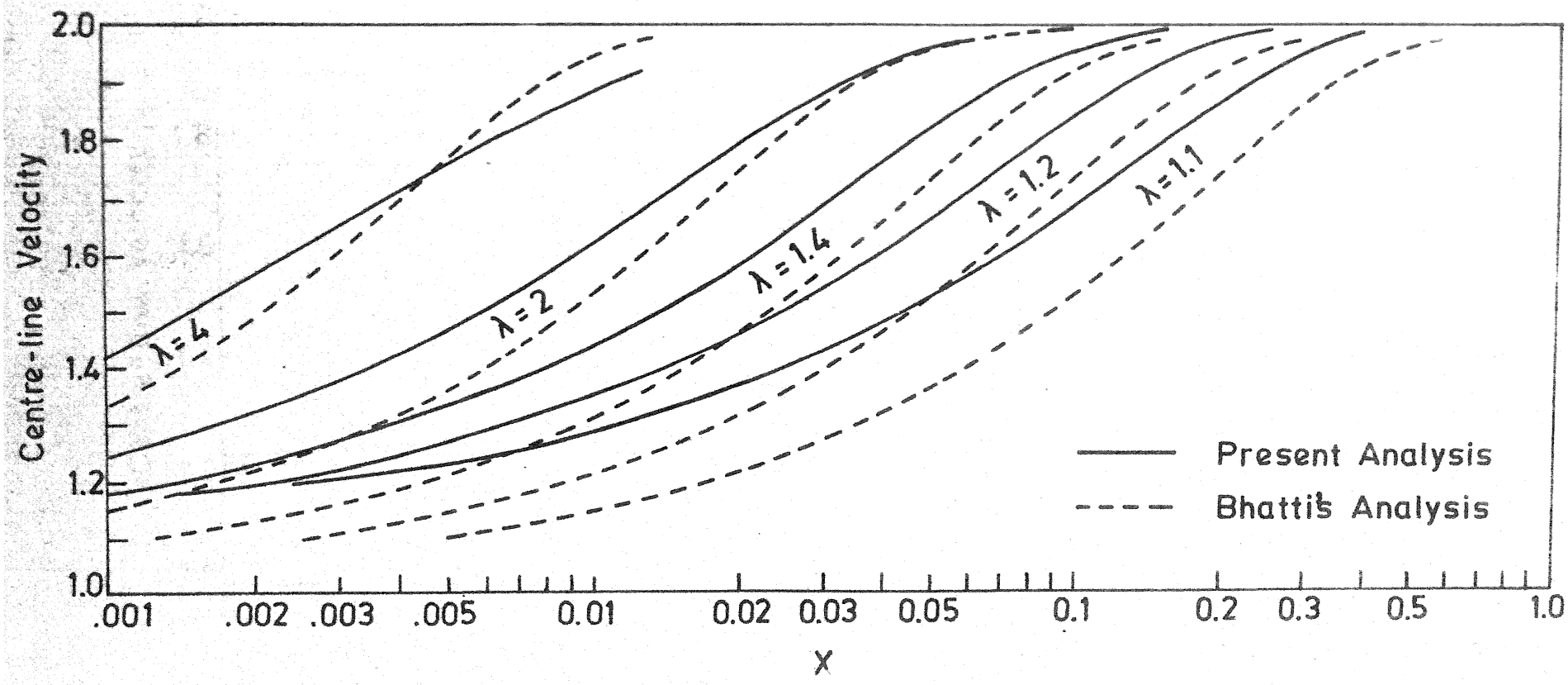

Fig. 5.2 (a) Development of centre-line velocity.

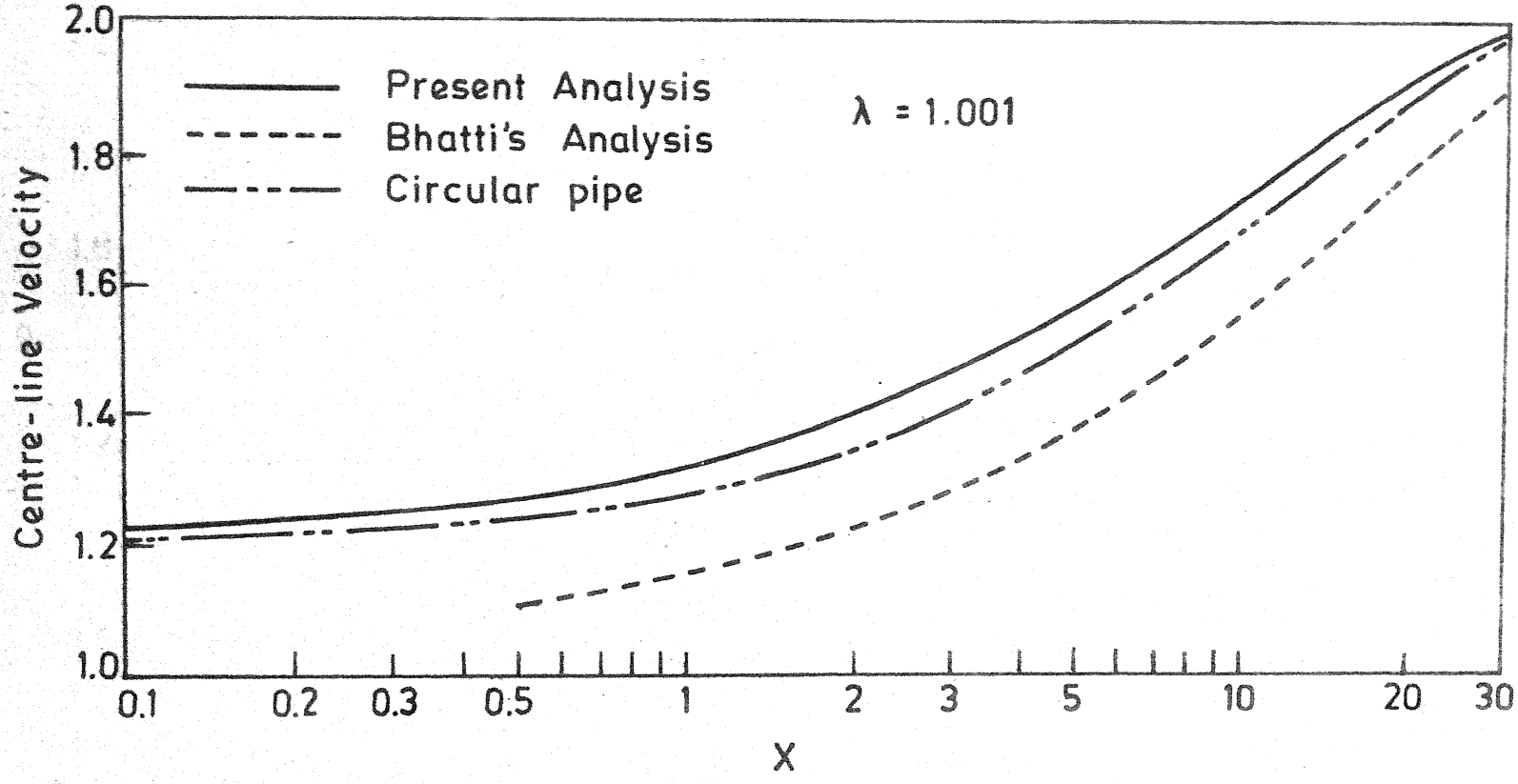

Fig. 5.2 (b) Development of centre-line velocity.

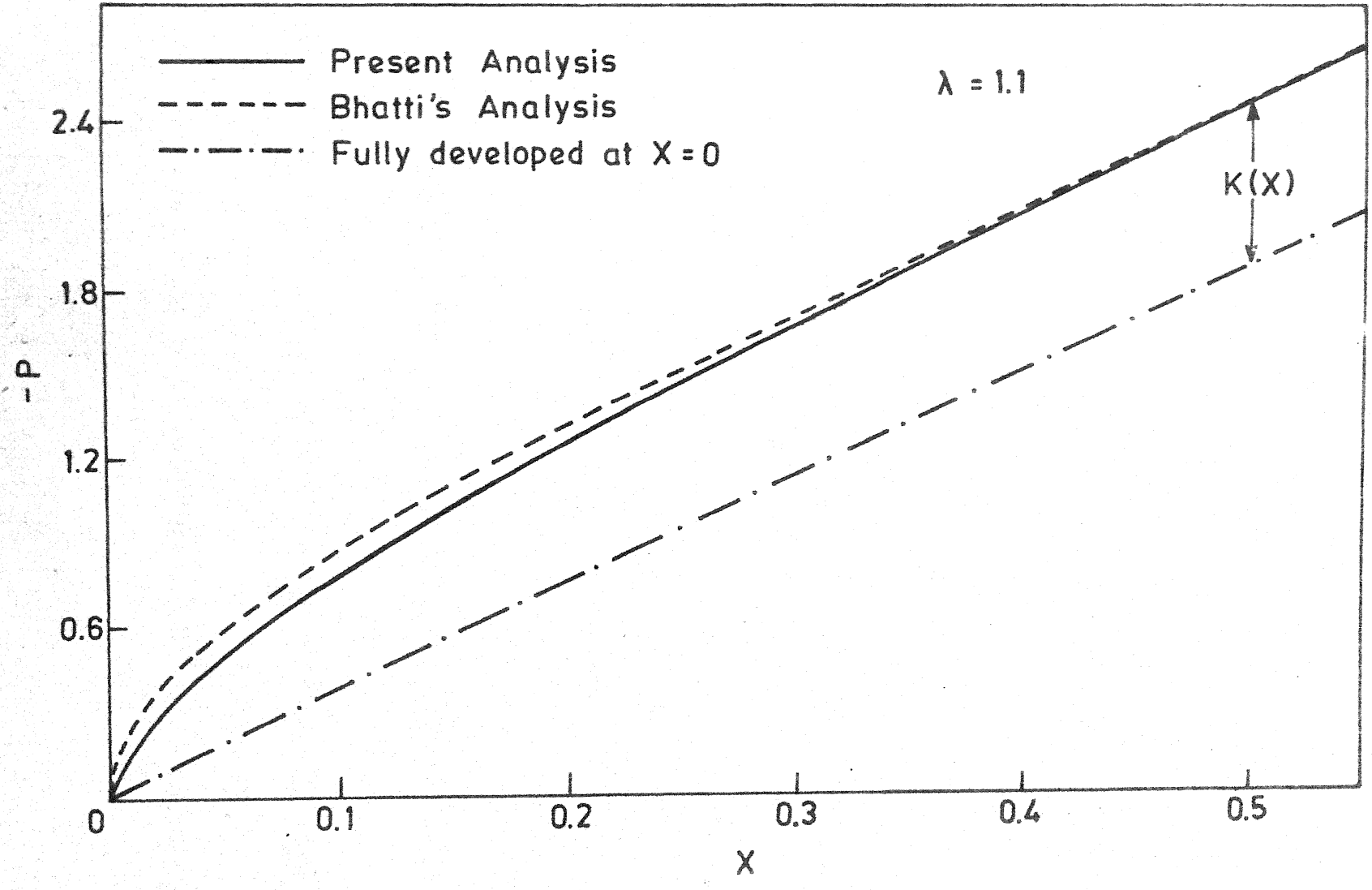

Fig. 5.3 (a) Axial Pressure - drop.

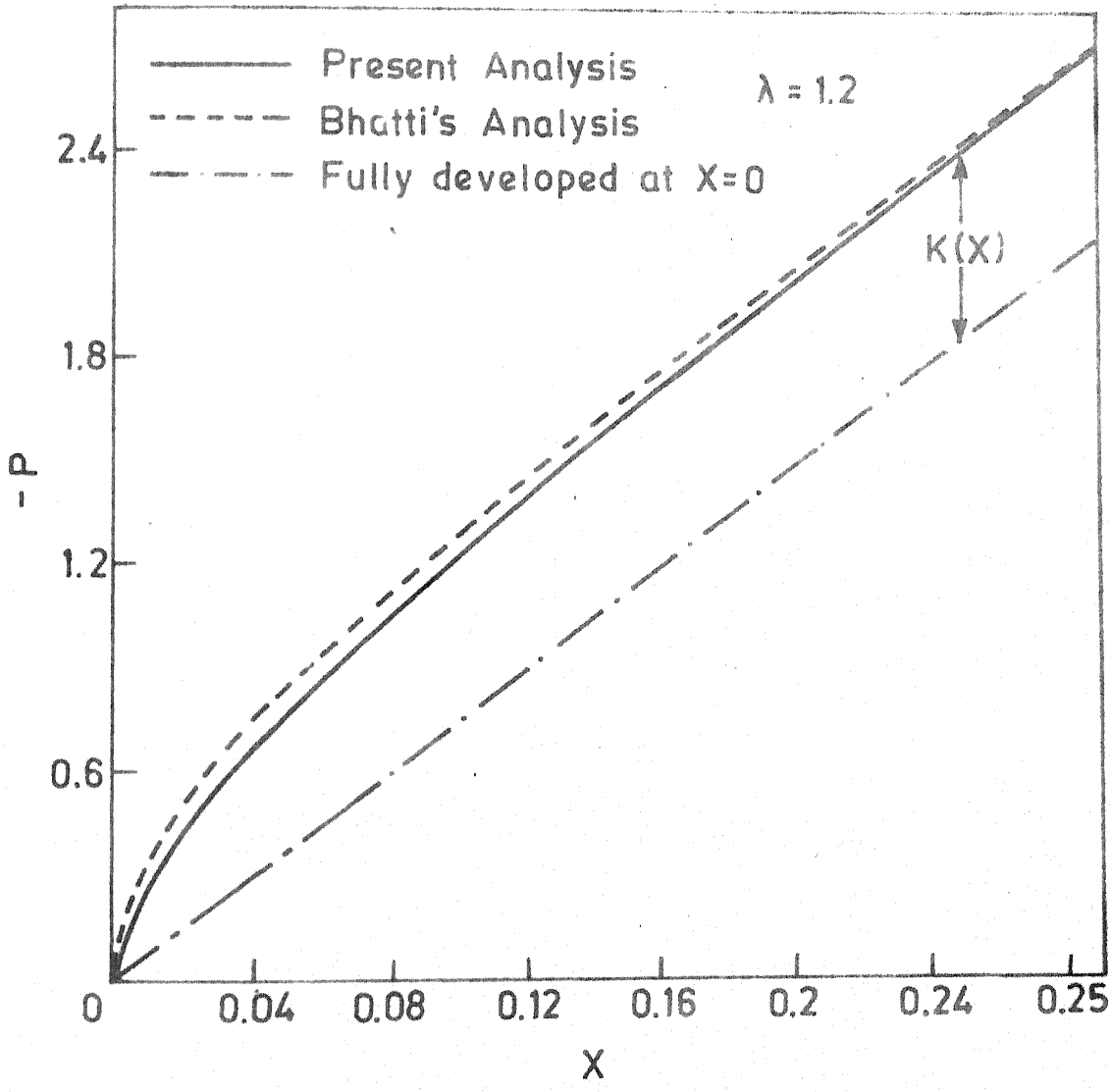

Fig.5.3 (b) Axial pressure-drop.

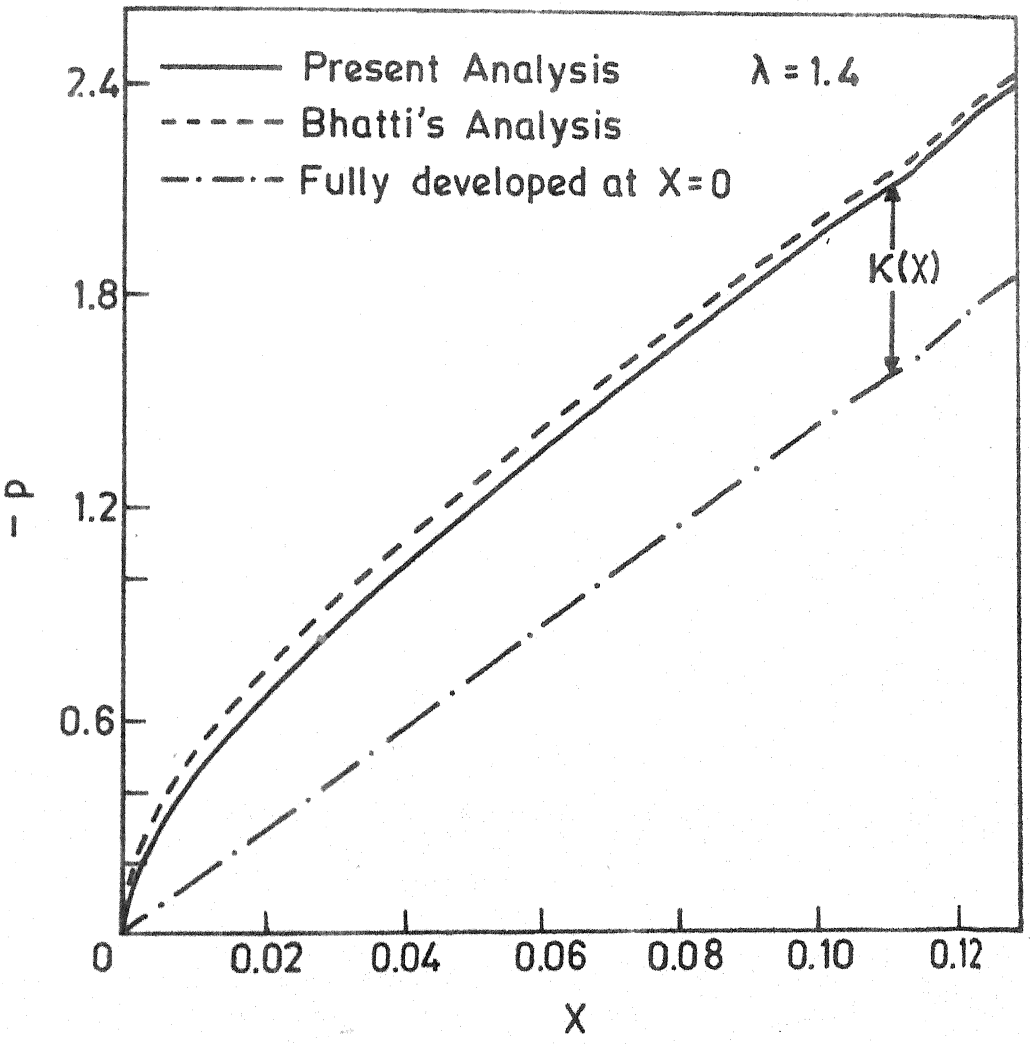

Fig.5.3 (c) Axial pressure-drop.

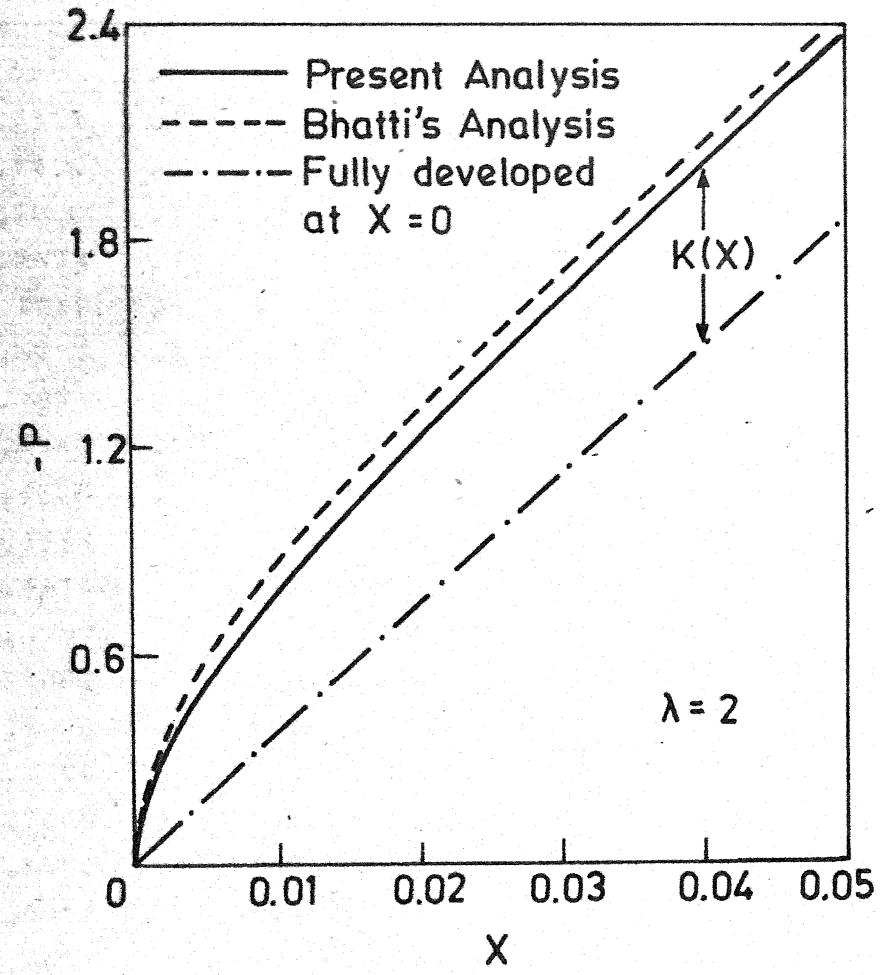

Fig. 5.3 (d) Axial pressure-drop.

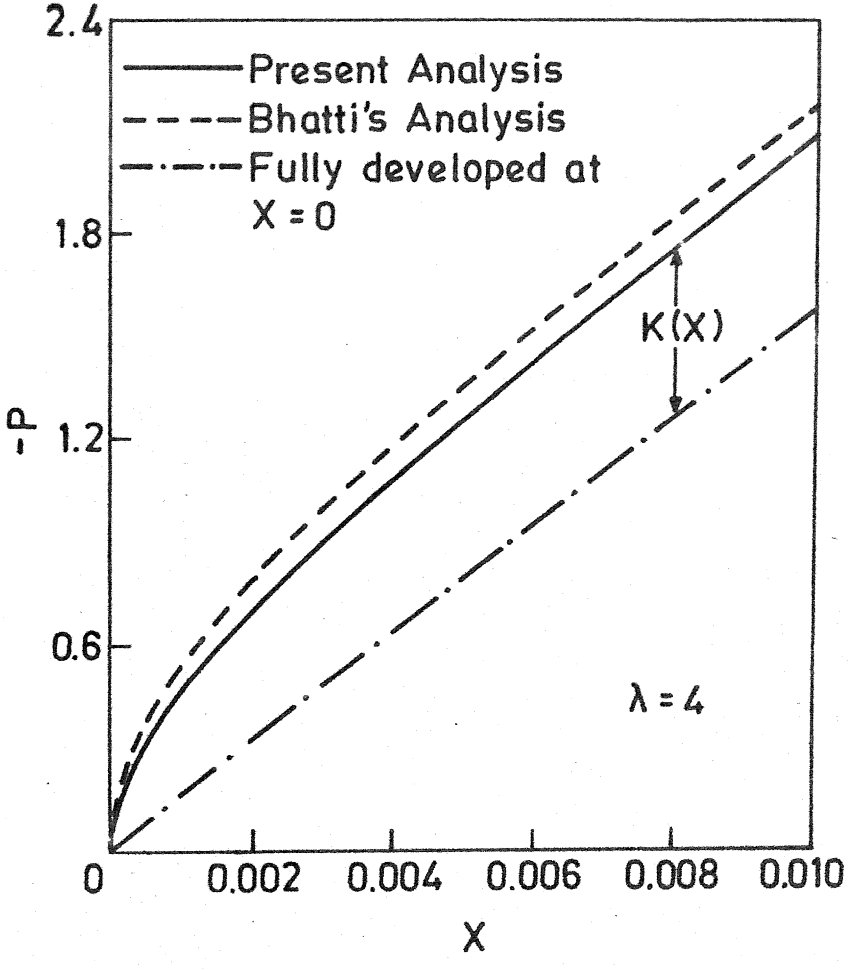

Fig. 5.3 (e) Axial pressure-drop.

Z	Y	Z/σ	X = .00100	X = .00500	X = .01000	X = .02000	X = .04000	X = .07000	X = .10000	X = .16000	X = .25000	X = .35000
			U	U	U	U	U	U	U	U	U	U
.0000	1.0		1.1827	1.2324	1.2877	1.3727	1.4879	1.6104	1.7037	1.8324	1.9351	1.9[illegible]
.0717	.9		1.1827	1.2324	1.2877	1.3727	1.4878	1.6100	1.7025	1.8291	1.9310	1.9[illegible]
.1416	.8		1.1827	1.2324	1.2877	1.3727	1.4878	1.6089	1.6986	1.8197	1.9132	1.9[illegible]
.2080	.7		1.1827	1.2324	1.2877	1.3727	1.4876	1.6065	1.6917	1.8015	1.8852	1.9[illegible]
.2694	.6		1.1827	1.2324	1.2877	1.3726	1.4871	1.6024	1.6813	1.7785	1.8623	1.8835
.3240	.5		1.1827	1.2324	1.2877	1.3726	1.4863	1.5961	1.6674	1.7510	1.8330	1.8352
.3707	.4		1.1827	1.2324	1.2877	1.3726	1.4848	1.5876	1.6509	1.7213	1.7988	1.8[illegible]
.4083	.3		1.1827	1.2324	1.2877	1.3725	1.4828	1.5778	1.6340	1.6934	1.7739	1.7825
.4358	.2		1.1827	1.2324	1.2877	1.3723	1.4808	1.5690	1.6204	1.6726	1.7399	1.7[illegible]
.4526	.1		1.1827	1.2324	1.2876	1.3722	1.4802	1.5641	1.6149	1.6635	1.6860	1.6905
.4583		0.0	1.1827	1.2324	1.2877	1.3723	1.4805	1.5633	1.6135	1.6609	1.6716	1.6[illegible]
2.4674		.1	1.1827	1.2324	1.2876	1.3718	1.4773	1.5578	1.6033	1.6464	1.6560	1.6718
.4797		.2	1.1827	1.2324	1.2876	1.3712	1.4730	1.5481	1.5870	1.6230	1.6304	1.6[illegible]
1.0000		.3	1.1827	1.2324	1.2875	1.3701	1.4660	1.5312	1.5610	1.5866	1.5977	1.6[illegible]
.9000		.4	1.1827	1.2323	1.2872	1.3676	1.4532	1.5024	1.5201	1.5317	1.5382	1.5329
.8000		.5	1.1827	1.2323	1.2861	1.3609	1.4278	1.4529	1.4653	1.4702	1.4727	1.4[illegible]
.7000		.6	1.1827	1.2317	1.2818	1.3420	1.3750	1.3873	1.3922	1.3940	1.3948	1.3[illegible]
.6000		.7	1.1826	1.2274	1.2622	1.2859	1.2645	1.2199	1.1980	1.1921	1.1905	1.1122
.5000		.8	1.1808	1.1945	1.1750	1.1251	1.0420	.9731	.9350	.9035	.8819	.8[illegible]
.4000		.9	1.1249	.9694	.8386	.7276	.6379	.5820	.5531	.5225	.5042	.4[illegible]
		X*	.00052	.00259	.00518	.01036	.02073	.03627	.05182	.07250	.10354	.14135

Table 5.1(a) Development of axial velocity at the major-axis
Aspect ratio = 1.1

Y	Z/σ	X = .00100	X = .00500	X = .01000	X = .02000	X = .04000	X = .07000	X = .10000	X = .16000	X = .25000	X = .35000
		U	U	U	U	U	U	U	U	U	U
.0000	0.0	1.1827	1.2324	1.2877	1.3727	1.4879	1.6101	1.7037	1.8325	1.9369	1.9924
.0700	.1	1.1827	1.2324	1.2877	1.3727	1.4878	1.6099	1.7021	1.8281	1.9298	1.9811
.1417	.2	1.1827	1.2324	1.2877	1.3727	1.4876	1.6078	1.6965	1.8146	1.9175	1.9644
.2166	.3	1.1827	1.2324	1.2877	1.3726	1.4868	1.6026	1.6842	1.7878	1.8696	1.9054
.2966	.4	1.1827	1.2324	1.2877	1.3724	1.4841	1.5905	1.6597	1.7419	1.8011	1.8302
.3835	.5	1.1827	1.2324	1.2876	1.3714	1.4756	1.5630	1.6128	1.6660	1.7019	1.7195
.4792	.6	1.1827	1.2323	1.2870	1.3659	1.4491	1.5017	1.5244	1.5410	1.5553	1.5603
.5861	.7	1.1826	1.2313	1.2813	1.3392	1.3720	1.3720	1.3341	1.3515	1.3416	1.3372
.7066	.8	1.1819	1.2167	1.2365	1.2245	1.1698	1.1185	1.0889	1.0568	1.0350	1.0250
.8435	.9	1.1432	1.0518	.9631	.8356	.7332	.6783	.6505	.6215	.6020	.5930
Pressure		-0.0150	-0.0750	-0.1447	-0.2577	-0.4225	-0.6146	-0.7800	-1.0732	-1.1679	-1.3782
X^*		.00052	.00259	.00518	.01036	.02073	.03627	.05182	.08290	.12954	.18135

Table 5.1(b) Development of axial velocity at the minor-axis and pressure
Aspect ratio = 1.1

Z	Y	Z/σ	X = .00010	X = .00100	X = .00200	X = .00500	X = .01000	X = .02000	X = .06000	X = .10000	X = .13000	X = .20000
			U	U	U	U	U	U	U	U	U	U
.0000	1.0		1.1357	1.1636	1.1936	1.2684	1.3522	1.4639	1.7249	1.8611	1.9209	1.9870
.1038	.9		1.1357	1.1636	1.1936	1.2684	1.3522	1.4639	1.7225	1.8544	1.9112	1.9737
.2050	.8		1.1357	1.1636	1.1936	1.2684	1.3522	1.4637	1.7142	1.8337	1.8820	1.9347
.3011	.7		1.1357	1.1636	1.1936	1.2684	1.3522	1.4633	1.6989	1.7977	1.8338	1.8731
.3899	.6		1.1357	1.1636	1.1936	1.2684	1.3522	1.4622	1.6767	1.7466	1.7696	1.7943
.4690	.5		1.1357	1.1636	1.1600	1.2684	1.3520	1.4601	1.6505	1.6838	1.6946	1.7057
.5366	.4		1.1357	1.1636	1.1936	1.2684	1.3518	1.4559	1.6216	1.6159	1.6169	1.6164
.5910	.3		1.1357	1.1636	1.1936	1.2683	1.3513	1.4493	1.5924	1.5521	1.5454	1.5355
.6309	.2		1.1357	1.1636	1.1936	1.2684	1.3510	1.4414	1.5837	1.5026	1.4899	1.4723
.6552	.1		1.1357	1.1636	1.1936	1.2681	1.3500	1.4401	1.6771	1.4804	1.4623	1.4357
.6633		0.0	1.1357	1.1636	1.1936	1.2684	1.3510	1.4408	1.6653	1.4732	1.4534	1.4243
2.4674		.1	1.1357	1.1636	1.1936	1.2678	1.3470	1.4281	1.5931	1.4523	1.4346	1.4099
.6825		.2	1.1357	1.1636	1.1936	1.2673	1.3429	1.4130	1.5178	1.4193	1.4021	1.3797
1.0000		.3	1.1357	1.1636	1.1936	1.2665	1.3374	1.3923	1.4499	1.3704	1.3527	1.3311
.9000		.4	1.1357	1.1636	1.1935	1.2647	1.3277	1.3610	1.3745	1.3013	1.2824	1.2606
.8000		.5	1.1357	1.1636	1.1932	1.2597	1.3074	1.3097	1.2748	1.2062	1.1861	1.1639
.7000		.6	1.1357	1.1634	1.1916	1.2440	1.2619	1.2230	1.1405	1.0778	1.0570	1.0349
.6000		.7	1.1357	1.1618	1.1819	1.1936	1.1605	1.0779	.9609	.9063	.8865	.8657
.5000		.8	1.1355	1.1439	1.1253	1.0414	.9499	.8440	.7230	.6799	.6634	.6461
.4000		.9	1.1160	.9750	.8443	.6607	.5708	.4926	.4096	.3838	.3737	.3631
		X*	.00011	.00109	.00217	.00543	.01086	.02171	.06514	.10857	.14114	.21713

Table 5.1(c) Development of axial velocity at the major-axis
Aspect ratio = 1.2

y	Z/σ	X = .00010	X = .00100	X = .00200	X = .00500	X = .01000	X = .02000	X = .06000	X = .10000	X = .13000	X = .20000
		U	U	U	U	U	U	U	U	U	U
.0000	0.0	1.1357	1.1636	1.1936	1.2684	1.3522	1.4639	1.7250	1.8611	1.9209	1.9870
.0797	.1	1.1357	1.1636	1.1936	1.2684	1.3522	1.4638	1.7217	1.8540	1.9117	1.9755
.1606	.2	1.1357	1.1636	1.1936	1.2684	1.3522	1.4634	1.7106	1.8310	1.8830	1.9399
.2438	.3	1.1357	1.1636	1.1936	1.2684	1.3521	1.4621	1.6875	1.7881	1.8310	1.8774
.3305	.4	1.1357	1.1636	1.1936	1.2684	1.3517	1.4579	1.6450	1.7185	1.7500	1.7835
.4219	.5	1.1357	1.1636	1.1936	1.2683	1.3497	1.4449	1.5709	1.6129	1.6318	1.6515
.5194	.6	1.1357	1.1636	1.1936	1.2671	1.3399	1.4063	1.4477	1.4587	1.4657	1.4724
.6244	.7	1.1357	1.1634	1.1926	1.2571	1.2972	1.3035	1.2532	1.2401	1.2378	1.2347
.7384	.8	1.1357	1.1590	1.1775	1.1903	1.1425	1.0708	.9624	.9388	.9315	.9233
.8630	.9	1.1253	1.0642	1.0064	.8658	.7257	.6436	.5529	.5339	.5270	.5196
Pressure		-0.0035	-0.0355	-0.0709	-0.1630	-0.2727	-0.4301	-0.8709	-1.2250	-1.4720	-2.0210
	X^*	.00011	.00109	.00217	.00543	.01086	.02171	.06514	.10857	.14114	.21713

Table 5.1(d) Development of axial velocity at the minor-axis and pressure
Aspect ratio = 1.2

Z	Y	Z/σ	X = .00010	X = .00050	X = .00100	X = .00200	X = .00500	X = .01000	X = .02000	X = .04000	X = .07000	X = .12000
			U	U	U	U	U	U	U	U	U	U
.0000	1.0		1.1090	1.1404	1.1766	1.2310	1.3330	1.4420	1.5908	1.7755	1.9097	1.9857
.1533	.9		1.1090	1.1404	1.1766	1.2310	1.3330	1.4420	1.5900	1.7692	1.8942	1.9637
.3028	.8		1.1090	1.1404	1.1766	1.2310	1.3330	1.4418	1.5865	1.7475	1.8469	1.8994
.4448	.7		1.1090	1.1404	1.1766	1.2310	1.3330	1.4410	1.5769	1.7047	1.7680	1.7930
.5759	.6		1.1090	1.1404	1.1766	1.2310	1.3330	1.4379	1.5564	1.6383	1.6626	1.6690
.6928	.5		1.1090	1.1404	1.1766	1.2310	1.3330	1.4281	1.5217	1.5501	1.5393	1.5250
.7927	.4		1.1090	1.1404	1.1766	1.2313	1.3311	1.4058	1.4664	1.4458	1.4093	1.3799
.8730	.3		1.1090	1.1404	1.1766	1.2303	1.3250	1.3997	1.3997	1.3414	1.2892	1.2490
.9318	.2		1.1090	1.1403	1.1767	1.2322	1.3133	1.3466	1.3438	1.2602	1.1981	1.1478
.9677	.1		1.1090	1.1403	1.1764	1.2298	1.3129	1.3409	1.3304	1.2351	1.1611	1.0930
.9798		0.0	1.1090	1.1403	1.1767	1.2322	1.3148	1.3424	1.3245	1.2254	1.1479	1.0750
2.4674		.1	1.1090	1.1403	1.1765	1.2291	1.2980	1.3080	1.2877	1.1910	1.1200	1.0573
.9955		.2	1.1090	1.1403	1.1762	1.2264	1.2793	1.2701	1.2433	1.1472	1.0809	1.0261
1.0000		.3	1.1090	1.1403	1.1757	1.2228	1.2554	1.2243	1.1875	1.0906	1.0282	.9798
.9000		.4	1.1090	1.1403	1.1744	1.2158	1.2209	1.1949	1.1157	1.0182	.9593	.9163
.8000		.5	1.1090	1.1399	1.1704	1.1996	1.1669	1.0845	1.0225	.9261	.8712	.8334
.7000		.6	1.1090	1.1379	1.1570	1.1608	1.0768	.9734	.9015	.8103	.7605	.7281
.6000		.7	1.1089	1.1269	1.1117	1.0692	.9330	.8204	.7459	.6659	.6233	.5969
.5000		.8	1.1056	1.0652	.9673	.8708	.7141	.6142	.5489	.4872	.4548	.4356
.4000		.9	1.0316	.7753	.5967	.5138	.4059	.3441	.3032	.2672	.2493	.2387
			X^* = .00024	.00118	.00237	.00474	.01184	.02369	.04737	.09475	.16581	.28424

Table 5.1(e) Development of axial velocity at the major-axis
Aspect ratio = 1.4

y	z/σ	X = .00010	X = .00050	X = .00100	X = .00200	X = .00500	X = .01000	X = .02000	X = .04000	X = .07000	X = .12000
		U	U	U	U	U	U	U	U	U	U
.0000	0.0	1.1090	1.1404	1.1766	1.2310	1.3330	1.4420	1.5908	1.7755	1.9097	1.9857
.0879	.1	1.1090	1.1404	1.1766	1.2310	1.3330	1.4420	1.5893	1.7692	1.8983	1.9713
.1765	.2	1.1090	1.1404	1.1766	1.2310	1.3330	1.4415	1.5838	1.7478	1.8625	1.9271
.2665	.3	1.1090	1.1404	1.1766	1.2310	1.3328	1.4396	1.5698	1.7061	1.7985	1.8512
.3587	.4	1.1090	1.1404	1.1766	1.2310	1.3321	1.4330	1.5392	1.6364	1.7014	1.7399
.4537	.5	1.1090	1.1404	1.1766	1.2309	1.3284	1.4124	1.4778	1.5286	1.5651	1.5893
.5534	.6	1.1090	1.1403	1.1765	1.2296	1.3114	1.3563	1.3656	1.3709	1.3822	1.3937
.6555	.7	1.1090	1.1401	1.1748	1.2182	1.2467	1.2254	1.1790	1.1510	1.1444	1.1462
.7639	.8	1.1087	1.1330	1.1510	1.1428	1.0523	.9708	.8977	.8570	.8420	.8386
.8784	.9	1.0816	1.0120	.9379	.8011	.6332	.5635	.5081	.4773	.4645	.4606
Pressure		-0.0085	-0.0437	-0.0857	-0.1512	-0.2818	-0.4332	-0.6628	-1.0344	-1.5176	-2.2649
X^*		.00024	.00118	.00237	.00474	.01184	.02369	.04737	.09475	.16581	.28424

Table 5.1(f) Development of axial velocity at the minor-axis and pressure
Aspect ratio = 1.4

Z	Y	Z/σ	X = .00010	X = .00040	X = .00100	X = .00300	X = .00500	X = .00800	X = .01000	X = .02000	X = .03000	X = .05000
			U	U	U	U	U	U	U	U	U	U
.0000	1.0		1.1012	1.1662	1.2414	1.3763	1.4693	1.5735	1.6271	1.8021	1.8893	1.9634
.2710	.9		1.1012	1.1662	1.2413	1.3763	1.4691	1.5724	1.6249	1.7920	1.8708	1.9338
.5352	.8		1.1012	1.1659	1.2427	1.3764	1.4683	1.5679	1.6161	1.7560	1.8095	1.8431
.7863	.7		1.1012	1.1651	1.2380	1.3754	1.4642	1.5533	1.5907	1.6777	1.6941	1.6930
1.0181	.6		1.1011	1.1639	1.2432	1.3727	1.4483	1.5110	1.5268	1.5410	1.5223	1.4950
1.2247	.5		1.1011	1.1619	1.2408	1.3571	1.3961	1.4128	1.4026	1.3511	1.3111	1.2753
1.4013	.4		1.1009	1.1681	1.2456	1.3036	1.2793	1.2589	1.2349	1.1379	1.0895	1.0520
1.5433	.3		1.1007	1.1473	1.2469	1.1964	1.1240	1.0962	1.0663	.9377	.8886	.8535
1.6473	.2		1.1004	1.1798	1.2220	1.0957	1.0091	.9899	.9278	.7866	.7384	.7258
1.7107	.1		1.1004	1.1382	1.2376	1.1046	1.0234	1.0059	.9624	.7369	.6817	.6860
1.7321		0.0	1.1004	1.1798	1.2217	1.0987	1.0222	1.0844	.9059	.7182	.6612	.6706
2.4674		.1	1.1004	1.1517	1.1704	1.0440	.9622	1.0002	.8623	.6858	.6338	.6391
1.7425		.2	1.1001	1.1289	1.1142	.9848	.8993	.9176	.8062	.6476	.6005	.6027
1.0000		.3	1.0995	1.1067	1.0518	.9181	.8311	.8337	.7389	.6026	.5601	.5600
.9000		.4	1.0978	1.0772	.9808	.8409	.7551	.7459	.6641	.5495	.5119	.5100
.8000		.5	1.0930	1.0290	.8956	.7502	.6687	.6516	.5837	.4874	.4547	.4516
.7000		.6	1.0772	.9468	.7880	.6431	.5697	.5484	.4955	.4151	.3878	.3840
.6000		.7	1.0250	.8126	.6495	.5169	.4556	.4339	.3956	.3314	.3099	.3062
.5000		.8	.8672	.6108	.4739	.3693	.3241	.3059	.2809	.2353	.2202	.2171
.4000		.9	.4919	.3381	.2581	.1978	.1731	.1621	.1495	.1253	.1173	.1155
		X*	.00074	.00296	.00740	.02221	.03701	.05922	.07402	.14804	.22207	.37011

Table 5.1(g) Development of axial velocity at the major-axis
Aspect ratio = 2.0

y	z/σ	X = .00010	X = .00040	X = .00100	X = .00300	X = .00500	X = .00800	X = .01000	X = .02000	X = .03000	X = .05000
		U	U	U	U	U	U	U	U	U	U
.0000	0.0	1.1012	1.1662	1.2414	1.3763	1.4693	1.5734	1.6271	1.8021	1.8893	1.9637
.0952	.1	1.1012	1.1662	1.2414	1.3762	1.4687	1.5707	1.6225	1.7909	1.8750	1.9468
.1907	.2	1.1012	1.1662	1.2414	1.3758	1.4659	1.5604	1.6066	1.7558	1.8308	1.8953
.2867	.3	1.1012	1.1662	1.2414	1.3738	1.4572	1.5367	1.5730	1.6925	1.7543	1.8079
.3836	.4	1.1012	1.1662	1.2411	1.3664	1.4341	1.4892	1.5122	1.5958	1.6419	1.6829
.4817	.5	1.1012	1.1662	1.2398	1.3425	1.3812	1.4042	1.4124	1.4594	1.4898	1.5182
.5812	.6	1.1012	1.1657	1.2314	1.2779	1.2765	1.2664	1.2616	1.2775	1.2943	1.3114
.6825	.7	1.1011	1.1603	1.1878	1.1342	1.0967	1.0629	1.0502	1.0449	1.0513	1.0599
.7859	.8	1.0972	1.1106	1.0225	.8759	.8258	.7858	.7721	.7570	.7573	.7692
.8916	.9	1.0048	.8186	.6109	.4948	.4599	.4320	.4236	.4101	.4082	.4083
Pressure		-0.0311	-0.1047	-0.1952	-0.3718	-0.5050	-0.6715	-0.7700	-1.2170	-1.6182	-2.3810
	X^*	.00074	.00296	.00740	.02221	.03701	.05922	.07402	.14804	.22207	.37011

Table 5.1(h) Development of axial velocity at the minor-axis and pressure
Aspect ratio = 2.0

z	Y	z/σ	X = .00001	X = .00002	X = .00005	X = .00010	X = .00020	X = .00050	X = .00100	X = .00500	X = .00800	X = .01000
			U	U	U	U	U	U	U	U	U	U
.0000	1.0		1.0711	1.0870	1.1219	1.1607	1.2110	1.3063	1.4188	1.7646	1.8527	1.8895
.6059	.9		1.0711	1.0870	1.1195	1.1594	1.2075	1.3052	1.4183	1.7546	1.8349	1.8674
1.1968	.8		1.0711	1.0856	1.1002	1.1511	1.2302	1.3108	1.4194	1.7202	1.7756	1.7945
1.7583	.7		1.0709	1.0760	1.0437	1.1228	1.1722	1.2957	1.4091	1.6449	1.6557	1.6530
2.2765	.6		1.0691	1.0459	.9738	1.1506	1.2357	1.3094	1.4008	1.4986	1.4502	1.4272
2.7386	.5		1.0619	1.0068	.9499	.9980	1.1778	1.2758	1.3347	1.2449	1.1627	1.1359
3.1333	.4		1.0459	.9810	.9699	1.1508	1.2733	1.2314	1.1812	.9228	.8515	.8320
3.4509	.3		1.0277	.8932	1.0040	1.1097	1.0606	1.0502	.8647	.6245	.5750	.5641
3.6834	.2		1.0171	.7667	.9679	1.1230	1.1965	.9708	.6275	.4105	.3750	.3945
3.8253	.1		1.0138	.7501	.9174	1.0894	1.2438	.9847	.6571	.3644	.3238	.4486
3.8730		0.0	1.0170	.7660	.9671	1.1227	1.1912	.9717	.6419	.3469	.3058	.4783
2.4674		.1	1.0116	.8219	.8910	1.0216	1.0566	.9024	.5879	.3110	.2929	.4319
3.8780		.2	1.0044	.8630	.8173	.9200	.9244	.8290	.5328	.2919	.2589	.3864
1.0000		.3	.9934	.8733	.7455	.8161	.7999	.7483	.4762	.2625	.2333	.3413
.9000		.4	.9731	.8445	.6740	.7101	.6856	.6586	.4176	.2315	.2062	.2962
.8000		.5	.9349	.7778	.5985	.6035	.5794	.5608	.3565	.1986	.1774	.2505
.7000		.6	.8624	.6782	.5127	.4959	.4753	.4568	.2926	.1638	.1466	.2038
.6000		.7	.7311	.5490	.4116	.3849	.3676	.3487	.2254	.1267	.1136	.1553
.5000		.8	.5181	.3931	.2924	.2670	.2529	.2371	.1545	.0872	.0733	.1061
.4000		.9	.2440	.2113	.1550	.1394	.1303	.1213	.0795	.0450	.0405	.0542
		X*	.00037	.00074	.00185	.00370	.00740	.01851	.03701	.18506	.29609	.37011

Table 5.1(1) Development of axial velocity at the major-axis
Aspect ratio = 4.0

y	z/σ	X = .00001	X = .00002	X = .00005	X = .00010	X = .00020	X = .00050	X = .00100	X = .00500	X = .00800	X = .01000
		U	U	U	U	U	U	U	U	U	U
.0000	0.0	1.0711	1.0870	1.1219	1.1607	1.2110	1.3063	1.4188	1.7646	1.8529	1.8895
.0989	.1	1.0711	1.0870	1.1219	1.1607	1.2110	1.3063	1.4182	1.7514	1.8367	1.8725
.1979	.2	1.0711	1.0870	1.1219	1.1607	1.2110	1.3061	1.4151	1.7103	1.7881	1.8211
.2971	.3	1.0711	1.0870	1.1219	1.1607	1.2110	1.3048	1.4055	1.6386	1.7051	1.7340
.3964	.4	1.0711	1.0870	1.1219	1.1607	1.2107	1.2993	1.3801	1.5323	1.5855	1.6095
.4960	.5	1.0711	1.0870	1.1219	1.1606	1.2088	1.2794	1.3229	1.3879	1.4274	1.4461
.5959	.6	1.0711	1.0870	1.1218	1.1591	1.1977	1.2207	1.2131	1.2015	1.2287	1.2422
.6961	.7	1.0711	1.0869	1.1199	1.1458	1.1441	1.0831	1.0312	.9711	.9879	.9963
.7969	.8	1.0699	1.0824	1.0938	1.0584	.9595	.8313	.7675	.6948	.7036	.7076
.8982	.9	1.0186	.9838	.8699	.6975	.5539	.4649	.4224	.3714	.3745	.3757
Pressure		-0.0149	-0.0320	-0.0705	-0.1148	-0.1745	-0.2944	-0.4486	-1.2470	-1.7513	-2.0775
	X^*	.00037	.00074	.00185	.00370	.00740	.01851	.03701	.18506	.29609	.37011

Table 5.1(j) Development of axial velocity at the minor-axis and pressure
Aspect ratio = 4.0

Lambda	Entrance-length $X_{infinity}$		Entrance-length $X^*_{infinity}$		Pressure defect $K_{infinity}$
	Present Analysis	Bhatti's Analysis	Present Analysis	Bhatti's Analysis	
1.1	0.3240	0.5450	0.1678	0.2824	0.580
1.2	0.1880	0.2800	0.2041	0.3040	0.565
1.4	0.1129	0.144	0.2674	0.3411	0.550
2.0	0.0916	0.0555	0.6780	0.4108	0.530

Table 5.2 Entrance length and fully developed pressure-defect

Chapter 6

CONCLUSIONS

The problem of flow development in an elliptical duct has been solved by a finite-difference method following transformation of the governing equations of motion into an elliptic-cylinder coordinate system. In order to solve the simultaneous finite-difference equations which result from the above method, an algorithm was developed to partition the coefficient matrix and thus utilise the banded structure of the partitioned matrix. This saves considerable computer time. The computed solution is compared with Bhatti's solution [24]. The differences between the present and Bhatti's results are more in the developing region near the entrance plane, specially within the boundary-layer, but they vanish as the flow develops. This is due to Bhatti's assumption regarding the growth of boundary-layer region and the velocity profile in this region that is based on the fully developed velocity profile. The present results compare better with those for the limiting case of developing flow in a circular pipe than Bhatti's results. However, comparison with experimental data, non-existant for developing flow in an elliptical duct, is the only real test.

It should be mentioned that the transformation from the Cartesian to the elliptic-cylinder system is not conducive to a numerical solution of the problem. First, it does not hold at the focus of the ellipse. Second, a uniform mesh in the elliptic-cylinder coordinate system implies a non-uniform mesh in the physical domain such that the grid size is small near

the focus of the ellipse and large near the wall. A numerical method on the other hand requires a non-uniform mesh of just the opposite nature due to large gradient near the wall. Thus a highly non-uniform mesh in the computational domain (elliptic-cylinder system) should be used. The present analysis and computer code (in Appendix C) is based on a non-uniform mesh but due to lack of time results could be obtained only for a uniform mesh in the computational domain.

Appendix A

Elliptic-cylinder coordinate system can be obtained by taking an orthogonal family of confocal ellipses and hyperbolas in a plane and translating them in the third direction, normal to the plane (Fig. A.1). The relation between the elliptic-cylinder coordinate (x, Ψ, η) and the Cartesian coordinate (x, y, z) may be written as

$$\begin{aligned} x &= x \,, \\ y &= c \sinh \eta \sin \Psi \,, \\ z &= c \cosh \eta \cos \Psi \,. \end{aligned} \tag{A.1}$$

The surfaces η = constant are the elliptic cylinders

$$\frac{z^2}{(c \cosh \eta)^2} + \frac{y^2}{(c \sinh \eta)^2} = 1, \tag{A.2}$$

while the surfaces Ψ = constant are the hyperbolic cylinders

$$\frac{z^2}{(c \cos \Psi)^2} - \frac{y^2}{(c \sin \Psi)^2} = 1. \tag{A.3}$$

Equation of the duct wall is

$$\frac{z^2}{a^2} + \frac{y^2}{b^2} = 1. \tag{A.4}$$

If equation (A.2) were to represent equation (A.4) for $\eta = \eta_w$,

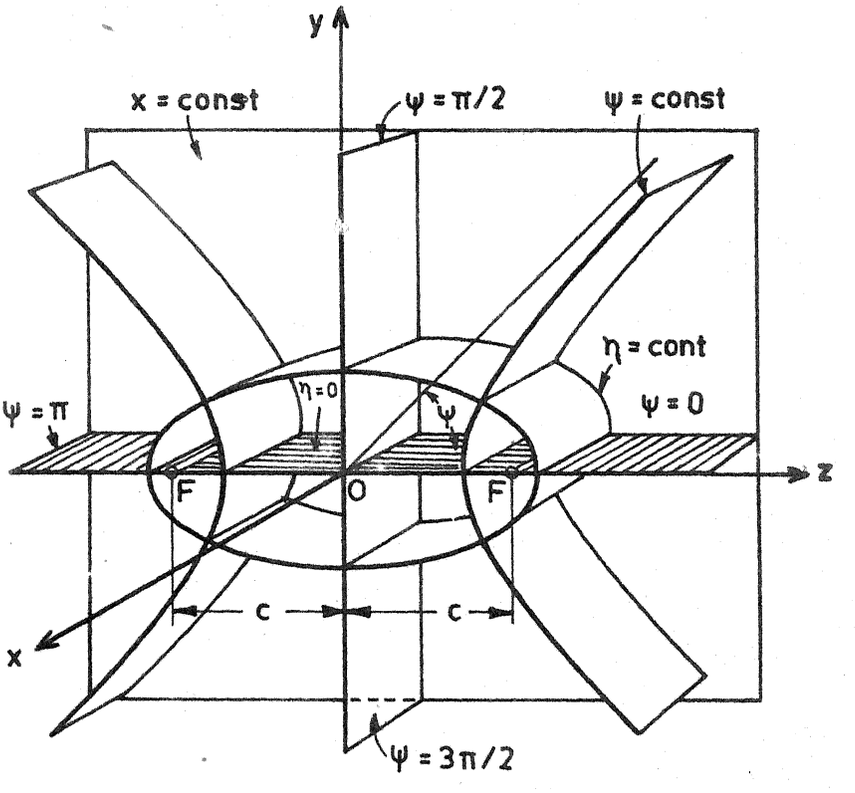

Fig. A1 Elliptic-cylinder coordinate system.

then

$$a = c \cosh \eta_w ,$$

$$b = c \sinh \eta_w , \qquad (A.5)$$

$$c = (a^2 - b^2)^{1/2} ,$$

and

$$\eta_w = \tanh^{-1}(b/a).$$

Appendix B

Elliptic cylinders represented by constant η surfaces are

$$\frac{z^2}{(c \cosh \eta)^2} + \frac{y^2}{(c \sinh \eta)^2} = 1. \qquad (B.1)$$

Slope of the tangent to this surface at any general point (Ψ, η) in the (y,z) plane is given by

$$\frac{dy}{dz} = -\cot \Psi \tanh \eta . \qquad (B.2)$$

Hence the slope of the normal to this surface at any general point (Ψ,η) in the (y,z) plane is given by

$$\frac{dy}{dz} = \tan \Psi \coth \eta . \qquad (B.3)$$

We shall define a variable $\theta(\Psi, \eta)$ (Fig. B.1) as

$$\tan \theta = \tan \Psi \coth \eta . \qquad (B.4)$$

The relationships between the transverse velocity components v_Ψ and v_η in the elliptic-cylinder coordinate system and the similar velocity components v and w in the Cartesian coordinate system are (Fig. B.1)

$$v_\Psi = v \cos \theta - w \sin \theta , \qquad (B.5)$$

and

$$v_\eta = v \sin \theta + w \cos \theta . \qquad (B.6)$$

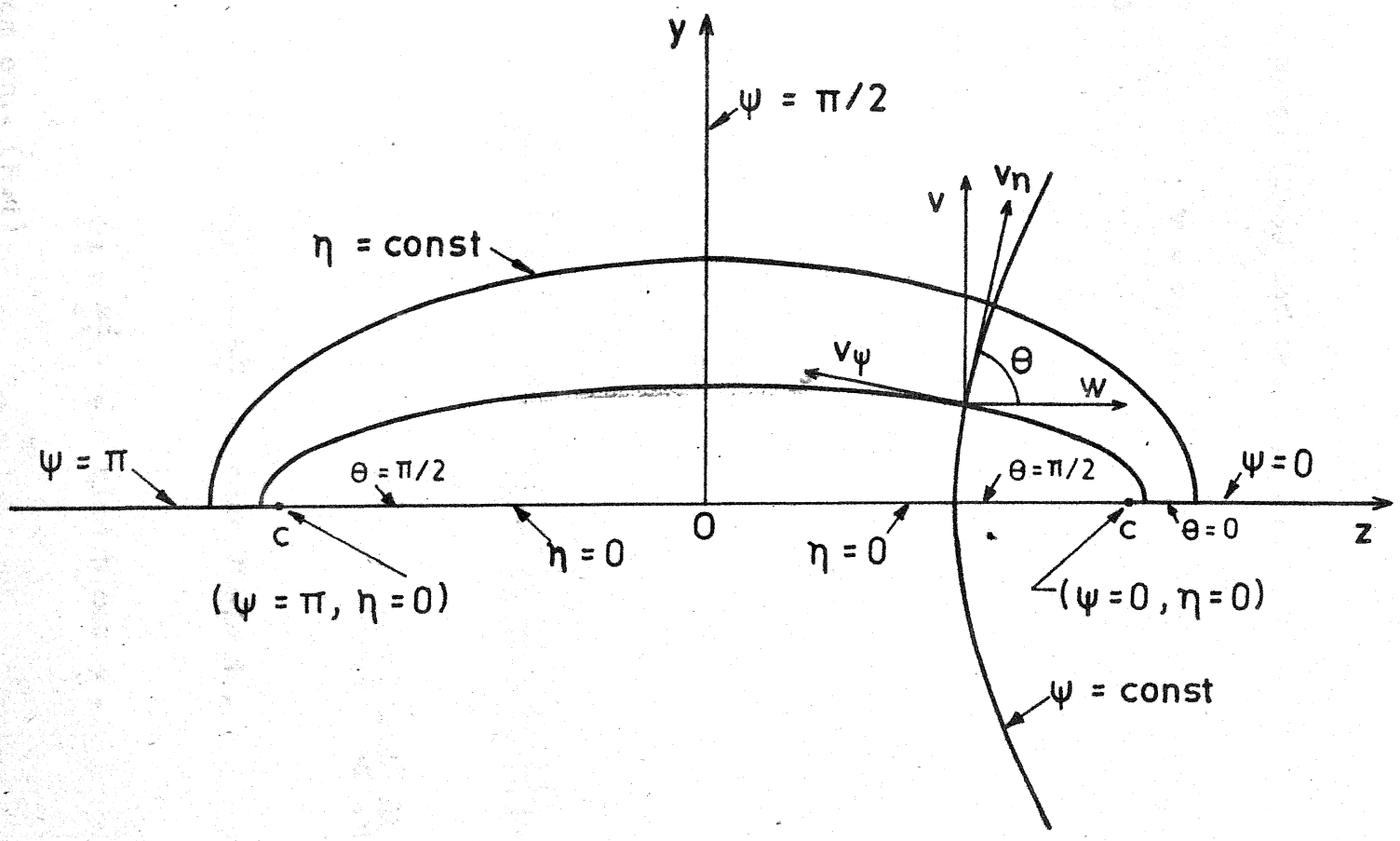

Fig. B.1 Velocity components in cartesian and elliptic-cylinder coordinate system.

From eqns. (B.5) and (B.6) it can also be seen that,

$$v = v_\Psi \cos\theta + v_\eta \sin\theta, \tag{B.7}$$

and

$$w = -v_\Psi \sin\theta + v_\eta \cos\theta. \tag{B.8}$$

We have the operators

$$\frac{\partial}{\partial \eta} = \frac{\partial z}{\partial \eta} \cdot \frac{\partial}{\partial z} + \frac{\partial Y}{\partial \eta} \cdot \frac{\partial}{\partial Y}, \tag{B.9}$$

and

$$\frac{\partial}{\partial \Psi} = \frac{\partial z}{\partial \Psi} \frac{\partial}{\partial z} + \frac{\partial Y}{\partial \Psi} \frac{\partial}{\partial Y}. \tag{B.10}$$

From (B.9) and (B.10)

$$\frac{\partial}{\partial Y} = \left[\frac{\partial z}{\partial \Psi} \frac{\partial}{\partial \eta} - \frac{\partial z}{\partial \eta} \cdot \frac{\partial}{\partial \Psi}\right] / \left[\frac{\partial Y}{\partial \eta} \frac{\partial z}{\partial \Psi} - \frac{\partial Y}{\partial \Psi} \frac{\partial z}{\partial \eta}\right], \tag{B.11}$$

and

$$\frac{\partial}{\partial z} = \left[-\frac{\partial z}{\partial \eta} \cdot \frac{\partial}{\partial \eta} - \frac{\partial z}{\partial \Psi} \frac{\partial}{\partial \Psi}\right] / \left[\frac{\partial Y}{\partial \eta} \frac{\partial z}{\partial \Psi} - \frac{\partial Y}{\partial \Psi} \frac{\partial z}{\partial \eta}\right], \tag{B.12}$$

since

$$\frac{\partial Y}{\partial \eta} = -\frac{\partial z}{\partial \Psi} = c \cosh\eta \sin\Psi, \tag{B.13}$$

and

$$\frac{\partial Y}{\partial \Psi} = \frac{\partial z}{\partial \eta} = c \sinh\eta \cos\Psi. \tag{B.14}$$

From eqn. (B.4)

$$\frac{\partial \theta}{\partial \eta} = -\tan\Psi \operatorname{cosech}^2\eta / \sec^2\theta, \tag{B.15}$$

and

$$\frac{\partial\theta}{\partial\Psi} = \sec^2\Psi \coth\eta \,/\, \sec^2\theta . \qquad (B.16)$$

When the operators (B.11) and (B.12) operate on eqns. (B.7) and (B.3) respectively, we get

$$\frac{\partial v}{\partial y} = \Big[-\Big(\frac{\partial v_\eta}{\partial\eta}\sin\theta + v_\eta\cos\theta\,\frac{\partial\theta}{\partial\eta} + \frac{\partial v_\Psi}{\partial\eta}\cos\theta - v_\Psi\sin\theta\,\frac{\partial\theta}{\partial\eta}\Big)\frac{\partial z}{\partial\Psi} + \Big(\frac{\partial v_\eta}{\partial\Psi}\sin\theta + v_\eta\cos\theta\,\frac{\partial\theta}{\partial\Psi} + \frac{\partial v_\Psi}{\partial\Psi}\cos\theta - v_\Psi\sin\theta\,\frac{\partial\theta}{\partial\Psi}\Big)\frac{\partial z}{\partial\eta}\Big] \Big/ \Big[\Big(\frac{\partial z}{\partial\Psi}\Big)^2 + \Big(\frac{\partial z}{\partial\eta}\Big)^2\Big], \qquad (B.17)$$

and

$$\frac{\partial w}{\partial z} = \Big[\Big(\frac{\partial v_\eta}{\partial\eta}\cos\theta - v_\eta\sin\theta\,\frac{\partial\theta}{\partial\eta} - \frac{\partial v_\Psi}{\partial\eta}\sin\theta - v_\Psi\cos\theta\,\frac{\partial\theta}{\partial\eta}\Big)\frac{\partial z}{\partial\eta} + \Big(\frac{\partial v_\eta}{\partial\Psi}\cos\theta - v_\eta\sin\theta\,\frac{\partial\theta}{\partial\Psi} - \frac{\partial v_\Psi}{\partial\Psi}\sin\theta - v_\Psi\cos\theta\,\frac{\partial\theta}{\partial\Psi}\Big)\frac{\partial z}{\partial\Psi}\Big] \Big/ \Big[\Big(\frac{\partial z}{\partial\Psi}\Big)^2 + \Big(\frac{\partial z}{\partial\eta}\Big)^2\Big] \qquad (B.18)$$

On addition and simplification (B.17) and (B.18) give

$$\frac{\partial v}{\partial Y} + \frac{\partial w}{\partial z} = [-c(v_\eta \sinh \eta \cosh \eta + v_\Psi \sin \Psi \cos \Psi)/(\cosh^2 \eta - \cos^2 \Psi)^{1/2} - c(\cosh^2 \eta - \cos^2 \Psi)^{1/2} (\frac{\partial v_\eta}{\partial \eta} + \frac{\partial v_\Psi}{\partial \Psi})] / [-c^2(\cosh^2 \eta - \cos^2 \Psi)] \quad (B.19)$$

Hence the continuity equation (2.1) transforms to

$$c(\cosh^2 \eta - \cos^2 \Psi) \frac{\partial u}{\partial x} + \frac{\partial}{\partial \eta} [v_\eta (\cosh^2 \eta - \cos^2 \Psi)^{1/2}] + \frac{\partial}{\partial \Psi} [v_\Psi (\cosh^2 \eta - \cos^2 \Psi)^{1/2}] = 0 \quad (B.20)$$

in the (x, Ψ, η) system.

Successive operations of (B.11) on u give

$$\frac{\partial u}{\partial Y} = [\frac{\partial z}{\partial \Psi} \frac{\partial u}{\partial \eta} - \frac{\partial z}{\partial \eta} \frac{\partial u}{\partial \Psi}] / D , \quad (B.21)$$

and

$$\frac{\partial^2 u}{\partial Y^2} = [\frac{\partial z}{\partial \Psi} \frac{\partial}{\partial \eta} (\frac{\partial u}{\partial Y}) - \frac{\partial z}{\partial \eta} \frac{\partial}{\partial \Psi} (\frac{\partial u}{\partial Y})] / D , \quad (B.22)$$

where $D = [\frac{\partial Y}{\partial \eta} \frac{\partial z}{\partial \Psi} - \frac{\partial Y}{\partial \Psi} \frac{\partial z}{\partial \eta}]$

$= -c^2(\cosh^2 \eta - \cos^2 \Psi)$.

Successive operations of (B•12) on u give

$$\frac{\partial u}{\partial z} = -\left[\frac{\partial z}{\partial \eta}\frac{\partial u}{\partial \eta} + \frac{\partial z}{\partial \Psi}\frac{\partial u}{\partial \Psi}\right]/D \,, \qquad (B•23)$$

and

$$\frac{\partial^2 u}{\partial z^2} = -\left[\frac{\partial z}{\partial \eta}\frac{\partial}{\partial \eta}\left(\frac{\partial u}{\partial z}\right) + \frac{\partial z}{\partial \Psi}\frac{\partial}{\partial \Psi}\left(\frac{\partial u}{\partial z}\right)\right]/D. \qquad (B•24)$$

Addition of eqns. (B•22) and (B•24) with further simplification gives

$$\frac{\partial^2 u}{\partial y^2} + \frac{\partial^2 u}{\partial z^2} = \left[\frac{\partial^2 u}{\partial \Psi^2} + \frac{\partial^2 u}{\partial \eta^2}\right]/\left[c^2(\cosh^2\eta - \cos^2\Psi)\right] \qquad (B•25)$$

From eqns. (B•7), (B•8), (B•21) and (B•23)

$$v\frac{\partial u}{\partial y} = (v_\eta \sin\theta + v_\Psi \cos\theta)\left(\frac{\partial z}{\partial \Psi}\frac{\partial u}{\partial \eta} - \frac{\partial z}{\partial \eta}\frac{\partial u}{\partial \Psi}\right)/D, \qquad (B•26)$$

and

$$w\frac{\partial u}{\partial z} = (v_\eta \cos\theta - v_\Psi \sin\theta)\left(-\frac{\partial z}{\partial \eta}\frac{\partial u}{\partial \eta} - \frac{\partial z}{\partial \Psi}\frac{\partial u}{\partial \Psi}\right)/D. \qquad (B•27)$$

Addition of eqns. (B•26) and (B•27), with the substitutions

$$\sin\theta = \sin\Psi\cosh\eta/(\cos^2\Psi\sinh^2\eta + \sin^2\Psi\cosh^2\eta),$$

and

$$\cos\theta = \cos\Psi\sinh\eta/(\cos^2\Psi\sinh^2\eta + \sin^2\Psi\cosh^2\eta),$$

and further simplifications reduces to

$$v\frac{\partial u}{\partial y} + w\frac{\partial u}{\partial z} = \left[v_\Psi\frac{\partial u}{\partial \Psi} + v_\eta\frac{\partial u}{\partial \eta}\right]/\left[c(\cosh^2\eta - \cos^2\Psi)^{1/2}\right]. \qquad (B•28)$$

Substitution of eqns. (B.25) and (B.28) in the axial momentum eqn. (2.6) gives

$$u\frac{\partial u}{\partial x} + \frac{\left[v_\Psi \frac{\partial u}{\partial \Psi} + v_\eta \frac{\partial u}{\partial \eta}\right]}{c(\cosh^2\eta - \cos^2\Psi)^{1/2}}$$

$$= -\frac{1}{\rho}\frac{dp}{dx} + \frac{\nu\left(\frac{\partial^2 u}{\partial \Psi^2} + \frac{\partial^2 u}{\partial \eta^2}\right)}{c^2(\cosh^2\eta - \cos^2\Psi)} . \qquad (B.29)$$

Substitution of eqns. (B.7), (B.8), (A.1) and (A.5) into eqn. (2.10) gives

$$\frac{v_\Psi \cos\theta + v_\eta \sin\theta}{-v_\Psi \sin\theta + v_\eta \cos\theta} = \coth^2\eta_w \tan\Psi \tanh\eta ,$$

or

$$\frac{v_\Psi}{v_\eta} = -\frac{[\cot\Psi + \coth^2\eta_w \tan\Psi]}{[\coth\eta - \coth^2\eta_w \tanh\eta]} . \qquad (B.30)$$

Boundary conditions :

(a) The condition $\partial u(x,0,z)/\partial y = 0$:

Now $$\frac{\partial u}{\partial y} = -c\left[\cosh\eta \sin\Psi \frac{\partial u}{\partial \eta} + \sinh\eta \cos\Psi \frac{\partial u}{\partial \Psi}\right] / \left[-c^2(\cosh^2\eta - \cos^2\Psi)\right] \qquad (B.31)$$

When $y = 0$, either Ψ or η is zero (Fig. B.1).

For $\eta = 0$, eqn. (B.31) gives

$$\frac{\partial u}{\partial \eta}(x, 0 < \Psi \leq \pi/2, 0) = 0 ,$$

and

for $\Psi = 0$ eqn. (B.31) gives

$$\frac{\partial u}{\partial \Psi}(x, 0, 0 < \eta \leq \eta_w) = 0.$$

(b) The condition $\partial u(x, y, 0)/\partial z = 0$:

Now $\frac{\partial u}{\partial z} = c\,[\sinh \eta \cos \Psi \frac{\partial u}{\partial \eta} - \cosh \eta \sin \Psi \frac{\partial u}{\partial \Psi}]/[c^2(\cosh^2 \eta - \cos^2 \Psi)]$. (B.32)

When $z = 0$, $\Psi = \pi/2$ and eqn. (B.32) gives

$$\frac{\partial u}{\partial \Psi}(x, \pi/2, \eta) = 0.$$

(c) The condition $v(x, 0, z) = 0$:

This gives

$$v_\eta (x, 0 < \Psi \leq \pi/2, 0) = 0 , \qquad (B.33)$$

since $\theta = \pi/2$ along $\eta = 0$ (Fig. B.1),

and

$$v_\Psi (x, 0, 0 < \eta \leq \eta_w) = 0 , \qquad (B.34)$$

since $\theta = 0$ along $\Psi = 0$ (Fig. B.1).

(d) The condition $\partial v(x, y, 0)/\partial z = 0$:

Now $\frac{\partial v}{\partial z} = [(\sinh \eta \cosh \eta \sin \Psi \cos \Psi)(\frac{\partial v_\eta}{\partial \eta} - \frac{\partial v_\Psi}{\partial \Psi})$

$+ (\cos^2 \Psi + \cosh^2 \eta) \sin \Psi \sinh \eta (v_\Psi \sin \Psi \cosh \eta$

$$- v_\eta \cos \Psi \sinh \eta)/(\cosh^2 \eta - \cos^2 \Psi)$$

$$+ (\sinh^2 \eta \cos^2 \Psi \frac{\partial v_\Psi}{\partial \eta}$$

$$+ \cosh^2 \eta \sin^2 \Psi \frac{\partial v_\eta}{\partial \Psi})]/[c(\cosh^2 \eta - \cos^2 \Psi)^{3/2}] .$$

(B.35)

When $z = 0$, $\Psi = \pi/2$ and eqn. (B.33) gives

$$\frac{\partial v_\eta}{\partial \Psi} = -v_\Psi \tanh \eta . \qquad \text{(B.36)}$$

(e) The condition $w(x,y,0) = 0$:

This gives

$$v_\Psi (x, \pi/2, \eta) = 0,$$

since $\theta = \pi/2$ along $\Psi = \pi/2$ (Fig. B.1).

Substitution of this in eqn. (B.36) results

$$\frac{\partial v_\eta}{\partial \Psi} (x, \pi/2, \eta) = 0.$$

(f) The condition $\partial w(x,0,z)/\partial y = 0$:

$$\text{Now } \frac{\partial w}{\partial y} = [(\sin^2 \Psi + \sinh^2 \eta)\cosh \eta \cos \Psi (v_\eta \cosh \eta \sin \Psi$$

$$+ v_\Psi \sinh \eta \cos \Psi)/(\cosh^2 \eta - \cos^2 \Psi)$$

$$+ \sinh \eta \cosh \eta \sin \Psi \cos \Psi (\frac{\partial v_\eta}{\partial \eta} + \frac{\partial v_\Psi}{\partial \Psi})$$

$$- (\cosh^2 \eta \sin^2 \Psi \frac{\partial v_\Psi}{\partial \eta}$$

$$+ \sinh^2 \eta \cos^2 \Psi \frac{\partial v_\eta}{\partial \Psi})] / [c(\cosh^2 \eta - \cos^2 \Psi)^{3/2}]. \quad (B.37)$$

For $\eta = 0$, eqn. (B.37) gives

$$\frac{\partial v_\Psi}{\partial \eta} (x, 0 < \Psi \leq \pi/2, 0) = v_\eta \cot \Psi . \quad (B.38)$$

For $\Psi = 0$, eqn. (B.37) gives

$$\frac{\partial v_\eta}{\partial \Psi} (x, 0, 0 < \eta \leq \eta_w) = v_\Psi \coth \eta . \quad (B.39)$$

Substitution of eqns. (B.33) and (B.34) respectively in eqns. (B.38) and (B.39) results

$$\frac{\partial v_\Psi}{\partial \eta} (x, 0 < \Psi \leq \pi/2, 0) = 0$$

and

$$\frac{\partial v_\eta}{\partial \Psi} (x, 0, 0 < \eta \leq \eta_w) = 0.$$

```
*** DFEC1.FOR *** Double precision version  *** Uniform - grid ***
for developing flow velocity profile in elliptical ducts

It uses the subroutine SOLVER (see Ch.4 in the text )

U,V,W are not stored on the duct wall as they are all zero there

The singularity at the focus of the ellipse (c,0) has been
eliminated as explained in Chapter.3

This code has been structured so that BREAK and subsequent RESTART
in the marching X-direction is possible

Exact curve fitting of order NR is included where NR is from
IG(N7,NR-1).For this purpose it calls subroutine CRVSET and
CRVSET calls PLYFIT and SOLVE
Besides this prog. calls NORMFN which intern calls PLTMOD

***** ----- ****** ----- ***** ----- ***** -+-+-+- ****** ----- *****

Variables:
    AL = duct half-width along the major-axis 'a'
    B  = duct half-width along the minor-asis 'b'
    DX = step size in the marching X-direction
    C  = focal length sqrt(a.a - b.b)
    SGM= 2.Eta-wall/PI
    EW = Eta-wall
    DZ = step size in the Z-direction (fig.3.2)
    DY = step size in the Y-direction (fig.3.2)
    X  = location the X-dir. upto which marching has been completed
    P0 = is the unknown pressure at location (i+1)
    R0 = known RHS of the integral continuity eqn.(3.17)
    U0 = corrected entrance velocity
    DEL= FF' (fig.3.3)
    XST= is the strating X after a break in the marching
    PR = storage variable for pressure P0
    CV = storage variable for centre-line velocity U(MM),where
         MM = m4*n8+1 (fig.3.2)
    IG(N7,NR-1) in this the first index represents 'j' and the
         second represents 'k'(fig.3.2)
    U,V,W are velocity components along X,Y,Z directions resply.
    AA = A in the eqn.(2.15)
    SA = sqrt of AA
    P  = C in eqn.(2.15)
    Q  = D in eqn.(2.15)
    BB = B in eqn.(2.17)
    BS = is one-dim. array for the elements of unsymmetric banded
         matrix [G] (see Chapter.4 and the subroutine SOLVER )
    R  = {R} is the right hand side column vector (see SOLVER )
    E  = {E} is the first row of the matrix [S] (see SOLVER )
    H  = {H} is the last column of [S]
    M  = m4 (fig.3.2)
    N  = n8 (fig.3.2)
    IREAD = 0 indicates starting from X=0
         N.E.to zero  indicates starting at some X>0
    IGRAP = 1 indicates plotting of W is needed and the output be
         stored in DFEC5.CDR
         N.E. 1 indicates plotting of W is not needed
***** ----- ****** ----- ****** ------- ******* ------- ****** --- **
    REAL *8 AL,B,DX,C2,C,BA,PI,SGM,CTH2,P4,P2,Y,Z,C1,Y1,Z1,Y2,Z2,F
   1,FX,EW,DZ,DY,X,P0,R0,U0,DEL,UL,XST
    REAL *8 PR(201),CV(201),WD(20),XG(21)
    INTEGER IG(11,4)
    REAL *8 U(220),V(220),W(220),AA(220),SA(220),P(220),Q(220)
   1,BB(200),BS(8810),R(220),E(220),H(220),A3K(220)
    OPEN (UNIT=2,DEVICE='DSK',FILE='DFEC1.CDR',ACCESS='SEQIN' )
    OPEN (UNIT=4,DEVICE='DSK',FILE='DFEC4.CDR',ACCESS='SEQIN' )
    OPEN (UNIT=6,DEVICE='DSK',FILE='DFEC1.OUT',ACCESS='SEQOUT')
    OPEN (UNIT=8,DEVICE='DSK',FILE='DFEC4.CDR',ACCESS='SEQOUT')
    OPEN (UNIT=10,DEVICE='DSK',FILE='DFEC5.CDR',ACCESS='SEQOUT')
```

```
      OPEN (UNIT=12,DEVICE='DSK',FILE='DFEC2.OUT',ACCESS='SEQOUT')
      READ(2,*)AL,B,M,N,IREAD,DEL,IGRAP,UL
      C2=AL*AL-B*B
      C=DSQRT(C2)
      BA=B/AL
      EW=0.5D0*DLOG((1.0D0+BA)/(1.0D0-BA))
      PI=3.14159265358979 3D0
      P2=0.5D0*PI
      P4=0.25D0*PI
      SGM=EW/P2
      DY=1.0D0/DFLOAT(N)
      DZ=SGM/DFLOAT(M)
      MN=M*N
      MN1=MN+M
      MN2=MN1+1
      M1=M+1
      N1=N+1
      N2=N+2
      MM1=M-1
      MM=MN+1
      MNM=MN1+M
      KKN=MN1-1
      MI2=2*M
      M2=MN-M
      M3=2*M+1
      NM1=N-1
      M8=M*M1+M3*NM1*M+2*M*M
! for curve fitting and subsequent interpolation for 'W'
! XG contains length Z for various K's
      XG(1)=0
      DO 18 L=1,MM1
      C2=L
8     XG(L+1)=C2*DZ
      XG(M1)=SGM
      WRITE(6,530)AL,B,C,EW,SGM,DY,DZ,M,N
      Z1=DEXP(EW)
      Z2=DEXP(-EW)
      CTH2=(Z1+Z2)/(Z1-Z2)
      CTH2=CTH2*CTH2
      C2=2.0D0*EW
      RO=(DEXP(C2)-DEXP(-C2))/(PI*DZ*DY)
! see eqn.(3.17) has been multiplied by 4
! FOR THE CALCULATION OF  AA  SA  P  Q  BB
      AL=P2*DZ
      B=P2*DY
      C=PI*DZ
      BA=PI*DY
! FOR J=1 AND K=1
      C2=P2*DEL
      Z=DEXP(C2)
      F=DEXP(-C2)
      Z=0.6D0*(Z+F)
      AA(1)=Z*Z-1.0D0
      SA(1)=DSQRT(AA(1))
      C2=PI*DEL
      Z=DEXP(C2)
      F=DEXP(-C2)
      P(1)=P4*0.5D0*(Z-F)/SA(1)
      Q(1)=P2
      WRITE(6,560)DEL,AA(1),P(1),Q(1)
      BB(1)=0
! FOR J=1 AND K=2(1)M
      DO 8 I=2,M
      C2=DFLOAT(I-1)
      Z1=C2*AL
      Z2=C2*C
      Z=DEXP(Z1)
      F=DEXP(-Z1)
      Z1=DEXP(Z2)
      Z2=DEXP(-Z2)
```

```
      Z=0.5D0*(Z+F)
      F=0.5D0*(Z1-Z2)
      AA(I)=Z*Z-1.0D0
      SA(I)=DSQRT(AA(I))
      Z=P4/SA(I)
      P(I)=Z*F
      Q(I)=0
8     BB(I)=0
C1 FOR J=2(1)N AND K=1
      K=0
      DO 12 I=M1,MN,M
      K=K+1
      C2=DFLOAT(K)
      Y1=C2*B
      Y2=C2*BA
      Y=DCOS(Y1)
      FX=DSIN(Y2)
      AA(I)=1.0D0-Y*Y
      SA(I)=DSQRT(AA(I))
      Y=P4/SA(I)
      P(I)=0
      Q(I)=Y*FX
12    BB(I)=0
C1 FOR J=N+1 AND K=1
      AA(MM)=1
      SA(MM)=1
      P(MM)=0
      Q(MM)=0
C1 FOR J=N+1 AND K=2(1)M
      DO 14 I=2,M
      K=MN+I
      C2=DFLOAT(I-1)
      Z1=C2*AL
      Z2=C2*C
      Z=DEXP(Z1)
      F=DEXP(-Z1)
      Z1=DEXP(Z2)
      Z2=DEXP(-Z2)
      Z=0.5D0*(Z+F)
      F=0.5D0*(Z1-Z2)
      AA(K)=Z*Z
      SA(K)=DSQRT(AA(K))
      P(K)=P4*F/SA(K)
14    Q(K)=0
C1 FOR J=2(1)N AND K=2(1)M
      DO 16 J=2,N
      K1=(J-1)*M
      C2=DFLOAT(J-1)
      Y1=C2*B
      Y2=C2*BA
      C1=DCOS(Y1)
      FX=DSIN(Y2)
      C2=DSIN(Y1)
      Y1=C2/C1
      Y2=C1/C2
      Y=Y2+CTH2*Y1
      C1=C1*C1
      DO 16 I=2,M
      K=K1+I
      C2=DFLOAT(I-1)
      Z1=C2*AL
      Z2=C2*C
      Z=DEXP(Z1)
      F=DEXP(-Z1)
      Z1=DEXP(Z2)
      Z2=DEXP(-Z2)
      Y2=(Z+F)/(Z-F)
      C2=(Z-F)/(Z+F)
      Z=0.5D0*(Z+F)
      Y1=0.5D0*(Z1-Z2)
```

```
      BB(K)=Y/(Y2-CTH2*C2)
      AA(K)=Z*Z-C1
      SA(K)=DSQRT(AA(K))
      C2=P4/SA(K)
      P(K)=C2*Y1
 15   Q(K)=C2*FX
      B=1.0D0/DY
      C=1.0D0/DZ
      X=0
      Y1=1.0D0/(DY*DY)
      Z1=1.0D0/(DZ*DZ)
      Y2=2.0D0*Y1
      Z2=2.0D0*Z1
      Y=1.0D0/(2.0D0*DY)
      Z=1.0D0/(2.0D0*DZ)
      F=Y2+Z2
C FIRST LINE IN THE UNPARTISIONED MATRIX
C THIS HAS BEEN MULTIPLIED BY " 4 " & IS UNCHANGED FROM THE SOLVER
      E(1)=AA(1)
      DO 105 L=2,M
105   E(L)=2.0D0*AA(L)
      J=M
      DO 110 K=M1,MN,M
      I=K-1
      J=J+1
      E(J)=2.0D0*AA(K)
      DO 110 L=2,M
      J=J+1
110   E(J)=4.0D0*AA(I+L)
      J=J+1
      E(J)=AA(MM)
      DO 115 L=2,M
      J=J+1
115   E(J)=2.0D0*AA(MN+L)
      IF(IREAD.EQ.1) GO TO 3
C CALCULATION OF THE INI." UO "
      DEL=0
      DO 120 L=1,MN1
120   DEL=DEL+E(L)
      U0=R0/DEL
      WRITE(6,500)U0
      DO 5 I=1,MN1
      U(I)=U0
      V(I)=0
5     W(I)=0
      P0=0
      GO TO 2
3     READ(4,515)(U(I),V(I),W(I),I=1,MN1)
      READ(4,580)P0,X
2     CONTINUE
      XST=X
C  SETTING UP THE NON-ZERO ELEMENTS OF THE PARTISIONED MATRIX "BS"
      READ(2,*)NOP
C     see NOP is NR-1
      READ(2,*)((IG(I,J),J=1,NOP),I=1,N1)
      WRITE(6,570)((IG(I,J),J=1,NOP),I=1,N1)
      READ(2,*)NDX
      DO 55 IN=1,NDX
      READ(2,*)DX,IWRIT,ILESS,IFULL,IFIT
C NDX = no of delta-X's at the present stretch
C IWRITE = no of steps in the marching X-direc. with delta-X=DX
C ILESS = 1 indicates writing U,V,W at (XST + IWRIT*DX) to 6-decimals
C     in the file DFEC1.OUT
C     otnewise no writing is done
C IFULL = 1 indicates writing U,V,W to 16 decimals in the file
C     DFEC2.COR
C     otnerwise no writing is done
C IFIT = 1 indicates curve fitting is required for 'W'
C     otnerwise no curve fitting is done
      FX=1.0D0/DX
```

```
      DO 125 L=1,MN1
125   ABX(L)=FX*AA(L)
      DO 255 KN=1,IWRIT
C SETTING (BS(I),1<=I<=M8) TO ZERO
      DO 305 L=1,M8
305   BS(L)=0
C MAIN DIAGONAL (I,I),FIRST M-ROWS
      BS(1)=-3.0D0*SA(1)*W(1)*Z+ABX(1)*U(1)-Z2+Y2
      J=1
      DO 310 L=1,MM1
      J=J+M1+L
      I=L+1
310   BS(J)=F+ABX(I)*U(I)
C MAIN DIAGONAL (I,I) UPTO "MN"TH ROW
      DO 315 L=M1,MN
      J=J+M3
315   BS(J)=F+ABX(L)*U(L)
C MAIN DIAGONAL (I,I), LAST M-ROWS
      I=0
      DO 320 L=MM,MN1
      I=I+1
      J=J+M3+1-I
320   BS(J)=F+ABX(L)*U(L)
C DIAGONAL (I,I+1),FIRST M-ROWS
      BS(2)=2.0D0*SA(1)*W(1)/DZ+5.0D0*Z1
      BS(3)=-SA(1)*W(1)*Z-4.0D0*Z1
      BS(4)=Z1
      J=2
      I=M1
      DO 325 L=2,MM1
      I=I+1
      J=J+I
325   BS(J)=Z*W(L)*SA(L)-Z1
      I=I+1
      J=J+I
      BS(J)=0
C DIAGONAL (I,I+1), UPTO "MN"TH ROW
      DO 330 L=MI2,MN,M
      I=L-M
      J=J+M3
      BS(J)=-Z2
      DO 335 K=2,MM1
      NS=I+K
      J=J+M3
335   BS(J)=Z*W(NS)*SA(NS)-Z1
      J=J+M3
330   BS(J)=0
C DIAGONAL (I,I+1),LAST M-ROWS
      I=M3
      J=J+I
      BS(J)=-Z2
      DO 340 L=2,MM1
      I=I-1
      NS=MN+L
      J=J+I
340   BS(J)=Z*W(NS)*SA(NS)-Z1
C DIAGONAL (I,I+M),FIRST M-ROWS
      I=M
      J=0
      DO 345 L=1,M
      I=I+1
      J=J+I
345   BS(J)=-Y2
C DIAGONAL (I,I+M),UPTO "MN"TH ROW
      DO 350 L=M1,MN
      J=J+M3
350   BS(J)=Y*V(L)*SA(L)-Y1
C DIAGONAL (I,I-1),FIRST M-ROWS
      I=M1
      J=0
```

```
      DO 355 L=2,M
      I=I+1
      J=J+I
355   BS(J)=-Z*W(L)*SA(L)-Z1
      I=I+1
      J=J+I
      BS(J)=0
C DIAGONAL (I,I-1),UPTO "MN"TH ROW
      DO 360 L=MI2,MN,M
      I=L-M
      DO 365 K=2,M
      NS=I+K
      J=J+M3
365   BS(J)=-Z*W(NS)*SA(NS)-Z1
      J=J+M3
360   BS(J)=0
C DIAGONAL (I,I-1),LAST M-ROWS
      I=M3
      DO 370 L=2,M
      I=I-1
      J=J+I
      NS=MN+L
370   BS(J)=-Z*W(NS)*SA(NS)-Z1
C DIAGONAL (I,I-M),ROW M+1 TO MN
      J=M*M1
      J=J/2+M*M+1-M3
      DO 375 L=M1,MN
      J=J+M3
375   BS(J)=-Y*V(L)*SA(L)-Y1
C DIAGONAL (I,I-M), LAST M-ROWS
      I=M3+1
      DO 380 L=MM,MN1
      I=I-1
      J=J+I
380   BS(J)=-Y2
C LAST COLUMN OF UNPARTIONED MATRIX, See this with R is destroyed
      DO 140 I=1,MN1
      H(I)=ABX(I)
140   R(I)=ABX(I)*(P0+U(I)*U(I))
C SOLUTION BY PARTISON OF THE MATRIX
      CALL SOLVER(R,BS,H,E,P0,R0,MN1,1,M,M,1.0D-15,IER)
C     WRITE(6,540)(R(I),I=1,MN1),P0
C FOR j=N AND k=M(-1)1
      V(MN)=-ABX(MN)*(R(MN)-U(MN))/(BB(MN)*(-P(MN)+C*SA(MN))+
     1Q(MN)-B*SA(MN))
      W(MN)=-BB(MN)*V(MN)
      DO 150 L=2,MM1
      I=MM-L
      K=I+1
      V(I)=-(ABX(I)*(R(I)-U(I))+C*SA(I)*W(K))/(BB(I)*(-P(I)+C*
     1SA(I))+Q(I)-B*SA(I))
150   W(I)=-BB(I)*V(I)
      I=I-1
      K=I+1
      V(I)=-(ABX(I)*(R(I)-U(I))+C*SA(I)*W(K))/(Q(I)-B*SA(I))
      W(I)=0
      IF(IFIT-1)405,410,405
410   CALL CRVSET(W,M,I,M1,N1,NOP,XG,IG,SGM,DEL)
      IX=I+1
      DO 152 KX=IX,MN
152   V(KX)=-W(KX)/BB(KX)
      V(I)=-(ABX(I)*(R(I)-U(I))+C*SA(I)*W(K))/(Q(I)-B*SA(I))
405   CONTINUE
C FOR j=(N-1)(-1)2 AND k=M(-1)1
      DO 155 J=2,NM1
      I=(N1-J)*M
      JX=I
      IM=I+M
      V(I)=-(ABX(I)*(R(I)-U(I))+B*SA(I)*V(IM))/(BB(I)*(-P(I)+C*
     1SA(I))+Q(I)-B*SA(I))
```

```
      W(I)=-BB(I)*V(I)
      DO 160 K=2,MM1
      I=I-1
      IM=I+M
      I1=I+1
      V(I)=-(ABX(I)*(R(I)-U(I))+SA(I)*(C*W(I1)+B*V(IM)))/(BB(I)*
     1(-P(I)+C*SA(I))+Q(I)-B*SA(I))
160   W(I)=-BB(I)*V(I)
      I=I-1
      IM=I+M
      I1=I+1
      V(I)=-(ABX(I)*(R(I)-U(I))+SA(I)*(C*W(I1)+B*V(IM)))/(Q(I)-B*
     1SA(I))
      W(I)=0
      IF(IFIT-1)155,415,155
415   CALL CRVSET(W,M,I,M1,N1,NOP,XG,IG,SGM,DEL)
      IX=I+1
      DO 158 KX=IX,JX
158   V(KX)=-W(KX)/BB(KX)
      V(I)=-(ABX(I)*(R(I)-U(I))+SA(I)*(C*W(I1)+B*V(IM)))/(Q(I)-B*
     1SA(I))
155   CONTINUE
C FOR j=1 AND <=M(-1)1
      W(M)=-(ABX(M)*(R(M)-U(M))+SA(M)*B*V(M+M))/(P(M)-C*SA(M))
      V(M)=0
      DO 165 L=2,M
      I=M1-L
      IM=I+M
      I1=I+1
      W(I)=-(ABX(I)*(R(I)-U(I))+SA(I)*(C*W(I1)+B*V(IM)))/(P(I)-C*
     1SA(I))
165   V(I)=0
      IF(IFIT-1)420,425,420
425   CALL CRVSET(W,M,I,M1,N1,NOP,XG,IG,SGM,DEL)
420   CONTINUE
C FOR j=N+1 AND k=M(-1)1
      W(MN1)=-(ABX(MN1)*(R(MN1)-U(MN1))-SA(MN1)*B*V(MN))/(P(MN1)-
     1C*SA(MN1))
      V(MN1)=0
      DO 170 L=2,MM1
      I=MN2-L
      IM=I-M
      I1=I+1
      W(I)=-(ABX(I)*(R(I)-U(I))+SA(I)*(C*W(I1)-B*V(IM)))/(P(I)-C*
     1SA(I))
170   V(I)=0
      V(MM)=0
      W(MM)=0
      IF(IFIT-1)430,435,430
435   CALL CRVSET(W,M,MM,M1,N1,NOP,XG,IG,SGM,DEL)
430   CONTINUE
C  TRANSFERING U'S STORED IN "R" TO "U"
      DO 175 I=1,MN1
175   U(I)=R(I)
      X=X+DX
      PR(KN)=P0
      CV(KN)=U(MM)
255   CONTINUE
      WRITE(12,600)XST,DX,IWRIT,X
      WRITE(12,602)(J,CV(J),PR(J),J=1,IWRIT)
      IF(ILESS-1)485,490,485
490   WRITE(6,585)(J,U(J),V(J),W(J),J=1,MN1)
      WRITE(6,590)P0,X,DX
485   IF(IFULL-1)498,495,498
495   WRITE(8,515)(U(J),V(J),W(J),J=1,MN1)
      WRITE(8,580)P0,X
498   IF(IGRAP-1)55,445,55
C
C The following steps are to plot the interpolated W's
```

```
445   DO 450 KG=1,N1
      NG=(KG-1)*M
      DO 455 LG=1,M
455   WD(LG)=W(NG+LG)
      CALL NORMFN(WD,DZ,M,X,KG,UL)
450   WRITE(10,460)
460   FORMAT(/)
55    CONTINUE
      STOP
500   FORMAT(' INI. VELOCITY U0 = ',D18.11)
505   FORMAT(10(1X,E12.5))
510   FORMAT(10(1X,E12.5))
530   FORMAT(' A=',F9.6,' B=',F9.6,' C=',F9.5,' EN=',F9.6,' SGM='
     1,F9.6 /' DY=',F6.4,' DZ=',F6.4,' M=',I2,' N=',I2)
540   FORMAT(8(1X,E15.8))
560   FORMAT(' DEL-Z = ',F11.9,' AA(1)= ',E13.6,' P(1)= ',E13.6,' Q(1
     1)= ',E13.6)
515   FORMAT(2(F19.16,2D23.16))
570   FORMAT(4I3)
580   FORMAT(D23.16,D15.8)
585   FORMAT(3(I4,F9.6,2E14.6))
590   FORMAT(D19.11,E12.4,E14.5)
600   FORMAT(' X-START=',F9.6,' DX=',F9.6,' NO.OF STEPS=',I3
     1,' X-END=',F9.6)
602   FORMAT(5(I3,F9.6,F10.6))
      END
```

```
      OPEN(UNIT=2,DEVICE='DSK',FILE='ELL1.CDR',ACCESS='SEQIN' )
      OPEN(UNIT=3,DEVICE='DSK',FILE='ELL2.CDR',ACCESS='SEQOUT'
     1,RECORD SIZE=132)
      OPEN(UNIT=4,DEVICE='DSK',FILE='ELL1.CDR',ACCESS='SEQOUT'
     1,RECORD SIZE=132)
      READ(1,*)DZ,AZ,BY,P,R1,Q,M1,M0,N1,N2,N0,IREAD
      C1=DSQRT(AZ*AZ-BY*BY)
      EW=BY/AZ
      EW=0.5D0*DLOG((1.0D0+EW)/(1.0D0-EW))
      PHI=3.14159265358979 3D0
      P2=0.5D0*PHI
      P4=0.25D0*PHI
      SGM=EW/P2
      M2=M1-1
      M3=M1+1
      N3=N1-1
      N4=N1+1
      N5=N2-1
      N6=N2+1
      N7=N0+1
      DZ1=P/DFLOAT(M2)
      DZ2=(SGM-P)/DFLOAT(M0-M2)
      DY1=R1/DFLOAT(N3)
      DY2=(Q-R1)/DFLOAT(N5-N3)
      DY3=(1.0D0-Q)/DFLOAT(N0-N5)
      WRITE(3,500)AZ,BY,C1,EW,SGM,DZ1,DZ2,DY1,DY2,DY3,M1,M0,N1
     1,N2,N0
      C1=DEXP(EW)
      C2=DEXP(-EW)
      CTH=(C1+C2)/(C1-C2)
      CTH=CTH*CTH
      C1=2.0D0*EW
      RD=0.25D0*(DEXP(C1)-DEXP(-C1))/(PHI*DZ1*DY1)
      MP1=M0+1
      M21=M2-1
      M01=M0-1
      N01=N0-1
      MN=N0*M0
      N3M=N3*M0
      N5M=N5*M0
      MN1=MN+1
      MN1=MN+M0
      K1=N1*M0+1
      K2=N2*M0+1
      K3=2*M0+1
      K4=(3*M0+1+K3*N01)*M0
      K5=(M0*MP1)/2+M0*M0+1-K3
      K6=MN1*(M0+M0+1)-(M0*MP1)/2
C! for curve fitting and subsequent interpolation for ' W '
      XG(1)=0
      DO 400 L=2,M1
      C5=L-1
400   XG(L)=C5*DZ1
      DO 405 L=M3,M0
      C5=L-M1
405   XG(L)=P+C5*DZ2
      XG(MP1)=SGM
C! CALCULATION OF  A , B , C , D & RA
C! FOR  I=1  AND  K=1
      C1=P2*DZ
      C2=DEXP(C1)
      C3=DEXP(-C1)
      C2=0.5D0*(C2+C3)
      A(1)=C2*C2-1.0D0
      RA(1)=DSQRT(A(1))
      C1=PHI*DZ
      C2=DEXP(C1)
      C3=DEXP(-C1)
      C(1)=P4*0.5D0*(C2-C3)/RA(1)
      D(1)=P2
```

```
      B(1)=0
      WRITE(3,530)DZ,A(1),RA(1),C(1),D(1)
      C1=P2*DZ1
      C2=P2*DZ2
      C3=PHI*DZ1
      C4=PHI*DZ2
      D1=P2*DY1
      D2=P2*DY2
      D3=P2*DY3
      D4=PHI*DY1
      D5=PHI*DY2
      D6=PHI*DY3
C1 FOR J=1 AND K=2(1)M1
      DO 2 L=2,M1
      C5=L-1
      F1=C5*C1
      F2=DEXP(F1)
      F3=DEXP(-F1)
      F2=0.5D0*(F2+F3)
      F1=C5*C3
      F3=DEXP(F1)
      F1=DEXP(-F1)
      F3=0.5D0*(F3-F1)
      A(L)=F2*F2-1.0D0
      RA(L)=DSQRT(A(L))
      C(L)=P4*F3/RA(L)
      D(L)=0
2     B(L)=0
C1 FOR J=1 AND K=M3(1)M0
      C6=P*P2
      C7=P*PHI
      DO 4 L=M3,M0
      C5=L-M1
      F1=C6+C5*C2
      F2=DEXP(F1)
      F3=DEXP(-F1)
      F2=0.5D0*(F2+F3)
      F1=C7+C5*C4
      F3=DEXP(F1)
      F1=DEXP(-F1)
      F3=0.5D0*(F3-F1)
      A(L)=F2*F2-1.0D0
      RA(L)=DSQRT(A(L))
      C(L)=P4*F3/RA(L)
      D(L)=0
4     B(L)=0
C1 FOR J=2(1)N1 AND K=1
      DO 6 K=2,N1
      I=K-1
      C5=I
      I=I*M0+1
      F5=DCOS(C5*D1)
      F6=DSIN(C5*D4)
      A(I)=1.0D0-F5*F5
      RA(I)=DSQRT(A(I))
      C(I)=0
      D(I)=P4*F6/RA(I)
6     B(I)=0
C1 FOR J=N4(1)N2 AND K=1
      C6=R1*P2
      C7=R1*PHI
      DO 8 K=N4,N2
      C5=K-N1
      I=(K-1)*M0+1
      F5=DCOS(C6+C5*D2)
      F6=DSIN(C7+C5*D5)
      A(I)=1.0D0-F5*F5
      RA(I)=DSQRT(A(I))
      C(I)=0
      D(I)=P4*F6/RA(I)
```

```
8       B(I)=0
CI FOR  J=N6(1)NO AND K=1
        C6=0*P2
        C7=0*PHI
        DO 10 K=N6,NO
        C5=K-N2
        I=(K-1)*MO+1
        F5=DCOS(C6+C5*D3)
        F6=DSIN(C7+C5*D6)
        A(I)=1.0D0-F5*F5
        RA(I)=DSQRT(A(I))
        C(I)=0
        D(I)=P4*F6/RA(I)
10      B(I)=0
CI FOR  J=N7 AND <=1
        A(MM)=1
        RA(MM)=1
        C(MM)=0
        D(MM)=0
CI FOR  J=N7 AND <=2(1)M1
        DO 12 L=2,M1
        I=MN+L
        C5=L-1
        F1=C5*C1
        F2=DEXP(F1)
        F3=DEXP(-F1)
        F2=0.5D0*(F2+F3)
        F1=C5*C3
        F3=DEXP(F1)
        F1=DEXP(-F1)
        F3=0.5D0*(F3-F1)
        A(I)=F2*F2
        RA(I)=F2
        C(I)=P4*F3/RA(I)
12      D(I)=0
CI FOR  J=N7 AND K=M3(1)MO
        C6=P*P2
        C7=P*PHI
        DO 14 L=M3,MO
        I=MN+L
        C5=L-M1
        F1=C6+C5*C2
        F2=DEXP(F1)
        F3=DEXP(-F1)
        F2=0.5D0*(F2+F3)
        F1=C7+C5*C4
        F3=DEXP(F1)
        F1=DEXP(-F1)
        F3=0.5D0*(F3-F1)
        A(I)=F2*F2
        RA(I)=F2
        C(I)=P4*F3/RA(I)
14      D(I)=0
CI FOR  J=2(1)N1 AND K=2(1)M1
        DO 20 K=2,N1
        I=K-1
        C5=I
        I=I*MO
        F4=C5*D1
        F5=DCOS(F4)
        F6=DSIN(F4)
        F4=DSIN(C5*D4)
        BY=F6/F5
        C5=F5/F6
        BY=C5+CTH*BY
        F5=F5*F5
        DO 18 L=2,M1
        J=I+L
        C5=L-1
        F1=C5*C1
```

```
      F2=DEXP(F1)
      F3=DEXP(-F1)
      AZ=(F2-F3)/(F2+F3)
      F1=(F2+F3)/(F2-F3)
      F2=0.5D0*(F2+F3)
      C5=C5*C3
      F3=DEXP(C5)
      C5=DEXP(-C5)
      F3=0.5D0*(F3-C5)
      B(J)=BY/(F1-CTH*AZ)
      A(J)=F2*F2-F5
      RA(J)=DSQRT(A(J))
      C5=P4/RA(J)
      C(J)=C5*F3
18    D(J)=C5*F4
C1 FOR I=2(1)M1 AND K=M3(1)MO
      DO 20 L=M3,MO
      J=I+L
      C5=L-M1
      F1=C6+C5*C2
      F2=DEXP(F1)
      F3=DEXP(-F1)
      AZ=(F2-F3)/(F2+F3)
      F1=(F2+F3)/(F2-F3)
      F2=0.5D0*(F2+F3)
      C5=C7+C5*C4
      F3=DEXP(C5)
      C5=DEXP(-C5)
      F3=0.5D0*(F3-C5)
      B(J)=BY/(F1-CTH*AZ)
      A(J)=F2*F2-F5
      RA(J)=DSQRT(A(J))
      C5=P4/RA(J)
      C(J)=C5*F3
20    D(J)=C5*F4
C1 FOR I=N4(1)N2 AND K=2(1)M1
      C8=R1*P2
      C9=R1*PHI
      DO 26 K=N4,N2
      I=(K-1)*MO
      C5=K-N1
      F4=CB+C5*D2
      F5=DCOS(F4)
      F6=DSIN(F4)
      F4=DSIN(C9+C5*D5)
      BY=F6/F5
      C5=F5/F6
      BY=C5+CTH*BY
      F5=F5*F5
      DO 24 L=2,M1
      J=I+L
      C5=L-1
      F1=C5*C1
      F2=DEXP(F1)
      F3=DEXP(-F1)
      AZ=(F2-F3)/(F2+F3)
      F1=(F2+F3)/(F2-F3)
      F2=0.5D0*(F2+F3)
      C5=C5*C3
      F3=DEXP(C5)
      C5=DEXP(-C5)
      F3=0.5D0*(F3-C5)
      B(J)=BY/(F1-CTH*AZ)
      A(J)=F2*F2-F5
      RA(J)=DSQRT(A(J))
      C5=P4/RA(J)
      C(J)=C5*F3
24    D(J)=C5*F4
C1 FOR I=N4(1)N2 AND K=M3(1)MO
      DO 26 L=M3,MO
```

```
      J=I+L
      C5=L-M1
      F1=C6+C5*C2
      F2=DEXP(F1)
      F3=DEXP(-F1)
      AZ=(F2-F3)/(F2+F3)
      F1=(F2+F3)/(F2-F3)
      F2=0.5D0*(F2+F3)
      C5=C7+C5*C4
      F3=DEXP(C5)
      C5=DEXP(-C5)
      F3=0.5D0*(F3-C5)
      B(J)=BY/(F1-CTH*AZ)
      A(J)=F2*F2-F5
      RA(J)=DSQRT(A(J))
      C5=P4/RA(J)
      C(J)=C5*F3
25    D(J)=C5*F4
C1 FOR  I=N6(1)N0 AND K=2(1)M1
      C8=Q*P2
      C9=Q*PHI
      DO 32 K=N6,N0
      I=(K-1)*M0
      C5=K-N2
      F4=C8+C5*D3
      F5=DCOS(F4)
      F6=DSIN(F4)
      F4=DSIN(C9+C5*D6)
      BY=F6/F3
      C5=F5/F5
      BY=C5+CTH*BY
      F5=F5*F5
      DO 30 L=2,M1
      J=I+L
      C5=L-1
      F1=C5*C1
      F2=DEXP(F1)
      F3=DEXP(-F1)
      AZ=(F2-F3)/(F2+F3)
      F1=(F2+F3)/(F2-F3)
      F2=0.5D0*(F2+F3)
      C5=C5*C3
      F3=DEXP(C5)
      C5=DEXP(-C5)
      F3=0.5D0*(F3-C5)
      B(J)=BY/(F1-CTH*AZ)
      A(J)=F2*F2-F5
      RA(J)=DSQRT(A(J))
      C5=P4/RA(J)
      C(J)=C5*F3
30    D(J)=C5*F4
C1 FOR  I=N6(1)N0 AND K=M3(1)M0
      DO 32 L=M3,M0
      J=I+L
      C5=L-M1
      F1=C6+C5*C2
      F2=DEXP(F1)
      F3=DEXP(-F1)
      AZ=(F2-F3)/(F2+F3)
      F1=(F2+F3)/(F2-F3)
      F2=0.5D0*(F2+F3)
      C5=C7+C5*C4
      F3=DEXP(C5)
      C5=DEXP(-C5)
      F3=0.5D0*(F3-C5)
      B(J)=BY/(F1-CTH*AZ)
      A(J)=F2*F2-F5
      RA(J)=DSQRT(A(J))
      C5=P4/RA(J)
      C(J)=C5*F3
```

```
32    D(J)=C5*F4
C FIRST ROW OF THE UNPARTITIONED MATRIX
      D1=DZ2/DZ1
      D2=DY2/DY1
      D3=D1*D2
      D4=DY3/DY1
      D5=D1*D4
      C1=0.5D0*D1
      C2=0.5D0*D2
      C3=0.5D0*D4
      C4=0.5D0*D5
      C5=0.5D0+C1
      C6=0.5D0+C2
      C7=0.5D0*(D1+D3)
      C8=C2+C4
      C9=0.5D0*(D2+D3)
      C10=C3+C5
      C11=C4+C5
      E(1)=0.25D0*A(1)
      DO 34 L=2,M2
34    E(L)=0.5D0*A(L)
      E(M1)=0.25D0*(1.0D0+D1)*A(M1)
      DO 36 L=M3,M0
36    E(L)=C1*A(L)
      DO 38 K=MP1,N3M,M0
38    E(K)=0.5D0*A(K)
      K=N3M+1
      E(K)=0.25D0*(1.0D0+D2)*A(K)
      DO 40 K=K1,N5M,M0
40    E(K)=C2*A(K)
      K=N5M+1
      E(K)=0.25D0*(D2+D4)*A(K)
      DO 42 K=K2,MN,M0
42    E(K)=C3*A(K)
      K=MN+1
      E(K)=0.25D0*D4*A(K)
      DO 44 K=2,N3
      I=(K-1)*M0
      DO 46 L=2,M2
      J=I+L
46    E(J)=A(J)
      J=I+M1
      E(J)=C5*A(J)
      DO 44 L=M3,M0
      J=I+L
44    E(J)=D1*A(J)
      DO 48 L=2,M2
      J=N3M+L
48    E(J)=C6*A(J)
      J=N3M+M1
      E(J)=0.25D0*(1.0D0+D1+D2+D3)*A(J)
      DO 50 L=M3,M0
      J=N3M+L
50    E(J)=C7*A(J)
      DO 52 K=N4,N5
      I=(K-1)*M0
      DO 54 L=2,M2
      J=I+L
54    E(J)=D2*A(J)
      J=I+M1
      E(J)=C9*A(J)
      DO 52 L=M3,M0
      J=I+L
52    E(J)=D3*A(J)
      DO 56 L=2,M2
      J=N5M+L
56    E(J)=C8*A(J)
      J=N5M+M1
      E(J)=0.25D0*(D2+D3+D4+D5)*A(J)
      DO 58 L=M3,M0
```

```
      J=N5M+L
58    E(J)=0.5D0*(D3+D5)*A(J)
      DO 60 K=N6,ND
      I=(K-1)*MD
      DO 62 L=2,M2
      J=I+L
62    E(J)=D4*A(J)
      J=I+M1
      E(J)=0.5D0*(D4+D5)*A(J)
      DO 60 L=M3,MD
      J=I+L
60    E(J)=D5*A(J)
      DO 64 L=2,M2
      J=MN+L
64    E(J)=C3*A(J)
      J=MN+M1
      E(J)=0.25D0*(D4+D5)*A(J)
      DO 66 L=M3,MD
      J=MN+L
66    E(J)=C4*A(J)
C     ***
C  see as in the uniform-grid code in this code the eqn.3.17 has not
C  been multiplied by '4'
C     ***
      IF(IREAD-1)68,70,68
70    READ(2,505)(U(I),V(I),W(I),I=1,MN1)
      READ(2,510)P0,X
      XST=X
      GO TO 72
C CALCULATION OF THE INI. U0
68    AZ=0
      DO 74 I=1,MN1
74    AZ=AZ+E(I)
      U0=R0/AZ
      WRITE(3,525)U0
      DO 76 I=1,MN1
      U(I)=U0
      V(I)=0
76    W(I)=0
      P0=0
C SETTING UP OF THE NON-ZERO ENTRIES OF PART. MATRIX "PM"
72    D1=0.5D0/DZ1
      D2=0.5D0/DY1
      D3=0.5D0/DZ2
      D4=0.5D0/DY2
      D5=0.5D0/DY3
      D6=1.0D0/(DZ1*DZ1)
      D7=1.0D0/(DY1*DY1)
      D8=1.0D0/(DZ2*DZ2)
      D9=1.0D0/(DY2*DY2)
      D10=1.0D0/(DY3*DY3)
      D11=2.0D0*D6
      D12=2.0D0*D7
      D13=2.0D0*D8
      D14=2.0D0*D9
      D15=2.0D0*D10
      C1=1.0D0/DZ1
      C2=1.0D0/DY1
      C3=1.0D0/DZ2
      C4=1.0D0/DY2
      C5=1.0D0/DY3
      T1=DZ2/DZ1
      T2=DY1/DY2
      T3=DY3/DY2
      F1=D11+D12
      F2=D13+D12
      F3=D11+D14
      F4=D13+D14
      F5=D11+D15
      F6=D13+D15
```

```
      READ(1,*)NOP
      READ(1,*)((IG(I,J),J=1,NOP),I=1,N7)
      READ(1,*)NDX
      DO 390 KLK=1,NDX
      READ(1,*)DX,IWRIT,ILESS,IFULL,IFIT

      NDX = is the no. of delta-x's at the present strech
      NOP = NR-1
      IWRIT = no of steps in the marching  X with delta-X=DX
      ILESS = 1 indicates writing of U,V,W  at (XST + IWRIT*DX ) to
              6 decimals with grid numbers
              otherwise no writing is done
      IFULL = 1 indicates writing of U,V,W to 16 deimals for starting
              of the marching
              otherwise no writing is done
      IFIT = 1 indicates curve fitting and interpolation is
              required for  W
              otherwise no no curve fitting is done
      FX=1.0D0/DX
      DO 85 I=1,MN1
85    ABX(I)=FX*A(I)
      DO 78 IJX=1,IWRIT
C SETTING (PM(I),1<=I<=K4) TO ZERO
      DO 80 I=1,K4
80    PM(I)=0
C DIAGONAL (I,I)
      PM(1)=ABX(1)*U(1)-3.0D0*RA(1)*W(1)*D1-D11+D12
      J=1
      DO 100 L=1,M21
      J=J+MP1+L
      I=L+1
100   PM(J)=F1+ABX(I)*U(I)
      J=J+MP1+M2
      I=M1
      PM(J)=ABX(I)*U(I)-RA(I)*W(I)*C3*(1.0D0-T1)+D13*T1+D12
      DO 105 L=M1,M01
      J=J+MP1+L
      I=L+1
105   PM(J)=F2+ABX(I)*U(I)
      DO 110 K=2,N3
      IJ=(K-1)*M0
      DO 115 L=1,M2
      J=J+K3
      I=IJ+L
115   PM(J)=F1+ABX(I)*U(I)
      J=J+K3
      I=IJ+M1
      PM(J)=ABX(I)*U(I)-RA(I)*W(I)*(1.0D0-T1)*C3+D13*T1+D12
      DO 110 L=M3,M0
      J=J+K3
      I=IJ+L
110   PM(J)=F2+ABX(I)*U(I)
      DO 120 L=1,M2
      J=J+K3
      I=N3M+L
120   PM(J)=ABX(I)*U(I)+RA(I)*V(I)*(1.0D0-T2)*C2+D11+D12*T2
      J=J+K3
      I=N3M+M1
      PM(J)=ABX(I)*U(I)-RA(I)*W(I)*(1.0D0-T1)*C3+RA(I)*V(I)*(1.0D0
     1-T2)*C2+D13*T1+D12*T2
      DO 125 L=M3,M0
      J=J+K3
      I=N3M+L
125   PM(J)=ABX(I)*U(I)+RA(I)*V(I)*(1.0D0-T2)*C2+D13+D12*T2
      DO 130 K=M4,N5
      IJ=(K-1)*M0
      DO 135 L=1,M2
      J=J+K3
      I=IJ+L
135   PM(J)=F3+ABX(I)*U(I)
```

```
      J=J+K3
      I=IJ+M1
      PM(J)=ABX(I)*U(I)-RA(I)*W(I)*(1.0D0-T1)*C3+D13*T1+D14
      DO 130 L=M3,M0
      J=J+K3
      I=IJ+L
  130 PM(J)=F4+ABX(I)*U(I)
      DO 140 L=1,M2
      J=J+K3
      I=N5M+L
  140 PM(J)=ABX(I)*U(I)-RA(I)*V(I)*(1.0D0-T3)*C5+D11+D15*T3
      J=J+K3
      I=N5M+M1
      PM(J)=ABX(I)*U(I)-RA(I)*W(I)*(1.0D0-T1)*C3-RA(I)*V(I)*C5*(1
     1.0D0-T3)+D13*T1+D15*T3
      DO 145 L=M3,M0
      J=J+K3
      I=N5M+L
  145 PM(J)=ABX(I)*U(I)-RA(I)*V(I)*(1.0D0-T3)*C5+D13+D15*T3
      DO 150 K=N5,N0
      IJ=(K-1)*M0
      DO 155 L=1,M2
      J=J+K3
      I=IJ+L
  155 PM(J)=F5+ABX(I)*U(I)
      J=J+K3
      I=IJ+M1
      PM(J)=ABX(I)*U(I)-RA(I)*W(I)*(1.0D0-T1)*C3+D13*T1+D15
      DO 150 L=M3,M0
      J=J+K3
      I=IJ+L
  150 PM(J)=F5+ABX(I)*U(I)
      DO 160 L=1,M2
      J=J+K3+1-L
      I=MN+L
  160 PM(J)=F5+ABX(I)*U(I)
      J=J+K3+1-M1
      I=MN+M1
      PM(J)=ABX(I)*U(I)-RA(I)*W(I)*(1.0D0-T1)*C3+D13*T1+D15
      DO 165 L=M3,M0
      J=J+K3+1-L
      I=MN+L
  165 PM(J)=F5+ABX(I)*U(I)
C DIAGONAL ( I , I+1 )
      PM(2)=2.0D0*RA(1)*W(1)*C1+5.0D0*D6
      PM(3)=-RA(1)*W(1)*D1-4.0D0*D6
      PM(4)=D6
      J=2
      I=MP1
      DO 170 L=2,M2
      I=I+1
      J=J+I
  170 PM(J)=RA(L)*W(L)*D1-D6
      I=I+1
      J=J+I
      PM(J)=(RA(M1)*W(M1)*C3-D13*T1)/(1.0D0+T1)
      DO 175 L=M3,M01
      I=I+1
      J=J+I
  175 PM(J)=RA(L)*W(L)*D3-D8
      I=I+1
      J=J+I
      PM(J)=0
      DO 180 K=2,N0
      IJ=(K-1)*M0
      J=J+K3
      PM(J)=-D11
      DO 185 L=2,M2
      I=IJ+L
      J=J+K3
```

```
185   PM(J)=RA(I)*W(I)*D1-D6
      I=IJ+M1
      J=J+K3
      PM(J)=(RA(I)*W(I)*C3-D13*T1)/(1.0D0+T1)
      DO 190 L=M3,M01
      I=IJ+L
      J=J+K3
190   PM(J)=RA(I)*W(I)*D3-D8
      J=J+K3
180   PM(J)=0
      IJ=K3
      J=J+IJ
      PM(J)=-D11
      DO 195 L=2,M2
      I=MN+L
      IJ=IJ-1
      J=J+IJ
195   PM(J)=RA(I)*W(I)*D1-D6
      I=MN+M1
      IJ=IJ-1
      J=J+IJ
      PM(J)=(RA(I)*W(I)*C3-D13*T1)/(1.0D0+T1)
      DO 200 L=M3,M01
      I=MN+L
      IJ=IJ-1
      J=J+IJ
200   PM(J)=RA(I)*W(I)*D3-D8
C DIAGONAL  ( I , I+M0 )
      I=M0
      J=0
      DO 205 L=1,M0
      I=I+1
      J=J+I
205   PM(J)=-D12
      DO 210 K=2,N3
      IJ=(K-1)*M0
      DO 210 L=1,M0
      I=IJ+L
      J=J+K3
210   PM(J)=RA(I)*V(I)*D2-D7
      C8=T2*T2/(1.0D0+T2)
      DO 215 L=1,M0
      I=N3M+L
      J=J+K3
215   PM(J)=(RA(I)*V(I)*C2-D12)*C8
      DO 220 K=N4,N5
      IJ=(K-1)*M0
      DO 220 L=1,M0
      I=IJ+L
      J=J+K3
220   PM(J)=RA(I)*V(I)*D4-D9
      C8=1.0D0+T3
      DO 225 L=1,M0
      I=N5M+L
      J=J+K3
225   PM(J)=(RA(I)*V(I)*C5-D15*T3)/C8
      DO 230 K=N6,N0
      IJ=(K-1)*M0
      DO 230 L=1,M0
      I=IJ+L
      J=J+K3
230   PM(J)=RA(I)*V(I)*D5-D10
C DIAGONAL ( I ,I-1 )
      I=MP1
      J=0
      DO 235 L=2,M2
      I=I+1
      J=J+I
235   PM(J)=-RA(L)*W(L)*D1-D6
      I=I+1
```

```
      J=J+I
      PM(J)=-(RA(M1)*W(M1)*C3+D13)*(T1*T1)/(1.0D0+T1)
      DO 240 L=M3,MO
      I=I+1
      J=J+I
240   PM(J)=-RA(L)*W(L)*D3-D8
      I=I+1
      J=J+I
      PM(J)=0
      C8=T1*T1/(1.0D0+T1)
      DO 245 K=2,NO
      IJ=(K-1)*MO
      DO 250 L=2,M2
      I=IJ+L
      J=J+K3
250   PM(J)=-RA(I)*W(I)*D1-D6
      I=IJ+M1
      J=J+K3
      PM(J)=-(RA(I)*W(I)*C3+D13)*C8
      DO 255 L=M3,MO
      I=IJ+L
      J=J+K3
255   PM(J)=-RA(I)*W(I)*D3-D8
      J=J+K3
245   PM(J)=0
      IJ=K3
      DO 260 L=2,M2
      IJ=IJ-1
      J=J+IJ
      I=MN+L
260   PM(J)=-RA(I)*W(I)*D1-D6
      IJ=IJ-1
      J=J+IJ
      I=MN+M1
      PM(J)=-(RA(I)*W(I)*C3+D13)*C8
      DO 265 L=M3,MO
      IJ=IJ-1
      J=J+IJ
      I=MN+L
265   PM(J)=-RA(I)*W(I)*D3-D8
C! DIAGONAL ( I , I-M )
      J=K5
      DO 270 K=2,N3
      IJ=(K-1)*MO
      DO 270 L=1,MO
      I=IJ+L
      J=J+K3
270   PM(J)=-RA(I)*V(I)*D2-D7
      C8=1.0D0/(1.0D0+T2)
      DO 275 L=1,MO
      I=N3M+L
      J=J+K3
275   PM(J)=-(RA(I)*V(I)*C2+D12*T2)*C8
      DO 280 K=N4,N5
      IJ=(K-1)*MO
      DO 280 L=1,MO
      I=IJ+L
      J=J+K3
280   PM(J)=-RA(I)*V(I)*D4-D9
      C8=T3*T3/(1.0D0+T3)
      DO 285 L=1,MO
      I=N5M+L
      J=J+K3
285   PM(J)=-(RA(I)*V(I)*C5+D15)*C8
      DO 290 K=N6,NO
      IJ=(K-1)*MO
      DO 290 L=1,MO
      I=IJ+L
      J=J+K3
290   PM(J)=-RA(I)*V(I)*D5-D10
```

```
      IJ=K3+1
      DO 295 L=1,MO
      IJ=IJ-1
      J=J+IJ
      I=MN+L
295   PM(J)=-D15
C  LAST COLUMN & THE R.H.S.  OF THE UNPARTITIONED MATRIX
      DO 300 L=1,MN1
      H(L)=ABX(L)
300   R(L)=H(L)*(P0+U(L)*U(L))
C  SOLUTION BY PARTITION
      CALL SOLVER(R,PM,H,E,P0,R0,MN1,1,M0,M0,1.0D-15,IER)
C  CALCULATION OF THE TRANSVERSE COMPONENTS  V  AND  W
C  FOR  I=N0 AND K=M0(-1)1
      V(MN)=-ABX(MN)*(R(MN)-U(MN))/(B(MN)*(C3*RA(MN)-C(MN))-C5*
     1RA(MN)+D(MN))
      W(MN)=-B(MN)*V(MN)
      I=0
      DO 305 L=M1,M01
      I=I+1
      J=MN-I
      J1=J+1
      V(J)=-(ABX(J)*(R(J)-U(J))+C3*RA(J)*W(J1))/(B(J)*(C3*RA(J)-
     1C(J))-C5*RA(J)+D(J))
305   W(J)=-B(J)*V(J)
      DO 310 L=2,M2
      I=I+1
      J=MN-I
      J1=J+1
      V(J)=-(ABX(J)*(R(J)-U(J))+C1*RA(J)*W(J1))/(B(J)*(C1*RA(J)-
     1C(J))-C5*RA(J)+D(J))
310   W(J)=-B(J)*V(J)
      I=I+1
      J=MN-I
      J1=J+1
      V(J)=-(ABX(J)*(R(J)-U(J))+C1*RA(J)*W(J1))/(-C5*RA(J)+D(J))
      W(J)=0
      IF(IFIT-1)410,415,410
415   CALL CRVSET(W,M0,J,MP1,N7,NOP,XG,IG,SGM,DZ)
      IX=J+1
      DO 420 KX=IX,MN
420   V(KX)=-W(KX)/B(KX)
      V(J)=-(ABX(J)*(R(J)-U(J))+C1*RA(J)*W(J1))/(-C5*RA(J)+D(J))
410   CONTINUE
C  FOR  I=(N0-1)(-1)N2 AND K=M0(-1)1
      DO 315 K=N2,N01
      IJ=(N01+N2-K)*M0
      JX=IJ
      JM=IJ+M0
      V(IJ)=-(ABX(IJ)*(R(IJ)-U(IJ))+RA(IJ)*C5*V(JM))/(B(IJ)*(C3*
     1RA(IJ)-C(IJ))-C5*RA(IJ)+D(IJ))
      W(IJ)=-B(IJ)*V(IJ)
      I=0
      DO 320 L=M1,M01
      I=I+1
      J=IJ-I
      J1=J+1
      JM=J+M0
      V(J)=-(ABX(J)*(R(J)-U(J))+RA(J)*(C3*W(J1)+C5*V(JM)))/(B(J)*(
     1C3*RA(J)-C(J))-C5*RA(J)+D(J))
320   W(J)=-B(J)*V(J)
      DO 325 L=2,M2
      I=I+1
      J=IJ-I
      J1=J+1
      JM=J+M0
      V(J)=-(ABX(J)*(R(J)-U(J))+RA(J)*(C1*W(J1)+C5*V(JM)))/(B(J)*(
     1C1*RA(J)-C(J))-C5*RA(J)+D(J))
325   W(J)=-B(J)*V(J)
      I=I+1
```

```
      J=IJ-I
      J1=J+1
      JM=J+MO
      V(J)=-(ABX(J)*(R(J)-U(J))+RA(J)*(C1*W(J1)+C5*V(JM)))/(-C5*RA
     1(J)+D(J))
      W(J)=0
      IF(IFIT-1)315,425,315
  425 CALL CRVSET(W,MO,J,MP1,N7,NOP,XG,IG,SGM,DZ)
      IX=J+1
      DO 430 KX=IX,JX
  430 V(KX)=-W(KX)/B(KX)
      V(J)=-(ABX(J)*(R(J)-U(J))+RA(J)*(C1*W(J1)+C5*V(JM)))/(-C5*RA
     1(J)+D(J))
  315 CONTINUE
C FOR I=N5(-1)N1 AND K=MO(-1)1
      DO 330 K=N1,N5
      IJ=(N5+N1-K)*MO
      JX=IJ
      JM=IJ+MO
      V(IJ)=-(ABX(IJ)*(R(IJ)-U(IJ))+RA(IJ)*C4*V(JM))/(B(IJ)*(C3*
     1RA(IJ)-C(IJ))-C4*RA(IJ)+D(IJ))
      W(IJ)=-B(IJ)*V(IJ)
      I=0
      DO 335 L=M1,M01
      I=I+1
      J=IJ-I
      J1=J+1
      JM=J+MO
      V(J)=-(ABX(J)*(R(J)-U(J))+RA(J)*(C3*W(J1)+C4*V(JM)))/(B(J)*
     1(C3*RA(J)-C(J))-C4*RA(J)+D(J))
  335 W(J)=-B(J)*V(J)
      DO 340 L=2,M2
      I=I+1
      J=IJ-I
      J1=J+1
      JM=J+MO
      V(J)=-(ABX(J)*(R(J)-U(J))+RA(J)*(C1*W(J1)+C4*V(JM)))/(B(J)*
     1(C1*RA(J)-C(J))-C4*RA(J)+D(J))
  340 W(J)=-B(J)*V(J)
      I=I+1
      J=IJ-I
      J1=J+1
      JM=J+MO
      V(J)=-(ABX(J)*(R(J)-U(J))+RA(J)*(C1*W(J1)+C4*V(JM)))/(-C4*R
     1A(J)+D(J))
      W(J)=0
      IF(IFIT-1)330,435,330
  435 CALL CRVSET(W,MO,J,MP1,N7,NOP,XG,IG,SGM,DZ)
      IX=J+1
      DO 440 KX=IX,JX
  440 V(KX)=-W(KX)/B(KX)
      V(J)=-(ABX(J)*(R(J)-U(J))+RA(J)*(C1*W(J1)+C4*V(JM)))/(-C4*R
     1A(J)+D(J))
  330 CONTINUE
C FOR I=N3(-1)2 AND K=MO(-1)1
      DO 345 K=2,N3
      IJ=(N3+2-K)*MO
      JX=IJ
      JM=IJ+MO
      V(IJ)=-(ABX(IJ)*(R(IJ)-U(IJ))+RA(IJ)*C2*V(JM))/(B(IJ)*(C3*
     1RA(IJ)-C(IJ))-C2*RA(IJ)+D(IJ))
      W(IJ)=-B(IJ)*V(IJ)
      I=0
      DO 350 L=M1,M01
      I=I+1
      J=IJ-I
      J1=J+1
      JM=J+MO
      V(J)=-(ABX(J)*(R(J)-U(J))+RA(J)*(C3*W(J1)+C2*V(JM)))/(B(J)*
     1(C3*RA(J)-C(J))-C2*RA(J)+D(J))
```

```
350   W(J)=-B(J)*V(J)
      DO 355 L=2,M2
      I=I+1
      J=II-I
      J1=J+1
      JM=J+M0
      V(J)=-(ABX(J)*(R(J)-U(J))+RA(J)*(C1*W(J1)+C2*V(JM)))/(B(J)*
     1(C1*RA(J)-C(J))-C2*RA(J)+D(J))
355   W(J)=-B(J)*V(J)
      I=I+1
      J=II-I
      J1=J+1
      JM=J+M0
      V(J)=-(ABX(J)*(R(J)-U(J))+RA(J)*(C1*W(J1)+C2*V(JM)))/(-C2*R
     1A(J)+D(J))
      W(J)=0
      IF(IFIT-1)345,450,345
450   CALL CRVSET(W,M0,J,MP1,N7,NOP,XG,IG,SGM,DZ)
      IX=J+1
      DO 455 KX=IX,JX
455   V(KX)=-W(KX)/B(KX)
      V(J)=-(ABX(J)*(R(J)-U(J))+RA(J)*(C1*W(J1)+C2*V(JM)))/(-C2*R
     1A(J)+D(J))
345   CONTINUE
C FOR  I=1  AND  K=M0(-1)1
      W(M0)=-(ABX(M0)*(R(M0)-U(M0))+RA(M0)*C2*V(M0+M0))
     1/(-C3*RA(M0)+C(M0))
      V(M0)=0
      I=0
      DO 360 L=M1,M01
      I=I+1
      J=M0-I
      J1=J+1
      W(J)=-(ABX(J)*(R(J)-U(J))+RA(J)*(C3*W(J1)+C2*V(J+M0)))
     1/(-C3*RA(J)+C(J))
360   V(J)=0
      DO 365 L=1,M2
      I=I+1
      J=M0-I
      J1=J+1
      W(J)=-(ABX(J)*(R(J)-U(J))+RA(J)*(C1*W(J1)+C2*V(J+M0)))
     1/(-C1*RA(J)+C(J))
365   V(J)=0
      IF(IFIT-1)465,470,465
470   CALL CRVSET(W,M0,J,MP1,N7,NOP,XG,IG,SGM,DZ)
465   CONTINUE
C FOR  I=N7  AND  K=M0(-1)1
      I=MN1
      W(I)=-(ABX(I)*(R(I)-U(I))-C5*RA(I)*V(MN))/(-C3*RA(I)+C(I))
      V(I)=0
      I=0
      DO 370 L=M1,M01
      I=I+1
      J=MN1-I
      J1=J+1
      JM=J-M0
      W(J)=-(ABX(J)*(R(J)-U(J))+RA(J)*(C3*W(J1)-C5*V(JM)))/(-C3*R
     1A(J)+C(J))
370   V(J)=0
      DO 375 L=2,M2
      I=I+1
      J=MN1-I
      J1=J+1
      JM=J-M0
      W(J)=-(ABX(J)*(R(J)-U(J))+RA(J)*(C1*W(J1)-C5*V(JM)))/(-C1*R
     1A(J)+C(J))
375   V(J)=0
      W(MM)=0
      V(MM)=0
      IF(IFIT-1)475,480,475
```

```
480   CALL CRVSET(N,MO,MM,MP1,N7,NOP,XG,IG,SGM,DZ)
475   CONTINUE
      DO 380 L=1,MN1
380   U(L)=R(L)
      X=X+DX
      PR(IJX)=PO
      CV(IJX)=U(MM)
78    CONTINUE
      WRITE(3,535)XST,DX,IWRIT,X
      WRITE(3,540)(J,CV(J),PR(J),J=1,IWRIT)
      IF(ILESS-1)482,485,482
485   WRITE(3,515)(J,U(J),V(J),W(J),J=1,MN1)
      WRITE(3,520)PO,X
482   IF(IFULL-1)390,490,390
490   WRITE(4,505)(U(J),V(J),W(J),J=1,MN1)
      WRITE(4,510)PO,X
390   CONTINUE
      STOP
500   FORMAT(' A=',F6.3,' B=',F6.3,' C=',F13.9,' EW=',F13.9,' SGM='
     1,F13.9,' DZ1=',F9.6,' DZ2=',F9.6,' DY1=',F9.6,
     1DY2=',F9.6,' DY3=',F9.6,' M1=',I3,' MO=',I3,' N1=',I3,' N2='
     1,I3,' NO=',I3)
505   FORMAT(2(F19.16,2D23.16))
510   FORMAT(D23.16,D16.8)
515   FORMAT(3(I4,F9.6,2E14.6))
520   FORMAT(D19.11,E12.4,E14.6)
525   FORMAT('  INI. VEL = ',F13.10)
530   FORMAT(' del-Z= ',F8.6,' A(1)= ',E13.6,' RA(1)= ',E13.6
     1,' C(1)= ',F9.6,' D(1)= ',F9.6)
535   FORMAT(' X-START= ',F13.9,' DX= ',E12.4,' NO.OF STPS= ',I4
     1,' X-END= ',F13.9)
540   FORMAT(5(I4,F9.6,F11.7))
161   FORMAT(10E13.5)
      END
```

```
C
C
C     This subroutine SOLVER solves the system [S] of order (n+1) in
C     eqn.(4.1)
C     where
C     n = m4(n8+1)
C           E  0
C     S = [     ]  is the coef. matrix
C           G  H
C     E = (E1,E2,E3,---,En) is the row vector arising from the coef. of the
C     axial vel. component U at location (i+1) in eqn.(3.17)
C     H = (H1,H2,H3,---,Hn) is the column vector arising from the pressure
C     terms at the location (i+1) in the axial momentum eqn.(3.2)
C     G =  is an unsymmtric banded matrix of order 'n' and band width
C     (2*m4+1) arising from coef. of axial velocity component U at location
C     (i+1) in eqn.(3.2)
C     U = (U1,U2,U3,---,Un) is the unknown axial velocity vector at location
C     (i+1)
C     P = is the unknown pressure at location (i+1)
C     Q = is the known RHS of eqn.(3.17)
C     R = (R1,R2,R3,---,Rn) is the known RHS column vector arising from the
C     terms at location (i) in eqn.(3.2).
C     **** ---- **** ---- **** ---- **** ---- **** -|-|- **** ---- **** ---
C     Usage:
C        CALL SOLVER(R,A,M,N,MUD,MLD,EPS,IER)
C
C     Description of the Arguments:
C     = the order of the matrix [G], i.e., 'n'
C        N = numper ofRHS vectors (in our case it is 1 )
C        MUD =  the number of the upper codiagonals ( in our case it is
C        m4)
C        MLD = the number of the lower codiagonals ( in our case same ass
C        MUD )
C        A = is unsymmetric banded matrix of MUD upper codiagonals and
C        MLD lower codiagonals ( in our case it is [G] )
C        R = is the RHS matrix of size (M*N) ( in our case it is (R) )
C        EPS = constant which is used as relative tolerance for test on
C        loss of significance )
C        IER = resulting error parameter
C                 IER=0 - no error
C                 IER=-1 no result because of wrong input parameters
C                 or because of pivot element at elimination step is  0
C                 IER=K  warning due to possible loss of significance
C                 inicated at elimination step K+1, where the pivot
C                 element was L.E. the internal tolerance EPS times
C                 absolutely greatest element of matrix A.
C
C        Band matrix A is to be stored rowwise in the first ME succes-
C        sive storage locations of totally needed MA storage locations,
C        where
C                 MA = M*MC-ML*(ML+1)/2
C                 ME = MA-MU*(MU+1)/2
C                 MC = min(M,MUD+MLD+1)
C                 ML = MC-1-MLD
C        and
C                 MU = MC-1-MUD.
C        RHS matrix is to be stored columnwise
C
C        On return the solution is stored in (R) ( in our case in (R) )
C
C        The solution is calculated by partion of the matrix [S] and
C        by Gauss elimination (ref.53) of the matrix [G].
C
C     ***** ----- ****** ------ ****** ----- ****** ------ ****** ------ ***
      SUBROUTINE SOLVER(R,A,H,E,PO,RO,M,N,MUD,MLD,EPS,IER)
      REAL *8 R(1),A(1),H(1),E(1),PIV,TB,TOL,PO,RO,SB,EPS
      MC=1+MLD+MUD
      MU=MLD
      ML=MUD
      MR=M-ML
```

```
      MZ=(MU*(MU+1))/2
      MA=M*MC-(ML*(ML+1))/2
      NM=N*M
C     Move elements backward and search for absolutely greatest element
C
      IER=0
      PIV=0
      JJ=MA
      J=MA-MZ
      KST=J
      DO 9 K=1,KST
      TB=A(J)
      A(JJ)=TB
      TB=DABS(TB)
      IF(TB-PIV)8,8,7
    7 PIV=TB
    8 J=J-1
    9 JJ=JJ-1
C
C     Insert zeros in first MU rows
C
      JJ=1
      J=1+MZ
      IC=1+MUD
      DO 13 I=1,MU
      DO 12 K=1,MC
      A(JJ)=0.D0
      IF(K-IC)11,11,12
   11 A(JJ)=A(J)
      J=J+1
   12 JJ=JJ+1
   13 IC=IC+1
C
C     Generate test value for singularity
C
      TOL=EPS*PIV
C
C     Start decomposition loop
C
      KST=1
      IDST=MC
      IC=MC-1
      DO 38 K=1,M
      IF(K-MR-1)16,16,15
   15 IDST=IDST-1
   16 ID=IDST
      ILR=K+MLD
      IF(ILR-M)18,18,17
   17 ILR=M
   18 II=KST
C
C     Pivot search in first column (row indexes from I=K upto I=ILR)
C
      PIV=0
      DO 22 I=K,ILR
      TB=DABS(A(II))
      IF(TB-PIV)20,20,19
   19 PIV=TB
      J=I
      JJ=II
   20 IF(I-MR)22,22,21
   21 ID=ID-1
   22 II=II+ID
      IF(PIV)47,47,23
   23 IF(IER)25,24,25
   24 IF(PIV-TOL)25,25,26
   25 IER=K-1
   26 PIV=1.D0/A(JJ)
C
C     Pivot row reduction and row interchange in  RHS
```

```
      ID=J-K
      DO 27 I=K,NM,M
      II=I+ID
      TB=PIV*H(II)
      H(II)=H(I)
      H(I)=TB
      TB=PIV*R(II)
      R(II)=R(I)
   27 R(I)=TB

     Pivot row reduction and row interchange in coef. matrix A

      II=KST
      J=JJ+IC
      DO 28 I=JJ,J
      TB=PIV*A(I)
      A(I)=A(II)
      A(II)=TB
   28 II=II+1

     Element reduction

      IF(K-ILR)29,34,34
   29 ID=KST
      II=K+1
      MU=KST+1
      MZ=KST+IC
      DO 33 I=II,ILR

     In matrix A

      ID=ID+MC
      JJ=I-MR-1
      IF(JJ)31,31,30
   30 ID=ID-JJ
   31 PIV=-A(ID)
      J=ID+1
      DO 32 JJ=MU,MZ
      A(J-1)=A(J)+PIV*A(JJ)
   32 J=J+1
      A(J-1)=0

     In matrix R

      J=K
      DO 33 JJ=I,NM,M
      R(JJ)=R(JJ)+PIV*R(J)
   33 H(JJ)=H(JJ)+PIV*H(J)
   34 J=J+M
      KST=KST+MC
      IF(ILR-MR)36,35,35
   35 IC=IC-1
   36 ID=K-MR
      IF(ID)38,38,37
   37 KST=KST-ID
   38 CONTINUE

     End decomposition loop


     Calculation of Ci and Di from Ei and Hi ( i=1(1)M )

      IC=2
      KST=MA+ML-MC+2
      II=M
      DO 145 I=2,M
      KST=KST-MC
      II=II-1
      J=II-MR
```

```
      IF(J)141,141,140
  140 KST=KST+J
  141 DO 143 J=II,NM,M
      SB=H(J)
      TB=R(J)
      MZ=KST+IC-2
      ID=J
      DO 142 JJ=KST,MZ
      ID=ID+1
      TB=TB-A(JJ)*R(ID)
  142 SB=SB-A(JJ)*H(ID)
      R(J)=TB
  143 H(J)=SB
      IF(IC-MC)144,145,145
  144 IC=IC+1
  145 CONTINUE
      SB=0
      TB=0
      DO 150 JJ=2,M
      TB=TB+E(JJ)*R(JJ)
  150 SB=SB+E(JJ)*H(JJ)
      PO=-(RO-TB)/SB
      DO 160 JJ=1,M
  160 R(JJ)=R(JJ)-PO*H(JJ)
   46 RETURN
C
C     Error return
C
   47 IER=-1
      RETURN
      END
C **** ---- **** ---- ***** ----- ***** -----| ***** ----- ****** ---- **
C SOLUTION OF N LINEAR EQUATIONS BY PROFESSOR HORNBECK'S PROGRAMME
C DIMENSION OF X = N, DIMENSION OF J = N+21. BOTH A & B ARE DESTROYED.
      SUBROUTINE SOLV(A,B,N)
      REAL *8 A(N,N),B(N),X(420),CO,SO
      INTEGER J(441)
C From here to statement No. 120, A inverse is computed & stored in A
      DO 10 I=1,N
   10 J(I+20)=I
      DO 80 I=1,N
      CO=0
      J1=I
      DO 20 K=I,N
      IF((DABS(CO)-DABS(A(I,K))).GE.0.0)GO TO 20
      J1=K
      CO=A(I,K)
   20 CONTINUE
      IF(I.EQ.J1)GO TO 40
      K=J(J1+20)
      J(J1+20)=J(I+20)
      J(I+20)=K
      DO 30 K=1,N
      SO=A(K,I)
      A(K,I)=A(K,J1)
   30 A(K,J1)=SO
   40 A(I,I)=1
      DO 50 J1=1,N
   50 A(I,J1)=A(I,J1)/CO
      DO 70 J1=1,N
      IF(I.EQ.J1)GO TO 70
      CO=A(J1,I)
      IF(CO.EQ.0.0)GO TO 70
      A(J1,I)=0
      DO 60 K=1,N
   60 A(J1,K)=A(J1,K)-CO*A(I,K)
   70 CONTINUE
   80 CONTINUE
      DO 120 I=1,N
      IF(J(I+20).EQ.I)GO TO 120
```

```
      J1=I
   90 J1=J1+1
      IF(J(J1+20).EQ.I)GO TO 100
      IF(N.GT.J1)GO TO 90
  100 J(J1+20)=J(I+20)
      DO 110 K=1,N
      CO=A(I,K)
      A(I,K)=A(J1,K)
  110 A(J1,K)=CO
      J(I+20)=I
  120 CONTINUE
C Multiply A inverse by the right side vector B & store the result in B
      DO 130 K=1,N
      X(K)=0
      DO 130 I=1,N
  130 X(K)=X(K)+A(K,I)*B(I)
      DO 140 K=1,N
  140 B(K)=X(K)
      RETURN
      END
C This suproutine NORMFN normalises the function A to be plotted,
C neglecting those values which exceed abs(UL) and calls the
C subroutine PLTMOD to plot these selected (normalised ) values.
      SUBROUTINE NORMFN(A,H,M,X,K,UL)
      REAL *8 A(M),B,H,FM,X,UL
      REAL *4 F(10)
      LOGICAL TF(10)
      FM=0
      DO 5 L=1,M
      B=DABS(A(L))
      IF(B.GT.UL)GO TO 2
      IF(B.LT.FM)GO TO 3
      FM=B
      NR=L
    3 TF(L)=.FALSE.
      GO TO 5
    2 TF(L)=.TRUE.
    5 CONTINUE
      WRITE(10,20)X,K,NR,A(NR)
      DO 10 L=1,M
      B=L-1
      R=H*B
      F(L)=A(L)/FM
      IF(TF(L))F(L)=0
      CALL PLTMOD(F(L),R,1.0,-1.0)
   10 CONTINUE
      RETURN
   20 FORMAT(' X ='F8.6,' K =',I2,' NR=',I2,' A(NR)=',F9.4)
      END
      SUBROUTINE PLTMOD (FRI,R,C,D)
      DIMENSION A(56),E(56)
      DATA A/' ',' ',' ',26*' ',' ','+',26*' ',' ','.'/,B/'*'/
      DATA E/' ',' ',' ',26*' ',' ','+',26*' ',' ','.'/
      I=(FRI-D)*50.0/(C-D)+2.0
      A(I)=B
  100 FORMAT(56A1,4X,6HF(X) =,F8.6,2X,3HR =,F4.2)
      WRITE(10,103)A
  103 FORMAT(56A1)
      DO 101 I=1,56
  101 A(I)=E(I)
      RETURN
      END
```

```
C  This subroutine CRVSET alongwith PLYFIT and SOLVE
C  fits an exact fit for the component W
      SUBROUTINE CRVSET(W,M,I,M1,N1,NOP,XG,IG,SGM,DEL)
      REAL *8 W(110),SGM,WF(11),XG(M1),XF(11),Y,DEL
      INTEGER IG(N1,NOP)
      K=I/M
      J2=K*M
      K=K+1
      N=NOP+2
      NO=N-1
      KK=K*M
      J1=1
      DO 5 L=1,NOP
      J1=J1+1
      J3=J2+IG(K,L)
      WF(J1)=W(J3)
5     XF(J1)=XG(IG(K,L))
      WF(1)=0
      XF(1)=0
      J1=J1+1
      WF(J1)=0
      XF(J1)=SGM
      CALL PLYFIT(WF,XF,N)
      DO 15 L=1,M1
      Y=1
      WF(L)=XF(1)
      DO 15 J=2,N
      Y=Y*XG(L)
15    WF(L)=WF(L)+XF(J)*Y
      J1=0
      DO 30 L=I,KK
      J1=J1+1
30    W(L)=WF(J1)
      RETURN
      END
      SUBROUTINE PLYFIT(F,X,N)
      REAL *8 F(N),X(N),A(6,6)
      DO 2 J=1,N
      A(J,1)=1
      DO 2 I=2,N
2     A(J,I)=A(J,I-1)*X(J)
      CALL SOLV(A,F,N)
      DO 4 I=1,N
4     X(I)=F(I)
      RETURN
      END
```

REFERENCES

1. L. Schiller, Die Entwicklung der laminaren Geschwindigkeitsverteilung und ihre Bedeutung fur Zähigkeitsmessungen, ZAMM, Vol. 2, pp. 96-106, 1922.

2. H. L. Langhaar, Steady Flow in the Transition Length of a Straight Tube, J. Appl. Mech., Vol. 9, pp. A55-A58, 1942.

3. L. Prandtl and O. G. Tietjens, Applied Hydro-and Aerodynamics, 1st ed., p. 27, Fig. 13, McGraw-Hill, New York, 1934.

4. N. A. Slezkin, Dynamics of Viscous Incompressible Fluids, Gostekhizdat, Moscow, Russia, 1955.

5. E. M. Sparrow, T.S. Lundgren and S. H. Lin, Slip Flow in the Entrance Region of a Parallel Plate Channel, Proc. Heat Transfer and Fluid Mech. Inst., Stanford University Press, Calif., pp. 223-238, 1962.

6. T. S. Lundgren, E.M. Sparrow and J. B. Starr, Pressure Drop Due to the Entrance Region in Ducts of Arbitrary Cross Section, J. Basic Engg., Trans. ASME, Vol. 86, pp. 620-626, 1964.

7. S. T. McComas, Hydrodynamic Entrance Lengths for Ducts of Arbitrary Cross Section, J. Basic Engg., Trans. ASME, Vol. 89, pp. 847-850, 1967.

8. E. M. Sparrow, S.H. Lin and T. S. Lundgren, Flow Development in the Hydrodynamic Entrance Region of Tubes and Ducts, Phys. Fluids, Vol. 7, pp. 338-347, 1964.

9. S. T. McComas and E. R.G. Eckert, Laminar Pressure Drop Associated With the Continuum Entrance Region and for Slip Flow in a Circular Tube, J. Appl. Mech., Vol. 32, pp. 765-770, 1965.

10. L. S. Han, Hydrodynamic Entrance Lengths for Incompressible Flow in Rectangular Ducts, J. Appl. Mech., Vol. 27, pp. 403-409, 1960.

11. E. M. Sparrow and S. H. Lin, The Developing Laminar Flow and Pressure Drops in the Entrance Region of Annular Ducts, J. Basic Engg., Trans. ASME, Vol. 86, pp. 827-834, 1964.

12. D. P. Flemming and E. M. Sparrow, Flow in the Hydrodynamic Entrance Region of Ducts of Arbitrary Cross Section, J. Heat Transfer, Trans. ASME, Vol. 91, pp. 345-354, 1959.

13. H. Schlichting, Laminare Kanaleinlaufstromung, ZAMM, Vol. 14, pp. 368-373, 1934.

14. Atkinson and S. Goldstein, in S. Goldstein (ed.), Modern Developments in Fluid Dynamics, Vol. 1, pp. 304-308, Clarendon Press, Oxford, England, 1938.

15. A. H. Shapiro, R. Siegel and S. J. Kline, Proc. 2nd U. S. Natl. Congr. Appl. Mech., ASME, pp. 773-741, New York, 1954.

16. R. Siegel, The Effect of Heating on Boundary Layer Transition for Liquid Flow in a Tube, D.Sc. thesis, Mass. Inst. Tech., Cambridge, Mass., 1953.

17. D. C. Bogue, Ind.Eng. Chem. J., Vol. 51, p. 894, 1959.

18. H. Schlichting, Boundary Layer Theory, 7th ed., McGraw-Hill, New York, 1979.

19. Y. Tomita, Soc. Chem. Engrs. Japan, Vol. 23, pp. 525-529, 1959.

20. Y. Tomita, Bull. JSME, Vol. 4, No. 13, pp. 77-86, 1961.

21. W. D. Campbell and J. C. Slattery, Flow in the Entrance of a Tube, J. Basic Engg., Trans. ASME, Vol. 85, pp. 41-44, 1963.

22. E. G. Christriansen and H. E. Lemmon, Entrance Region Flow, AIChE J., Vol. 11, pp. 995-999, 1965.

23. R. Y. Chen, Flow in the Entrance Region at Low Reynolds number, J. Fluids Engg., Trans. ASME, Vol. 95, pp. 153-158, 1973.

24. M. S. Bhatti, Laminar Flow in the Entrance Region of Elliptical Ducts, J. Fluids Engg., Trans. ASME, Vol. 105, pp. 290-296, 1983.

25. L. S. Han and A. L. Coopar, Approximate Solutions of Two Internal Flow Problems - Solution by an Integral Method, Proc. 4th U.S. Natl. Cong. Appl. Mech., ASME, Vol. 2, pp. 1269-1278, 1962.

26. E. M. Sparrow, Analysis of Laminar Forced Convection Heat Transfer in Entrance Region of Flat Rectangular Ducts, NACA TN 3331, 1955.

27. W. T. Rouleau and J. F. Osterle, The Application of Finite Difference Methods to Boundary Layer Type Flows, J. Aero. Sci., Vol. 22, pp. 249-254, 1955.

28. J. R. Bodoia and J. F. Osterle, Finite Difference Analysis of Plane Poiseuille and Coutte Flow Developments, Applied Scientific Research, Sec. A, Vol. 10, pp. 265-276, 1961.

29. Y. L. Wang and P. A. Longwell, Laminar Flow in the inlet section of parallel plates, AIChE J., Vol. 10, pp. 323-329, 1964.

30. F. W. Schmidt and B. Zeldin, Laminar Flow in Inlet Sections of Tubes and Ducts, AIChE. J., Vol. 15, pp. 612-614, 1969.

31. A. Brandt and J. Gillis, Magnetohydrodynamic Flow in the Inlet Region of a Straight Channel, Phys. Fluids, Vol. 9, pp. 690-699, 1966.

32. S. Abarbanel, S. Bennet, A. Braudt and J. Gillis, Velocity profiles at Low Reynolds numbers, J. Appl. Mech., Vol. 37, pp. 2-4, 1970.

33. J. A. Miller, Laminar Incompressible Flow in the Entrance Region of Ducts of Arbitrary Cross Section, J. Engg. Power, Vol. 93, pp. 113-118, 1971.

34. G. Comini, S. Del Giudice and M. Strada, Finite Element Analysis of Laminar Flow in the Entrance Region of Ducts, Int. J. Num. Meth. Engg., Vol. 15, pp. 507-517, 1980.

35. T. F. Irvine and E. R. G. Eckert, Comparison of Experimental Information and Analytical Prediction for Laminar Entrance Pressure Drop in Ducts With Rectangular and Triangular Cross Sections, J. Appl. Mech., Vol. 25, pp. 283-290, 1958.

36. E. R. G. Eckert and T. F. Irvine, Incompressible Friction Factor, Transition and Hydrodynamic Entrance-Length Studies of Ducts with Triangular and Rectangular Cross Sections, WADC Tech. Rept. 58-85, ASTIA D.N. AD-151027, 1957.

37. E. R. G. Eckert and T. F. Irvine, Incompressible Friction Factor, Transition and Hydrodynamic Entrance-Length Studies with Triangular and Rectangular Cross Sections, Proc. 5th Midwest. Conf. Fluid Mech., pp. 122-145, 1957.

38. G. G. Beavers, E.M. Sparrow and R.A. Magnuson, Experiments on Hydrodynamically Developing Flow in Rectangular Ducts of Arbitrary Aspect Ratio, Int. J. Heat Mass. Transfer, Vol. 13, pp. 689-702, 1970.

39. E. M. Sparrow, C.W. Hixon and G. Shavit, Experiments on Laminar Flow development in rectangular ducts, J. Basic Engg., Trans. ASME, Vol. 89, pp. 116-124, 1967.

40. S. V. Patankar and D. B. Spalding, A calculation procedure for Heat, Mass and Momentum Transfer in Three-Dimensional Parabolic Flows, Int. J. Heat Mass Transfer, Vol. 15, pp. 1787-1806, 1972.

41. L. S. Caretto, A. D, Gosman, S. V. Patankar and D. B. Spalding, Two calculation procedures for steady three-dimensional flows with recirculation, Proc. 3rd. Int. Conf. Num. Meth. Fluid Dynamics, Paris, July 1972.

42. V. S. Pratap and D. B. Spalding, Fluid flow and heat transfer in three-dimensional duct flows, Int.J. Heat Mass Transfer, Vol. 19, pp. 1183-1188, 1976.

43. R. J. Goldstein and D. K. Kreid, Measurement of Laminar Flow Development in a Square-Duct Using a Laser-Doppler Flow-meter, J. Appl. Mech., Vol. 34, pp. 813-818, 1967.

44. R. K. Shah and A. L. London, Laminar Flow Forced Convection in Ducts, Academic Press, New York, 1978.

45. G. A. Carlson, Laminar Entrance Flow in a Square Duct, Ph.D. thesis, Carnegie Inst. Tech., 1966.

46. V. K. Garg, Developing Flow in a Rectangular Duct, in C. Taylor, J. A. Johnson and W. R. Smith, (eds.), Numerical Methods in Laminar and Turbulent Flows, Pineridge Press, pp. 58-68, 1983.

47. E. E. Feldman, R. W. Hornbeck and J. F. Osterle, A Numerical Solution of Laminar Developing Flow in Eccentric Annular Ducts, Int. J. Heat Mass Transfer, Vol. 25, pp. 231-241, 1982.

48. G. E. Forsythe and W. R. Wasow, Finite-Difference Methods for Partial Differential Equations, John Wiley, New York, 1960.

49. D. N. de G. Allen, Relaxation Methods in Engineering and Science, McGraw-Hill, New York, 1954.

50. R.W. Hornbeck, Numerical Marching Techniques for Fluid Flows with Heat Transfer, NASA SP-297, Washington, D.C., 1973.

51. R.W. Hernbeck, Numerical Methods, Quantum Publishers, New York, 1975.

52. S.K. Gupta and K.K. Tanji, Computer Program for Solution of Large Sparse Unsymmetric Systems of Linear Equations, Int. J.Num. Meth. Engg., Vol. 11, pp. 1251-1259, 1977.

53. A. Ralston, A first course in Numerical Analysis, McGraw-Hill, 1965.